MOLECULAR SIZE AND CONFIGURATION

OF

CELLULOSE TRINITRATE IN SOLUTION

A

THESIS

BY

Md. Mahbubul Huque, B.Sc. (Honours), M.Sc.
(University of Dacca,
Pakistan)

Submitted to the Faculty of Graduate
Studies and Research of McGill Univer-
sity in partial fulfilment of the
requirements for the degree of
Doctor of Philosophy.

McGill University,
Montreal, Canada.

August 21, 1957

ACKNOWLEDGMENTS

FOREWORD

The arrangement of this thesis may require some explanation. The main text has been written to be published with little modification. Additional information is contained in a series of Appendices which include a historical survey, details of experimental procedures and calculation of hydrodynamic parameter. The last two Appendices contain the data from which the results described in the text were computed. The main text and the series of Appendices have separate bibliographies, lists of Figures and lists of Tables.

SUMMARY

Viscosity and light-scattering measurements were made on several fractions and two unfractionated samples of cellulose trinitrate. The samples were prepared from bleached ramie, unbleached ramie and cotton linters. Solvents were acetone and ethyl acetate.

Viscosity was measured in a multi-shear viscometer designed for the purpose. Light-scattering measurements were made in a Brice-Phoenix Light-scattering Photometer modified to accommodate a cell which could be centrifuged.

The range of molecular weight investigated was from 6.5×10^5 to 25.0×10^5. The relationship between the z-average mean-square radius of gyration, $\overline{s_z^2}$, and the z-average molecular weight was approximately linear in both solvents. The ratio of $(\overline{s_o^2})_z / \overline{M}_z$ (where $(\overline{s_o^2})_z$ is the value of $\overline{s_z^2}$ in the unperturbed state) was found to be constant in acetone but increased with $\overline{M}_z$ in ethyl acetate. This indicated that, whereas in acetone random coil configuration was attained, a configurational transition occurred in ethyl acetate in the molecular weight range investigated.

v

The intrinsic viscosity was found to be independent of shear rate in acetone. In ethyl acetate it was independent of shear rate for $[\eta] < 30$ dl. g.$^{-1}$. At higher values the intrinsic viscosity was linearly related to the rate of shear in the range of shear rate of 700 sec.$^{-1}$ to 300 sec.$^{-1}$.

The value of the exponent a in the relationship between intrinsic viscosity and molecular weight was found to be lower than unity but approximately equal in both solvents.

The hydrodynamic parameter Φ' was calculated for both solvents. In acetone its value increased with molecular weight but in ethyl acetate a constant value of Φ' was obtained.

The Huggins' interaction constant, k', increased with decrease in shear rate; k' at constant shear rate was higher in acetone than in ethyl acetate. Both k' and the second virial coefficient, A_2, decreased irregularly with increasing molecular weight. A possible correlation between the irregularities and the nitrogen content of the samples was observed.

Certain persistent anomalies at high concentration were observed during light-scattering measurements. The plot of reduced intensity vs. concentration deviated from linearity above a certain critical concentration which decreased approximately linearly with increasing molecular weight. At about the same concentration vertical bands of diminished and increased intensities (striations) were observed. Several experiments were carried out to ascertain the origin of these phenomena. Results suggest that the effects were not trivial but related to some basic property of the solutions studied.

TABLE OF CONTENTS

LIST OF FIGURES

Main Text

Appendices

LIST OF TABLES

Main Text

Appendices

No.   Page

LIST OF SYMBOLS

A_2 – Second virial coefficient

$\overset{\circ}{A}$ – Ångstrom unit (10^{-8} cm.)

a – Exponent in the empirical relationship between intrinsic viscosity and molecular weight

C – Calibration constant for light-scattering apparatus

c – Concentration; g./cc. for light-scattering and g./100 cc. for viscosity measurements

c_c – Critical concentration

G – Mean rate of shear

g – Acceleration due to gravity

I_θ – Scattering intensity at angle θ multiplied by sin θ

i_θ – Scattering intensity at angle θ , expressed as the ratio of galvanometer readings for scattered and transmitted beams.

K – Constant in empirical equation relating intrinsic viscosity to molecular weight

K – Constant in the equation for light-scattering

k – Arbitrary constant used in Zimm's equation for plotting light-scattering data

k' – Huggins' interaction constant

k'_{500} – Huggins' interaction constant at a shear rate of 500 sec.$^{-1}$

M_O - Molecular weight of the monomer

$\overline{M}$ - Average molecular weight

$\overline{M}_n$, $\overline{M}_w$, $\overline{M}_z$ - Number, weight and z-average molecular weight respectively

N - Avogadro number

n - Refractive index of solution

n_s - Refractive index of solvent

n_w - Refractive index of water

$P(\theta)$ - Factor expressing the reduction in scattered intensity at the angle θ owing to intraparticle interference

q - Persistence length defined by Kratky and Porod

q_Φ - Polydispersity correction factor in the calculation of Φ'

R_θ - Rayleigh ratio at angle θ

R_θ^o - Rayleigh ratio at angle θ in the absence of intra-particle interference

$r_{max.}$ - Maximum extension of the polymer molecule

$\sqrt{\overline{s_o^2}}$ - Unperturbed radius of gyration

$\overline{s^2}$, $\sqrt{\overline{s^2}}$ - Mean-square and root-mean-square radii of gyration

x - Number of units of length q in the fully extended molecule

$\propto$ - Extension factor

η_{sp} -   Specific viscosity

$[\eta]$ -   Intrinsic viscosity

$[\eta]_{500}$ -   Intrinsic viscosity at a shear rate of 500 sec.$^{-1}$

$[\eta]_{o}$ -   Intrinsic viscosity at zero shear rate

$[\eta]^{T}$ -   Intrinsic viscosity corrected to the value for the trinitrate

θ -   Angle between transmitted and scattered beam

Θ -   "Ideal" temperature at which van't Hoff's law is obeyed for a given poor solvent-polymer system

λ -   Wave length of light in vacuum

τ -   Turbidity as determined by the spectrophotometer

Φ' -   Parameter relating the intrinsic viscosity to the radius of gyration of a polymer molecule

Φ -   Parameter relating the intrinsic viscosity to the end-to-end distance of the polymer molecule

PREFACE

PREFACE

The molecular configuration of cellulose derivatives
in solution is known to differ considerably from that of
an ideal Gaussian coil. This is because the β -glucosidic
chain is relatively stiff compared with many synthetic
polymers. At very high molecular weight, however, random
coil statistics would be expected to apply. Reliable data
are lacking in this range largely because of the experi-
mental difficulties in preparing fractions and handling
solutions.

The object of the present investigation was to study
the configurational behaviour of cellulose trinitrates of
high molecular weight in acetone and ethyl acetate. Nitrates
were made from raw ramie, bleached ramie and cotton. Several
fractions and two unfractionated samples were used. Visco-
sity and light-scattering measurements were made on these
samples in the two solvents.

Viscosity was measured in an Ubbelohde capillary
viscometer. The instrument was designed to permit deter-
minations at different rates of shear and dilution in situ.

Light-scattering measurements were complicated by
the high viscosity of the solutions, even at low concentra-
tion, and the consequent difficulty in removing the extra-

neous dust particles and gel-like material. This difficulty
was overcome by ultracentrifugal clarification in small
glass cells which were placed directly into the light-
scattering apparatus after centrifuging. A Brice-Phoenix
Light-scattering Photometer was modified to accommodate
the special type of cells needed for this technique.

The intrinsic viscosity and the Huggins' interaction
constant were obtained from viscosity measurements. Light-
scattering measurements yielded the molecular weight, radius
of gyration and the second virial coefficient. From a com-
parison of molecular weight and dimensions information was
derived concerning the configuration of the cellulose tri-
nitrate chain in dilute solution.

Certain unexpected but persistent anomalies in light-
scattering were found at higher concentrations. Above a
certain critical concentration an unusual increase in the
scattered intensity occurred and visible discontinuities
were noted in the beam as it passed through the solution.
Several types of experiments were carried out in order to
ascertain whether these effects were spurious or due to
inherent properties of high molecular weight cellulose tri-
nitrate in solution.

INTRODUCTION

INTRODUCTION

Modern theories of high polymer solutions are based
on the concept of the ideal Gaussian chain in which the
orientation of a segment is independent of the direction
of its predecessor in the chain. In real polymers bond
angle restrictions and steric hindrances to free rotation
can severely restrict the degree of randomness in inter-
segment orientation.

As first shown by Kuhn (23), the real polymer may
be replaced by a model random coil containing fewer seg-
ments, each of which is considerably longer than the ori-
ginal monomer unit. If the molecular weight is high compared
with the segment length of the model, the molecule will show
the configurational behaviour of a random coil, in spite of
restraint on random orientation between the monomer units.
Conversely, for a stiff chain at low molecular weights,
the configuration may differ markedly from that of an ideal
random coil. In such a case, as the molecular weight in-
creases from a low value, configurational changes should
occur by which the molecule approaches Gaussian behaviour
more nearly. If the chain is flexible, random flight

statistics will apply at a relatively low value of the aver-age molecular weight, M, e.g., 30,000 for polystyrene (31). Cellulose nitrate (15, 18) has been shown to be a rather stiff chain for which non-Gaussian behaviour is observed for samples having molecular weight as high as 400,000 (31).

The configurational transition in the case of cellu-lose trinitrate (designated CTN hereafter) can be studied by following the change of molecular dimension with molecu-lar weight. A suitable parameter is the root-mean-square radius of gyration, $\sqrt{\overline{s^2}}$, which in the case of a polymer is defined as the average distance of a segment from the centre of gravity of the molecule; $\sqrt{\overline{s^2}}$ is readily deter-mined by the light-scattering method. As shown by Benoit and Doty (4), for a stiff rod-like chain $\sqrt{\overline{s^2}}$ is propor-tional to M and $\overline{s^2}/M$ will increase with M. For a Gaussian coil $\overline{s^2}$ varies as M and $\overline{s^2}/M$ is constant. Inferences about the configuration of the molecules can, therefore, be drawn from the variation of $\overline{s^2}/\overline{M}$ with M. The data of Hunt et al (18) for CTN in ethyl acetate show an increase in $\overline{s^2}/\overline{M}$ with increasing molecular weight. The authors worked only with low molecular weight material, and pre-dicted an asymptotic approach to a constant value of $\overline{s^2}/M$

at high $\overline{M}$. The earlier light-scattering measurements of
Holtzer et al (15) over a wide range of molecular weight
also demonstrated such an increase of $\overline{s^2}/\overline{M}$ with M at low
$\overline{M}$. But because of experimental difficulties the authors
regarded their data for samples of molecular weight higher
than 1.5×10^6 as unreliable. An unambiguous demonstration
of random coil behaviour of CTN at very high molecular
weight has not yet been given.

The intrinsic viscosity, $[\eta]$, of a polymer solu-
tion is also related to molecular configuration. Hydro-
dynamic theories developed by Debye and Bueche (11), Kirk-
wood and Riseman (20) and Brinkman (5) have lent support to
the empirical equation

$$[\eta] = k \, \overline{M}^{\,a} \qquad\qquad \dots\dots (1)$$

put forward by Houwink (16) . In Eqn. (1) K and a are con-
stants. The value of the exponent a depends on the configu-
ration of the molecule. According to the above theories,
for a stiff chain several regions may be distinguished in
the $[\eta]$ -$\overline{M}$ relation as the molecular weight increases;
each region is characterized by a value of a. At low $\overline{M}$
when the molecule is rod-like a has a value which approaches
2. With increasing $\overline{M}$, the molecule passes through a non-

Gaussian coil to a free-draining Gaussian coil when $\underline{a}$ becomes 1. With further increase in $\overline{M}$ the coil develops a solvent immobilizing character which decreases $\underline{a}$ until it approaches 0.5; this is the value for a solvent impermeable coil. With CTN the evidence for such change of the value of $\underline{a}$ with molecular weight is conflicting. For example, Badger and Blaker (2) and Münster (29) obtained a definite curvature in the plot of $\log \left[\eta\right]$ vs. $\log \overline{M}$ while Holtzer et al (15) have indicated that their data gave constant $\underline{a}$ throughout the molecular weight range.

The flexibility and the configurational characteristics of polymers are affected by the nature of the solvent used. Good solvents (with negative heat of mixing) prefer solvent-solute contact; reacting with or solvating the polymers, they stiffen and stretch the molecules. In poor solvents, on the other hand, solute-solute contact is preferred and the polymer has a more compact structure. Such change in configuration results in a change of the exponent $\underline{a}$ in Eqn. (1), $\underline{a}$ being less in the poor solvent than in the good solvent. This has been demonstrated in the case of synthetic polymers, e.g., polystyrene (3). For CTN the data are incomplete. In the only such investigation on CTN in more than one solvent Immergut, Ranby and Mark (19) related

$[\eta]$ to the osmotic molecular weight. The values of $\underline{a}$ obtained by them were 1.03 and 0.91 in ethyl acetate and acetone respectively. On the other hand, Holtzer et al (15), Hunt et al (18) and Newman et al (32) report near unity values of $\underline{a}$ in acetone and ethyl acetate.

It is evident that complete and reliable data are lacking in the high molecular weight range, both in regard to the relation of $\overline{s^2}/\overline{M}$ with $\overline{M}$ and in the value of $\underline{a}$ in Eqn. (1) in different solvents. The purpose of this work was, therefore, to study the configuration of high molecular weight CTN in a good (ethyl acetate) and a poor (acetone) solvent. Viscosity and light-scattering methods were used and the results interpreted in the light of modern theories of the solution properties of polymers.

A more detailed survey of earlier work in this field is given in Appendix I.

EXPERIMENTAL

EXPERIMENTAL

The experimental part is divided into several sections. Materials together with the procedure of fractionation are described first. Viscosity and light-scattering methods are described in the two following sections. A short description of the refractive index measurements is included at the end.

MATERIALS

Cellulose Nitrates

Cellulose trinitrates prepared from unbleached raw ramie, bleached ramie and cotton linters (designated respectively by H, M and T) were used in this investigation. The method of nitration has been described by Timell (44). Nitrogen contents are given in Table I.

Fractionation

The samples were fractionated by adding water to an acetone solution following the method of Mitchell (28). The exact quantities of water necessary for precipitation were ascertained from exploratory fractionations. Frac-

TABLE I

Analytical Data of Cellulose Nitrates

Source	#Nitrogen content %N	Degree of substitution	Base molecular weight
Unbleached raw ramie (H)	13.68	2.90	288
Bleached ramie (M)	13.80	2.93	290
Cotton linters (T)	13.57	2.88	285

#Complete nitration to cellulose trinitrate would correspond to 14.14% N with a base molecular weight of 297.

tionation data for samples M and H are given in Tables II and III respectively.

For sample M, 4.5 gm. was soaked in acetone-water mixture (91:9) for 24 hours and then stirred vigorously for six hours to yield a 0.1% solution; solutions of higher concentration were too viscous for convenient handling. The solution was then centrifuged at 500 g for 20 minutes to remove any undissolved material. The decanted solution was placed in a $25^{\circ}C$ bath and distilled water added to it dropwise with vigorous stirring. When the previously determined quantity of water had been added, the system was allowed to stand for one hour in the bath while the stirring continued. The precipitate was separated by centrifuging for 20 minutes at 500 g. The precipitate in the centrifuge cups was gel-like in appearance. It was found that addition of methanol facilitated removal of the precipitate from the cups. Excess liquid was squeezed out of the solid which was then vacuum-dried at about $45^{\circ}C$. This procedure was repeated to yield four fractions (M-1, M-2A, M-2B and M-3).

The solution remaining after separation of M-3 was evaporated to dryness to yield M-4.

TABLE II

Fractionation Data on Sample M

Fraction	Water added cc.	Weight gm.	Yield %
M-1	31.0	1.190	28.4
#M-2A	4.8	0.723	17.0
#M-2B	5.2	0.524	12.3
M-3	12.1	0.578	13.8
M-4		0.880	19.5
Undissolved material		0.320	7.1
Loss			1.9

#Fractions M-2A and M-2B had nearly identical
 intrinsic viscosities and were, therefore,
 blended by dissolving in acetone and precipi-
 tating by addition of water. The blended sample
 is referred to as M-2 hereafter.

Sample H was fractionated in essentially the same way from a 0.1% solution of 2 gm. in acetone. The solution left after separation of the third fraction was evaporated to about 1/4 its original volume by blowing air through it and stirring. The resulting suspension was centrifuged to take out the fourth fraction. The final fraction was obtained as before by evaporating the remaining liquid to dryness.

All fractions were stored over fused calcium chloride in a refrigerator.

Sample T, also, was fractionated after the method of Mitchell (28). Ten fractions were obtained of which only T-6 and T-8 were used in this study. These fractions were chosen in order to extend the range to a somewhat lower molecular weight than values found for the fractions of M and H.

Finally a fraction, P, from an exploratory fractionation of bleached ram ramie nitrate was used to fill the gap of molecular weights between M-2 and M-3.

In the fractionation of samples M and H the solutions developed a cloudiness which increased as the fractionation proceeded. Repeated centrifugations did not remove the

TABLE III

Fractionation Data on Sample H

Fraction	Water added cc.	Weight gm.	Yield %
H-1	34.0	0.369	18.5
H-2	10.3	0.548	27.4
H-3	40.0	0.397	19.8
H-4	-	0.265	13.3
H-5	-	0.340	17.0
Undissolved material		0.020	1.0
Loss			3.0

cloudiness. The effect seemed greater in sample H, possibly because of its lower nitrogen content. Evidently part of the precipitate remained suspended as colloidal material. It is probable that the non-sedimentable aggregates from one cycle were precipitated on the next addition of water. However, this is an assumption and must be recognized as such when considering the effectiveness of the fractionation procedure.

Solvents

Reagent grade acetone was used in fractionation. For viscosity and light-scattering measurements reagent grade solvents were redistilled. Boiling ranges for acetone and ethyl acetate were $56.3-56.8^\circ C$ and $77-77.3^\circ C$ respectively.

Preparation of Solutions

Solutions were made up by shaking CTN in solvent for 24 hours in a wrist-action shaker. This was followed by centrifugation in stainless steel tubes at 24,000 g for 30 minutes to remove any undissolved material. Three-fourths of the liquid in the centrifuge tubes were decanted into a glass-stoppered flask. This served as stock solution from which solutions were made for viscosity and light-

scattering measurements. A calibrated 10 cc. hypodermic syringe was used for transfer of liquids.

It was thought possible that CTN might form aggregates on repeating cycles of dissolution recovery (by precipitation or evaporation) and re-solution, in which case erroneous results would be obtained from the light-scattering measurements. Since such cycles were inevitable in fractionation and recovery, light-scattering experiments, which are described later, were carried out to test the possibility of aggregate formation.

VISCOSITY MEASUREMENTS

Since the viscosity of solutions of high DP cellulose nitrate is shear-dependent, a standard shear rate of 500 sec.$^{-1}$ was adopted following the convention of Newman et al and others (32, 42). A modified form of the suspended-level dilution capillary viscometer of Schurz and Immergut (40) was used. The viscometer had four bulbs which enabled measurements to be made at different rates of shear calculable from the expression (22)

$$G_i = \frac{8V_i}{3\pi r^3 t_i} \qquad \ldots \ldots (2)$$

where G_i = mean rate of shear corresponding to bulb i

V_i = volume of bulb i

t_i = efflux time of V_i

r = radius of viscometer capillary.

Efflux times were measured at $25.00 \pm 0.01^{\circ}C$ to 0.1 sec. for each of the four bulbs for pure solvent and over a range of concentrations of the solutions obtained by progressive dilution of the solution first introduced in the viscometer. Efflux times for five or six concentrations were measured on each sample. Kinetic energy corrections (amounting to 0.2 to 3 percent) were applied in the usual way (10) and values of the specific viscosity, η_{sp}, at shear rates calculated from Eqn. (2) were obtained.

The concentration, c, of the initial solution was determined in a duplicate measurement by evaporation and weighing. The solid from 10 cc. of the solution was dried in vacuum to constant weight in a weighed aluminium cup. In determining the concentration of ethyl acetate solutions, filtered ethyl alcohol was added during evaporation to aid in the complete removal of ethyl acetate (18).

From this data, plots of log $\frac{\eta_{sp}}{c}$ against log G for different concentrations were obtained. Fig. 1 shows an example. From these plots the values of $\frac{\eta_{sp}}{c}$ for G = 500

Fig. 1

Log of reduced viscosity vs. log of rate
of shear at different concentrations for
fraction H-2 in acetone.
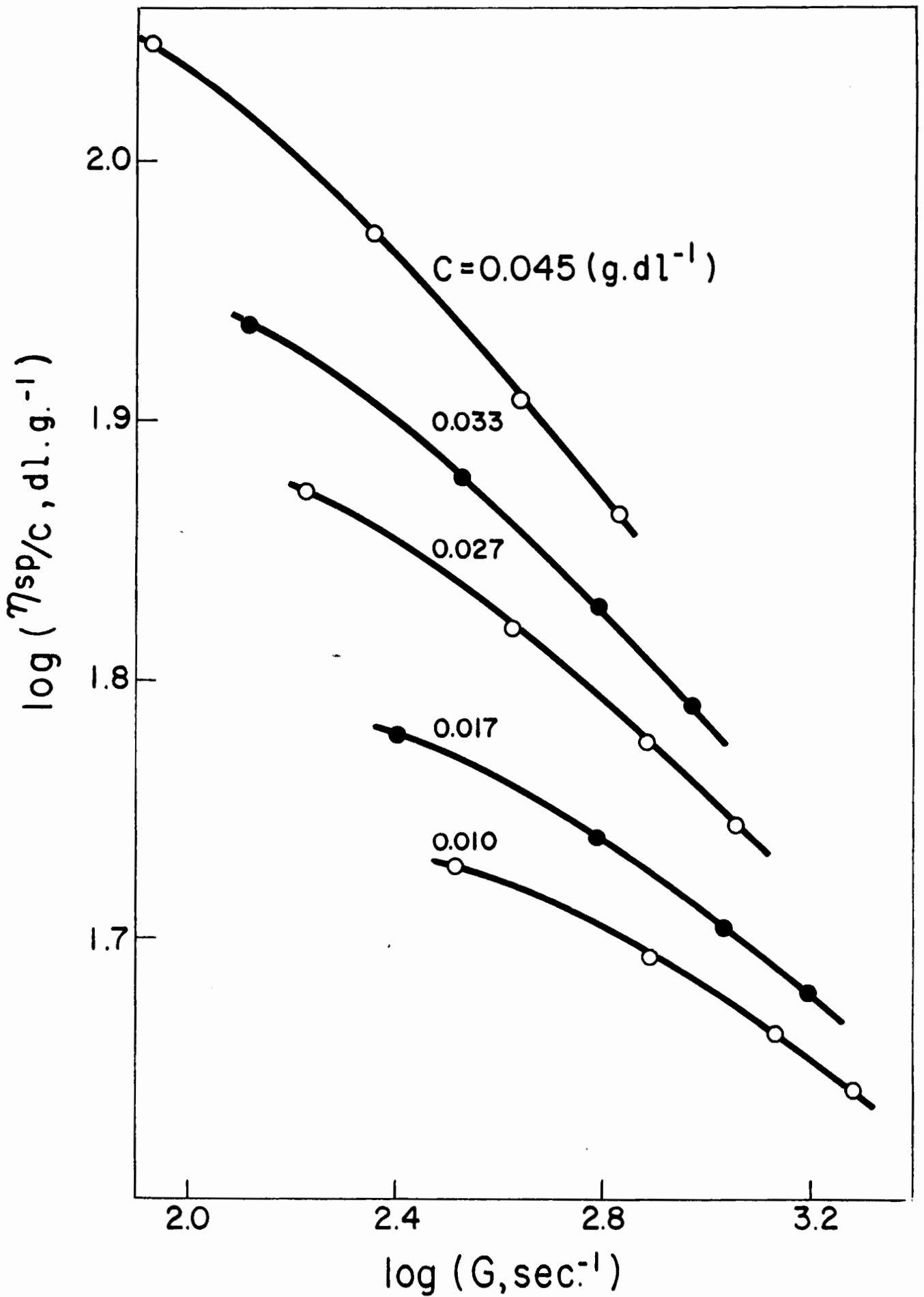
sec.$^{-1}$ were obtained by interpolation. A plot of $\frac{\eta_{sp}}{c}$ vs.
c was then made as shown in Fig. 2. Linear extrapolation
to zero concentration gave the intrinsic viscosity, $[\eta]_{500}$.
In a similar manner intrinsic viscosities were obtained
for a range of G values between 300 and 700 sec.$^{-1}$.

The Huggins' interaction constant (17), k'_{500}, was
calculated from the slope of the $\frac{\eta_{sp}}{c}$ vs. c line at 500 sec.$^{-1}$
in the equation

$$\frac{\eta_{sp}}{c} = [\eta] + k'[\eta]^2 c \qquad \qquad \ldots\ldots (3)$$

A more detailed description of the viscometer is
given in Appendix II.

LIGHT-SCATTERING

Apparatus

Light-scattering measurements were made in a Brice-
Phoenix photometer. The instrument was modified to accom-
modate cells of the type described by Dandliker and Kraut
(9) in which the solution is clarified by ultra-centrifu-
gation in situ. This course was found necessary after at-
tempts to remove stray dust from the solutions by conventional
means such as centrifugation (outside the measuring cell) and

Fig. 2

Reduced viscosity vs. concentration
for fraction H-2 in acetone at a shear
rate of 500 sec.$^{-1}$.
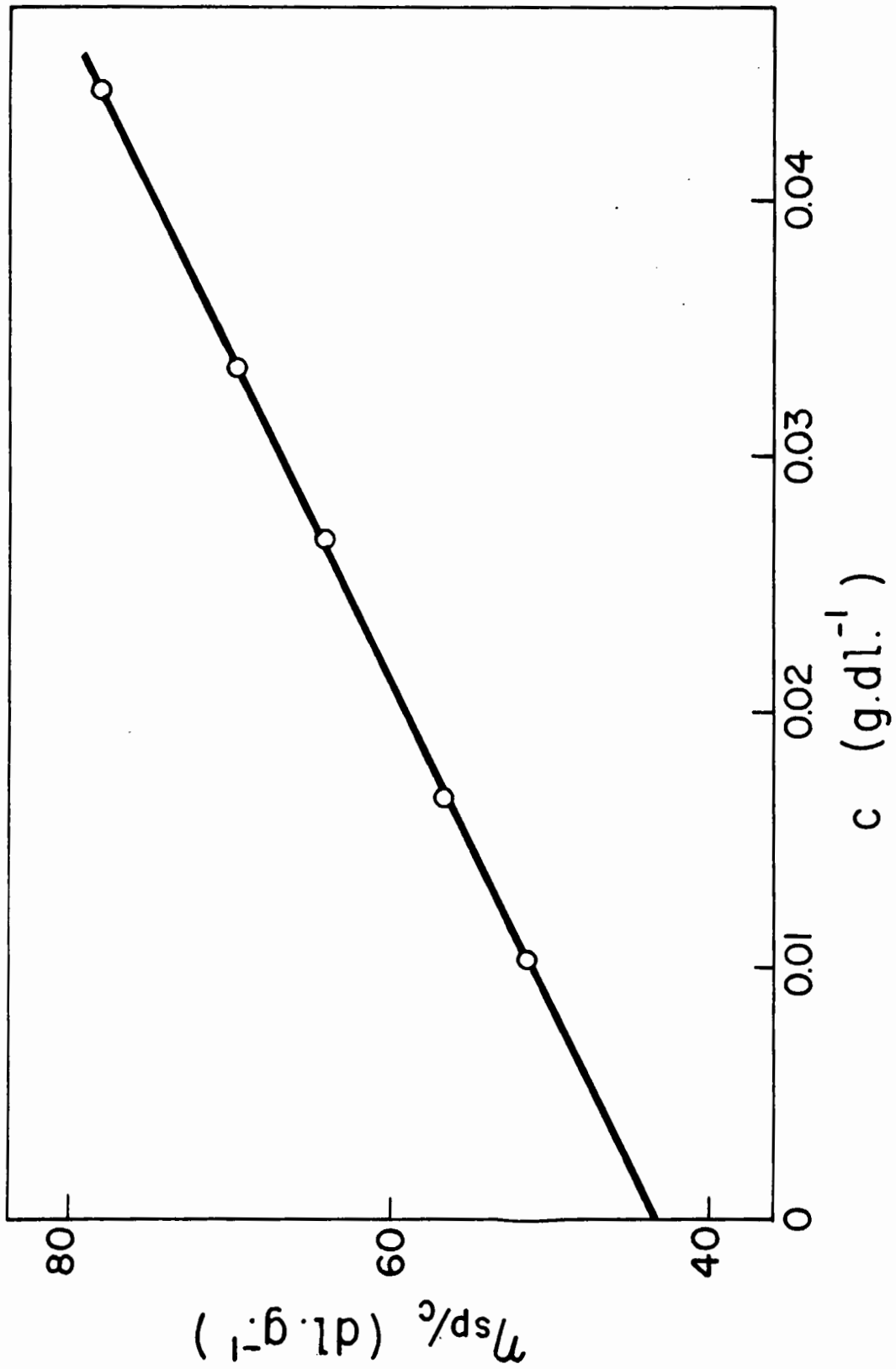
filtration proved unsatisfactory. Despite elaborate care the solution clarified by centrifuging became contaminated with dust in transferring it to the measuring cell; when ultrafine sintered glass filters were used, the solute was retained by adsorption on the filter.

The modified optical system is shown in Fig. 3. Fig. 4 is a photograph of the mounting of the cell SC in the bath B. This bath always contained distilled and filtered solvent. A 8 mm. x 4 mm. slit S_1 in front of the mercury lamp L is focussed by lens L_1 at the centre of the scattering cell. The beam is 4 mm. x 2 mm. at the centre of the cell. Scattered light is collected by an opening (4 mm. x 2.5 mm.) in front of the lens L_2. Horizontal convergences in the incident and scattered beams are 5° and the vertical convergences are 9°. All measurements were made with blue light ($\lambda = 4358$ Å).

The Light-scattering Cell

The cells were of the same shape as described by Dandliker and Kraut (9). The dimensions were larger to allow use of about 8 to 10 cc. of liquid. The cells were capped with serological stoppers.

Fig. 3

The optical system in the light-
scattering apparatus after modifica-
tion for use of small cells.

Legend:

L - Light source

MF - Monochromatic filter

PS - Photographic shutter

NF - Neutral filters

L_1 - Lens in the incident beam

CL_1 - Cylindrical lens in the incident
beam

SC - Scattering cell

B - Bath

L_2 - Lens in the receiving system

CL_2 - Cylindrical lens in the receiving
system

PM - Photomultiplier

S_1, S_2, S_3 and S_4 - Diaphragms
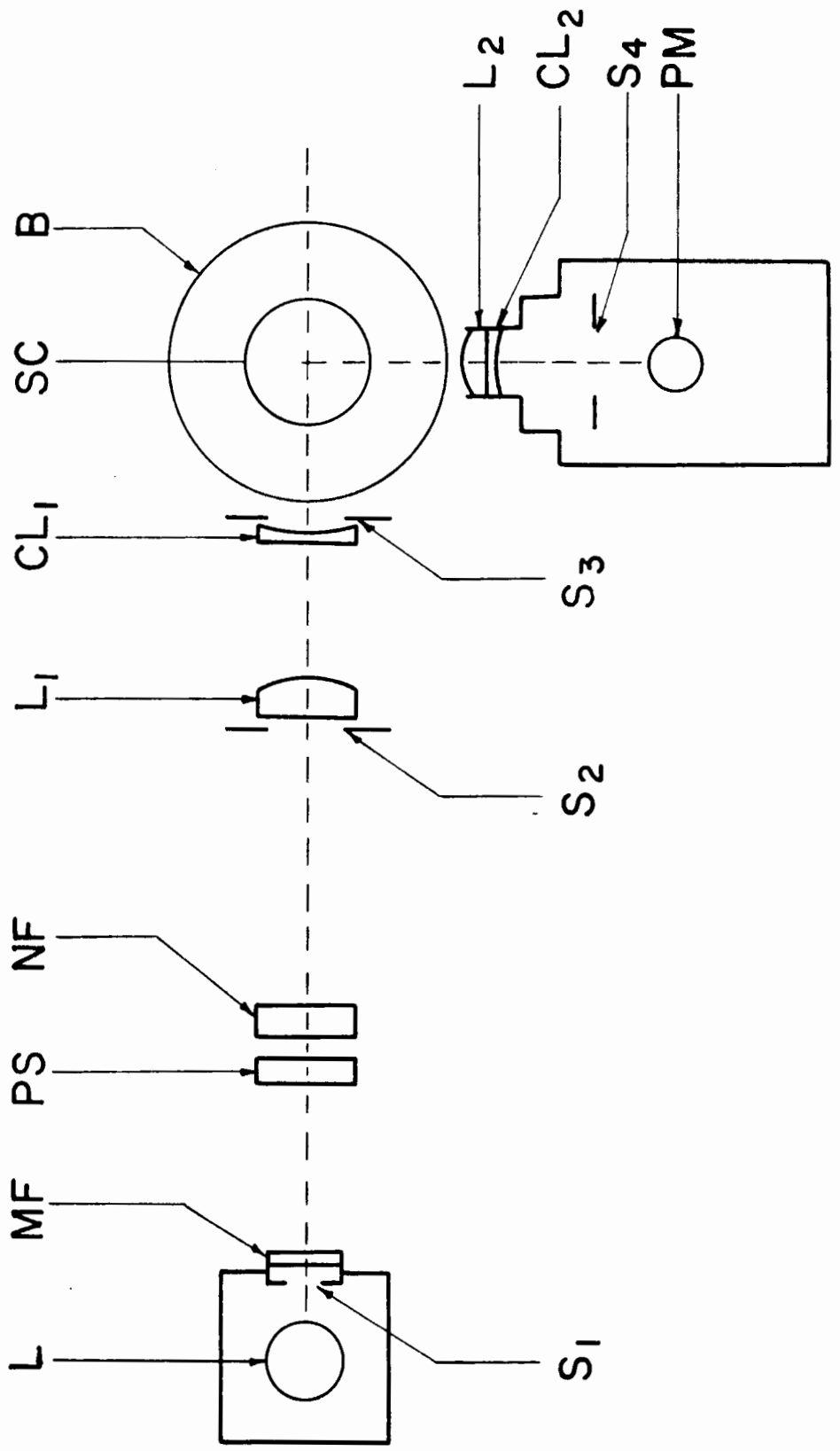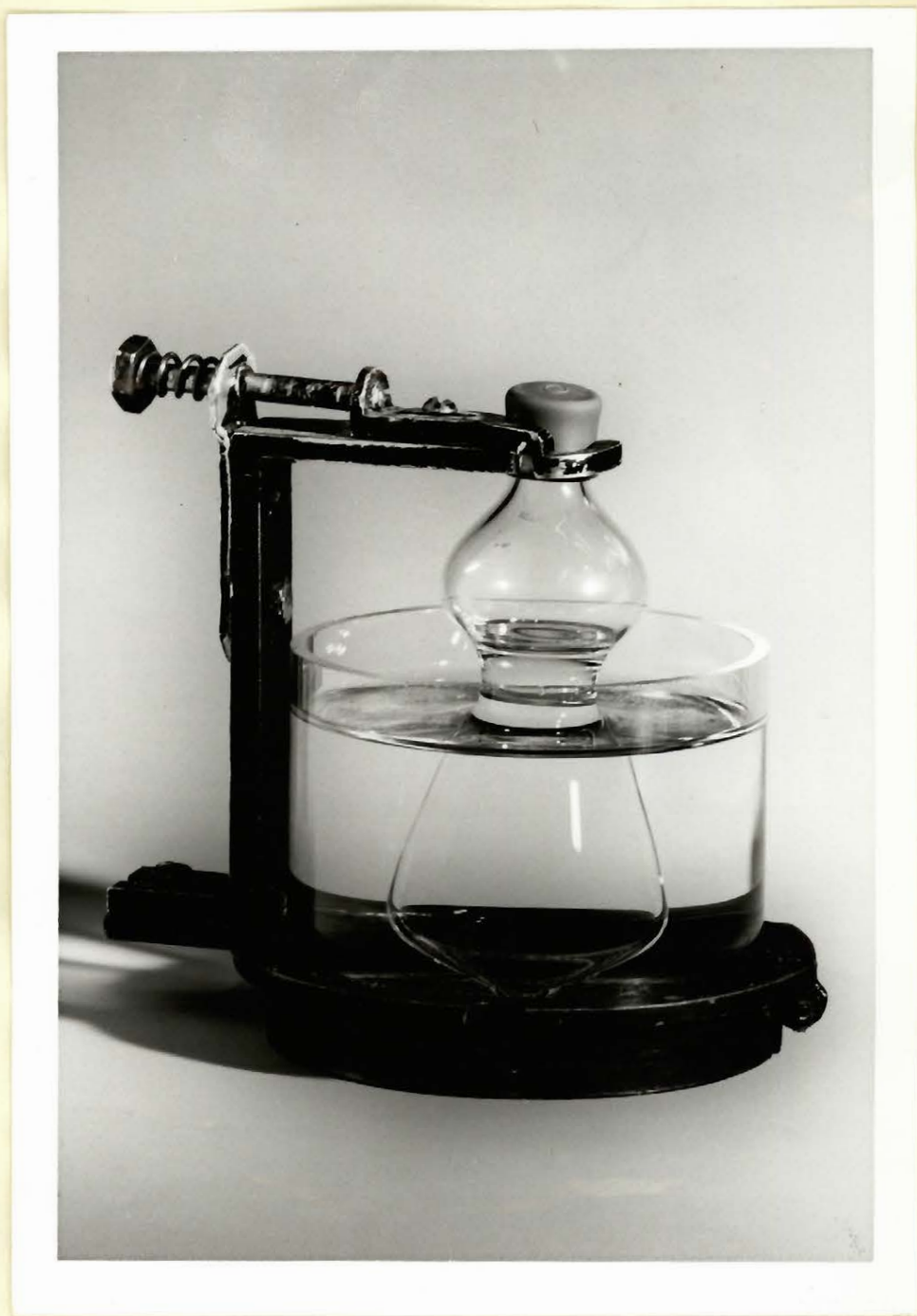
Tests and Calibration of the Apparatus

The apparatus was tested for symmetry with a dilute solution of fluorescein. After correction for volume change, the scattered intensity was constant to $\pm 1\%$. Negligible background scattering was found with toluene and acetone. The photomultiplier response to vertically polarized light was only 1.2% higher than that to horizontally polarized light. No correction was made for this small effect.

The calibration for each cell was carried out with Ludox suspension in 0.05 M aqueous NaCl (13). The spectrophotometric turbidity was determined with a Beckman DU spectrophotometer using 10 cm. cells. The calibration was checked by measuring the excess turbidity of a 0.50% solution of Cornell standard polystyrene in toluene. The value found was 3.26×10^{-3} cm.$^{-1}$ which is in good agreement with the National Bureau of Standards value (24) of 3.30×10^{-3} cm.$^{-1}$. The Rayleigh ratio of redistilled and filtered benzene was found to be 49.6×10^{-6} cm.$^{-1}$, also in good agreement with the Maron and Lou (26) value of 49.7×10^{-6} cm.$^{-1}$.

Measurements

Five or six solutions of decreasing concentration were prepared by diluting aliquot portions of the stock

solution, the preparation of which has been described above. Each solution in its cell was centrifuged in a Spinco model L ultracentrifuge at about 55,000 g for 30 minutes using the swinging bucket rotor, No. SW25.1. After light-scattering measurements, concentrations were determined by evaporation of 5 cc. of solution from each cell to dryness under vacuum to constant weight.

The angular variation of scattered intensity was measured from θ of 30° to 135° as soon after centrifugation as possible. Solvent scattering was always measured and, at each angle, subtracted from that of the solution to give the scattering due to the solute alone. The scattering intensity, i_θ, was expressed as the ratio of the galvanometer readings for the scattered light and the transmitted beam. This procedure eliminated errors due to lamp intensity fluctuation, photocell fatigue and attenuation of the incident beam by scattering or absorption.

The Rayleigh ratio, R_θ, was obtained from i_θ by means of the relationship:

$$R_\theta = \frac{3}{16\pi} \cdot C \cdot \left(\frac{n_s}{n_w}\right)^2 \cdot i_\theta \cdot \frac{\sin \theta}{1 + \cos^2 \theta} \cdot \quad \dots \quad (4)$$

the derivation of which is given in greater detail in Appendix IV. Here C is the calibration constant, $\left(\frac{n_s}{n_w}\right)^2$ is a refraction

correction factor (14) in which n_s is the refractive index of solvent and n_w that of water. Multiplication by the factor $\dfrac{\sin \theta}{1 + \cos^2 \theta}$ yields the vertically polarized component normalized to constant scattering volume.

The effect of depolarization and fluorescence of CTN solution on scattered intensity has been shown to be negligible (18). No correction was, therefore, made for these effects.

After the manner of Zimm (46), Kc/R_θ was plotted against $\sin^2 \theta/2 + kc$ when a grid-like plot as shown in Fig. 5 was obtained; k is a convenient constant and K is given by $K = 2\pi^2 n_s^2 (dn/dc)^2 / N \lambda^4$, where dn/dc is the refractive index increment, N is the Avogadro number and λ, the wave length (4358 Å) of light _in vacuo_.

The lines at $\theta = 0$ and $c = 0$ produced by multiple extrapolation were themselves extrapolated to give a common intercept,

$$\left(Kc/R_\theta\right)_{\substack{c=0\\\theta=0}},$$

the reciprocal of which gives the weight-average molecular weight, M_w. The z-average radius of gyration, $\sqrt{\overline{s^2}_z}$, was obtained from the initial slope of the $c = 0$ line by means of the expression

Fig. 5

Zimm plot of light-scattering data
for fraction M-2 in acetone.
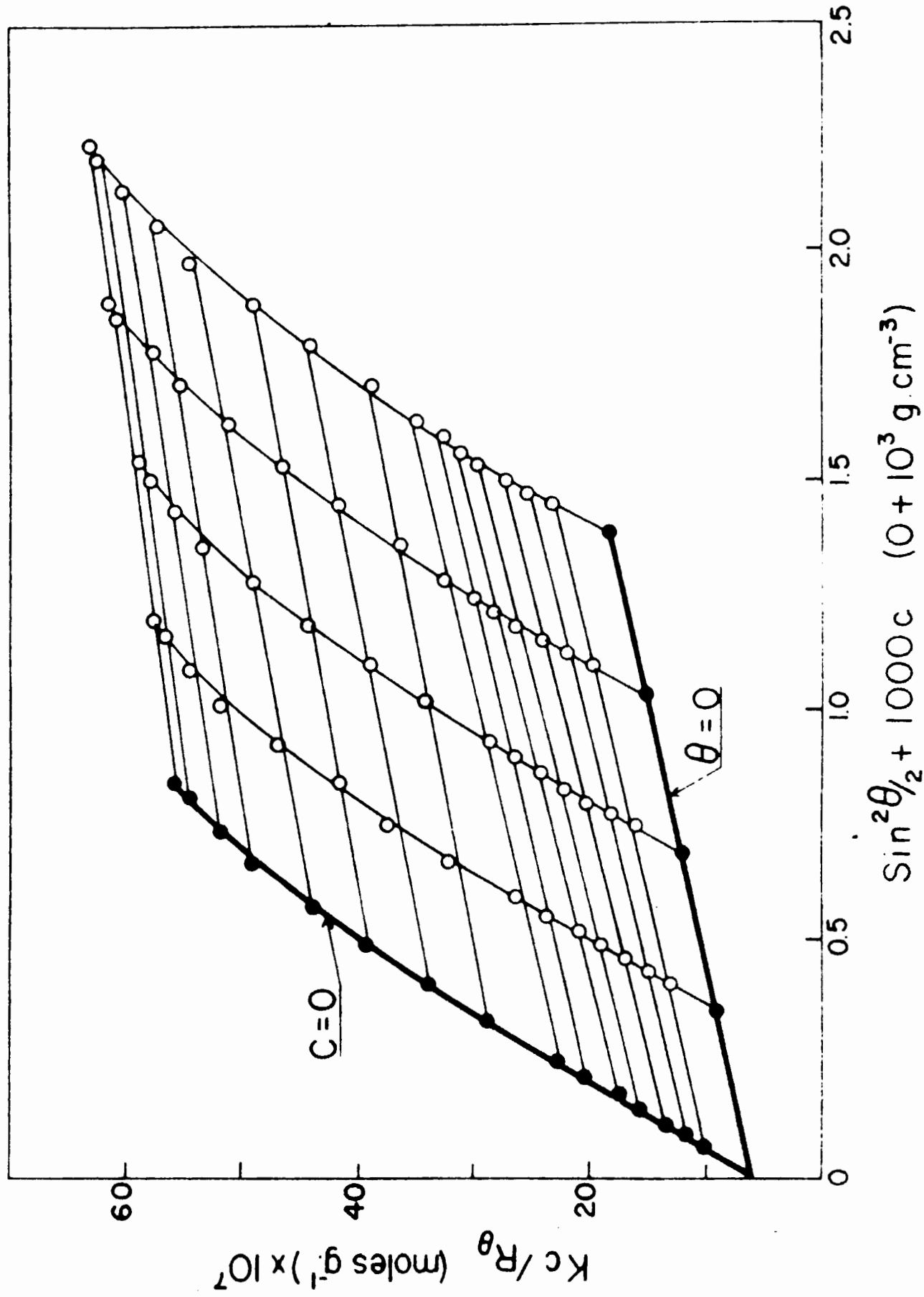
$$\frac{\text{Initial slope}}{\text{Intercept}} = \frac{16\pi^2}{3} \cdot \overline{s}_z^2 \cdot (n/\lambda)^2 \qquad \cdots (5)$$

where n is the refractive index of the solution.

The concentration dependence of the intensity can be written as

$$Kc/R_\theta = \frac{1}{MP(\theta)} + 2A_2 c \qquad \cdots (6)$$

where $P(\theta) = \dfrac{R_\theta^o}{R_\theta} \cdot R_\theta^o$ is the Rayleigh ratio if there were no intraparticle interference. A_2 is the second virial coefficient and is computed from the slope of the $(Kc/R_\theta)_{\theta=0}$ vs. c line in the Zimm plot (46).

Further details of the development of light-scattering techniques are given in Appendix IV.

REFRACTIVE INDEX MEASUREMENTS

The increment of refractive index $\dfrac{dn}{dc}$ of the solution over that of the solvent was measured by means of a Brice-Phoenix differential refractometer for $\lambda = 4358\ \overset{o}{A}$ at 25°C. The instrument was calibrated with sucrose solutions of different concentrations using sodium light ($\lambda = 5890\ \overset{o}{A}$). The calibration was checked by measurement of $\triangle n$ for a 4% aqueous KCl solution. The measured value was within 0.4% of the value calculated from data obtained from the International Critical Tables.

RESULTS

RESULTS

The experimental results are described in several sections. The results of aggregation experiments are described first, followed by a short section on capillary adsorption. Light-scattering and viscosity data on all samples are presented next. Finally, an account is given of certain anomalous observations made during light-scattering measurements.

Aggregation

The possibility of irreversible aggregation on repeating cycles of dissolution, recovery by drying or precipitation and re-dissolving, of CTN was checked by measuring the light-scattering dissymmetry. The presence of aggregates would give rise to a marked increase in the dissymmetry during each cycle.

A sample of bleached ramie nitrate was studied in acetone and ethyl acetate solutions. The procedure for both solvents was identical and is described below.

An approximately 0.2% solution was made by shaking the vacuum-dried solid for 24 hours with the solvent. This was centrifuged at 500 g for 20 minutes to remove any

undissolved material. The light-scattering dissymmetry,

$i_{45^{\circ}}/i_{135^{\circ}}$, was measured and concentration determined by the method previously described. The remaining

solution was then evaporated to dryness in a vacuum-evaporator at about 25°C. The vacuum-dried CTN was then redissolved

and the dissymmetry and concentration were measured without

further centrifugation.

As shown in Table IV, there was no increase in dis-

symmetry in either solvent after drying and redissolving.

This proved absence of significant aggregate formation.

Similar results were obtained in another experiment

in acetone solution where the solid was precipitated out by

adding water, instead of being evaporated to dryness.

Anomalous Viscosity Behaviour at Low Concentration

Marked upward curvature of the graph of $\frac{\eta_{sp}}{c}$ vs. c

was observed at very low concentration of CTN in ethyl

acetate. An example of this behaviour is given in Fig. 6.

The deviation from linearity of the $\frac{\eta_{sp}}{c}$ vs. c graph has also

been observed in the case of other polymers (34, 41) at low

concentration. The effect is probably a spurious one arising

from a small decrease in capillary diameter due to an adsorbed

TABLE IV

Results of Aggregation Experiments

	Acetone		Ethyl Acetate	
	Before drying	After drying and re-dissolving	Before drying	After drying and re-dissolving
$c(\text{g.dl.}^{-1})$	0.1935	0.2075	0.1850	0.2015
$i_{45°}/i_{135°}$	2.11	2.19	2.20	2.20

Fig. 6

Reduced viscosity vs. concentration
for fraction H-2 in ethyl acetate at
very low concentrations.

$\dfrac{\eta_{sp}}{C}$ (dl. g⁻¹)

85

75

65

C (g . dL⁻¹)

0.005

0.010

0.015
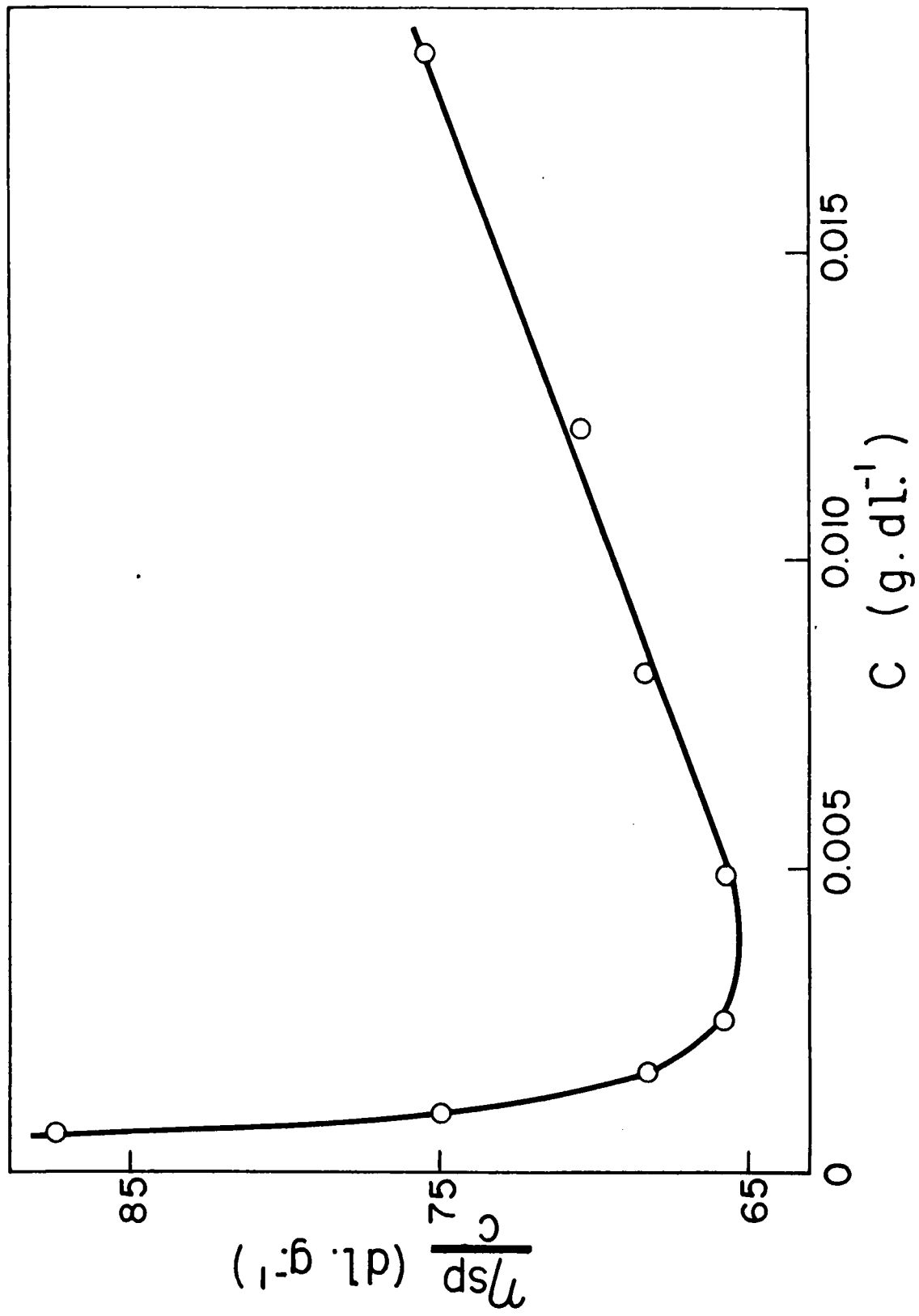
layer of polymer on the walls of the capillary. It was perceptible at low concentrations when the time of flow for the solution was only a few seconds greater than for the pure solvent.

In measuring viscosities the effect was avoided by working with a viscometer of comparatively wide capillary and at concentrations at which the effect was negligible.

An experiment in this connection is described in Appendix III.

Viscosity and Light-scattering

The experimental results from viscosity and light-scattering measurements are listed in two tables. Table V contains the results in acetone solution while the contents of Table VI are for ethyl acetate solutions. The quantities given for each sample are the weight average molecular weight, $\overline{M}_w$, z-average root-mean-square radius of gyration, $\sqrt{\overline{s^2}}_z$, the second virial coefficient, A_2, the intrinsic viscosity, $[\eta]_{500}$ and the Huggins' interaction constant k'_{500}. The data which were reduced to yield these results are given in Appendices VII and VIII.

In order to derive the configurational parameters

TABLE V

Results of Viscosity and Light-scattering Measurements
in Acetone

Sample	$[\eta]_{500}$	k'_{500}	$M_w \times 10^{-5}$	$\sqrt{\overline{s^2}}_z$	$A_2 \times 10^4$
	dl.g.$^{-1}$			$\overset{\circ}{A}$	mole cc. g.$^{-2}$
T-8	12.1	0.83	6.5	869	7.3
T-6	15.6	0.95	8.4	958	7.4
M-3	18.9	0.62	9.9	1060	3.2
P	20.5	0.55	11.4	1150	4.1
M	22.1	0.52	15.3	1440	4.9
M-2	26.0	0.56	16.9	1480	4.6
M-1	36.8 *44.7*	0.33	22.8	1610	3.8
H	43.4 *52.5*	0.39	23.8	1670	5.1
H-2	43.6	0.41	25.0	1730	3.8

TABLE VI

Results of Viscosity and Light-scattering Measurements in
Ethyl Acetate

Sample	$[\eta]_{500}$ dl.g^{-1}	k'_{500}	$\bar{M}_w \times 10^{-5}$	$\sqrt{\overline{s^2}_z}$ Å	$A_2 \times 10^4$ mole cc. g.$^{-2}$	$[\eta]_0$ dl.g.$^{-1}$
T-8	16.9	0.58	6.8	972	7.3	16.9
T-6	20.4	0.74	7.8	1097	7.8	20.4
M-3	24.6	0.52	9.8	1430	3.1	24.6
P	-	-	-	-	-	-
M	32.4	0.50	16.1	1520	6.6	32.9
M-2	32.8	0.55	15.9	1630	4.4	34.4
M-1	44.6	0.35	23.2	2100	4.8	46.5
H	-	-	-	-	-	-
H-2	58.6	0.27	25.0	2190	3.6	61.3

from the light-scattering data, certain assumptions as to the molecular weight distribution were necessary since polydispersity is inevitable even in carefully fractionated material (15, 18). A suitable distribution is one in which the z-average, weight average and number average molecular weights, represented respectively by $\overline{M}_z$, $\overline{M}_w$ and $\overline{M}_n$, are related in the proportion 3:2:1. Such a distribution has been used by others (15, 46) and was assumed by Hunt et al (18) for their high molecular weight samples. This proportionality will be assumed in computing $\overline{M}_z$ and $\overline{M}_n$ from the values of $\overline{M}_w$ obtained from light scattering.

The initial concentrations of solutions employed for light-scattering measurements varied from 0.12 to 0.35 g./$_{100}$ cc. depending on the molecular weight. At the lowest concentration the solvent scattering intensity was 50 percent of the scattering intensity from solution. The initial concentration range in viscometry was 0.035 to 0.085 g./$_{100}$ cc. depending on the molecular weight. The lowest concentration in viscometric measurements were a fifth or sixth of the initial concentration.

The refractive index increment, dn/dc, at 25°C used for the calculation of K were 0.104 cc. g^{-1} and 0.105 cc. g^{-1}

for ethyl acetate and acetone solution respectively. These were the mean values from solutions of bleached and unbleached (raw) ramie nitrate. The corresponding K values were 1.85 x 10^7 and 1.84 x 10^7 respectively for ethyl acetate and acetone.

Shear Dependence of Viscosity

Shear dependence of intrinsic viscosity in the range of rate of shear between 300 and 700 sec.$^{-1}$ was estimated. For the complete range of molecular weight studied $\left[\eta\right]$ was found to be independent of G in acetone solution over the range of shear rates mentioned. A typical plot of $\frac{\eta_{sp}}{c}$ vs. c for different G is shown in Fig. 7.

In ethyl acetate solution, on the other hand, $\left[\eta\right]$ showed slight dependence on the rate of shear for the higher molecular weight samples. An example is shown in Fig. 8, where the values for H-2 have been plotted. The magnitude of the dependence decreased with decreasing molecular weight and below $\left[\eta\right] = 30$ the dependence was no longer observed. Similar results for the shear dependence in ethyl acetate solution was obtained by Timell (42).

In those cases where such dependence was noticed, $\left[\eta\right]$ values at different G were linearly related to the rate

Fig. 7

Reduced viscosity vs. concentration
for fraction H-2 in acetone at different
rates of shear.
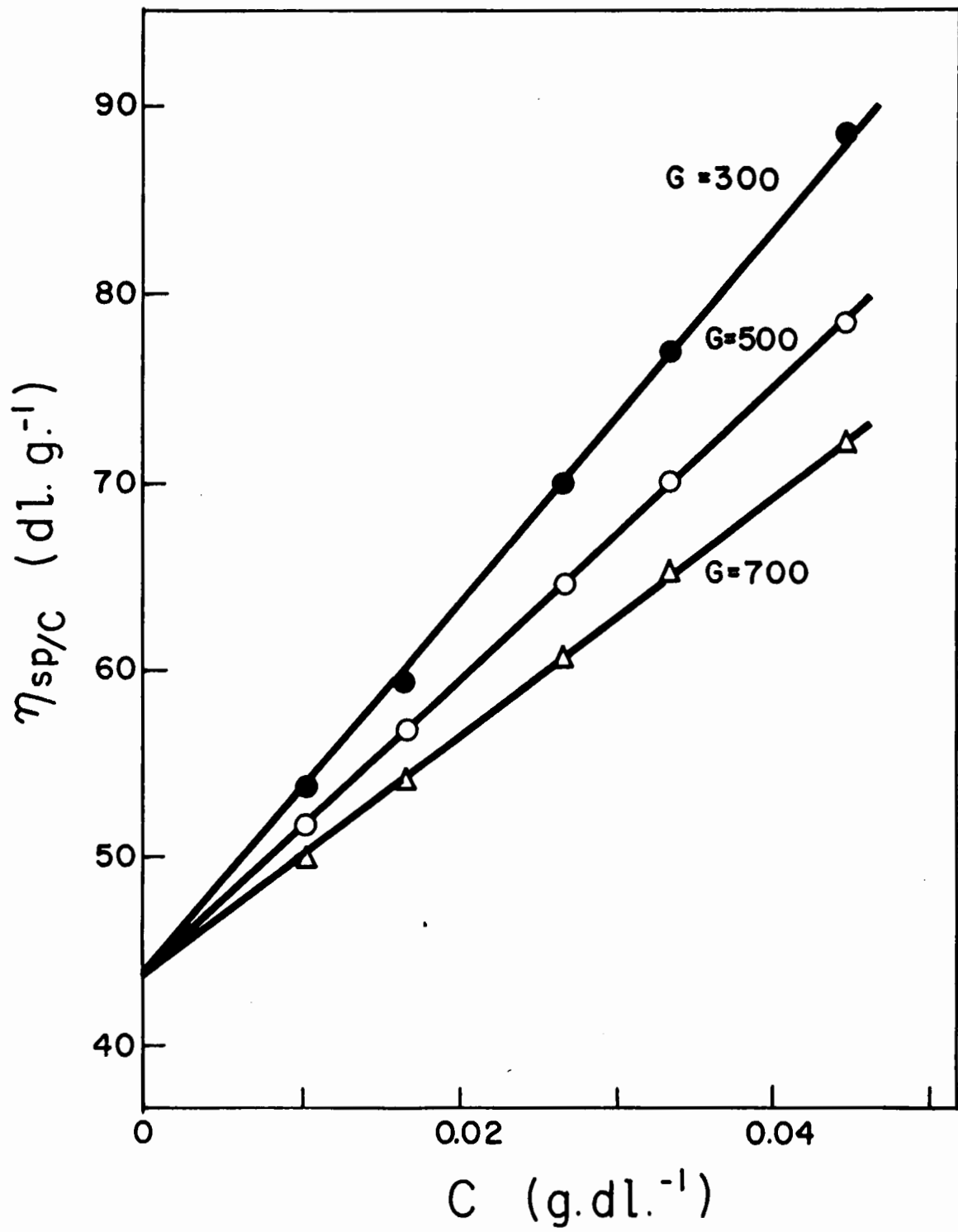
Fig. 8

Reduced viscosity vs. concentration
for fraction H-2 in ethyl acetate at
different rates of shear.
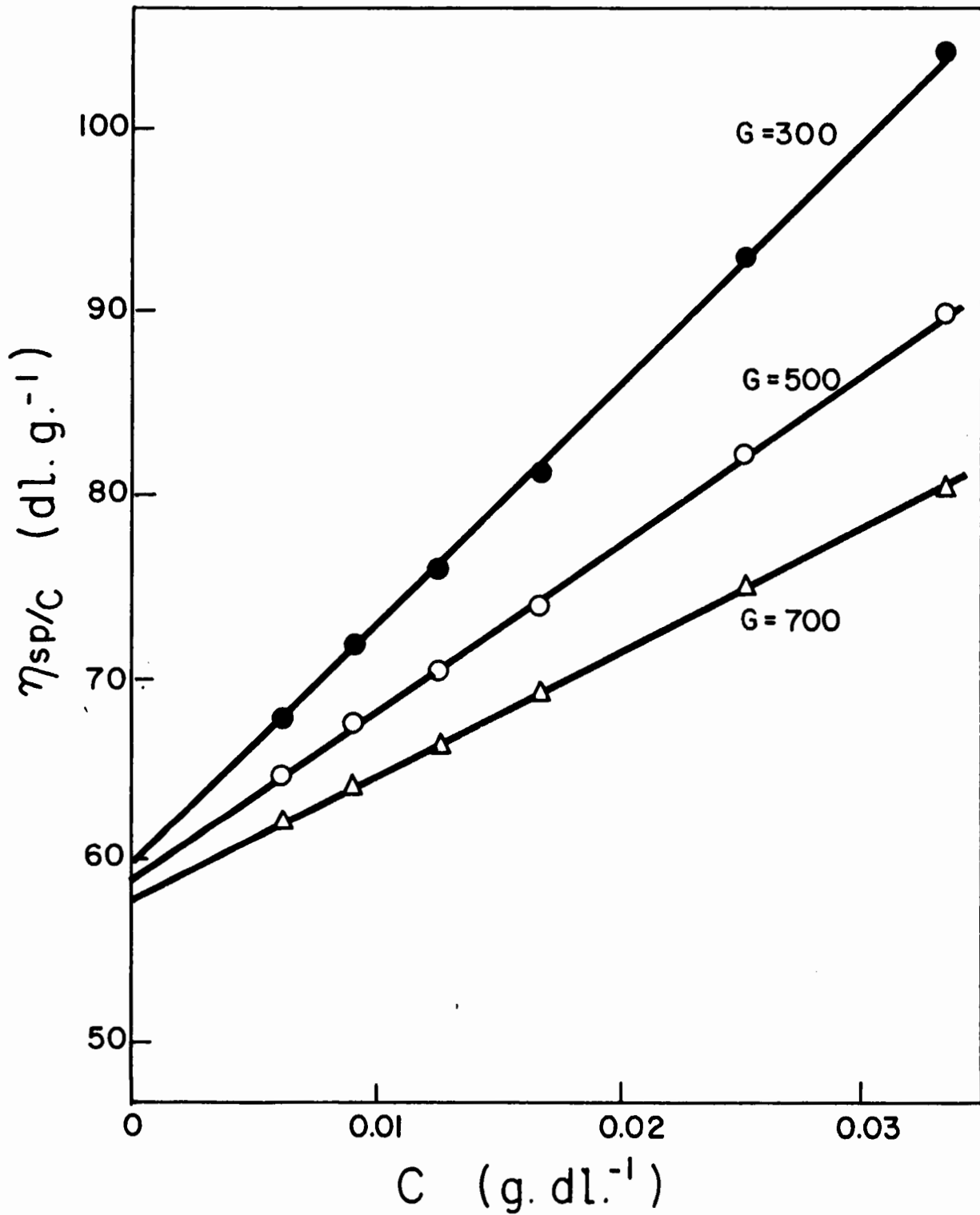
Fig. 9

Intrinsic viscosity vs. rate of shear
for samples M, M-1, M-2 and H-2 in
ethyl acetate.
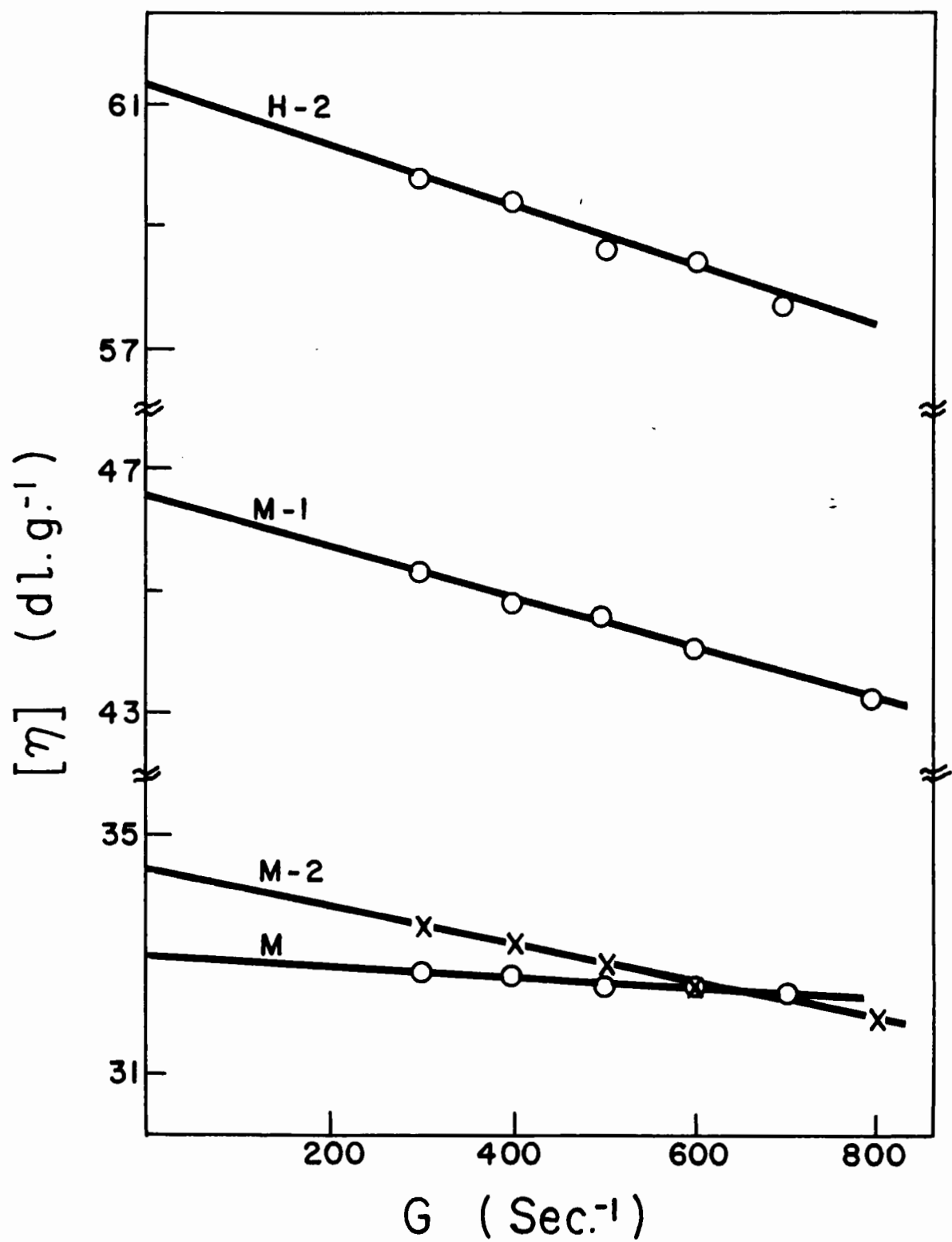
of shear. Fig. 9 shows the variation of $[\eta]$ with G for samples M, M-2, M-1 and H-2. Extrapolation of these lines gave values of the intrinsic viscosity at zero rate of shear, $[\eta]_o$ which have been included in Table VI.

These results show a small or no dependence of $[\eta]$ on G in the range of shear studied. As clearly shown in Figs. 6 and 7 marked shear dependence of $\dfrac{\eta_{sp}}{c}$ occurs at finite concentration. This shear dependence is probably not related to an intrinsic property of the molecule but is due to molecular interaction which will increase as concentration increases. A similar result has been noted recently by Nawab (30) for suspensions of model filaments. In the present work the reservation must be made that the range of shear was somewhat narrow and a more marked variation of $[\eta]$ with G may have been detected if measurements were made at much lower shear rates.

Anomalous Light-scattering

Early in the work it was noted that the graph of Kc/R_θ vs. $\sin^2 \theta/2 + kc$ at $\theta = 0$ curved downwards after a certain concentration was reached. Fig. 10 is a Zimm plot showing this effect. Such deviation from linearity was found in all the samples. The concentration, c_c, at which

Fig. 10

Zimm plot of light-scattering data for
fraction M-1 in acetone showing deviation
from linearity of $(Kc/R_\theta)_{\theta=0}$ vs c line at
high concentration.
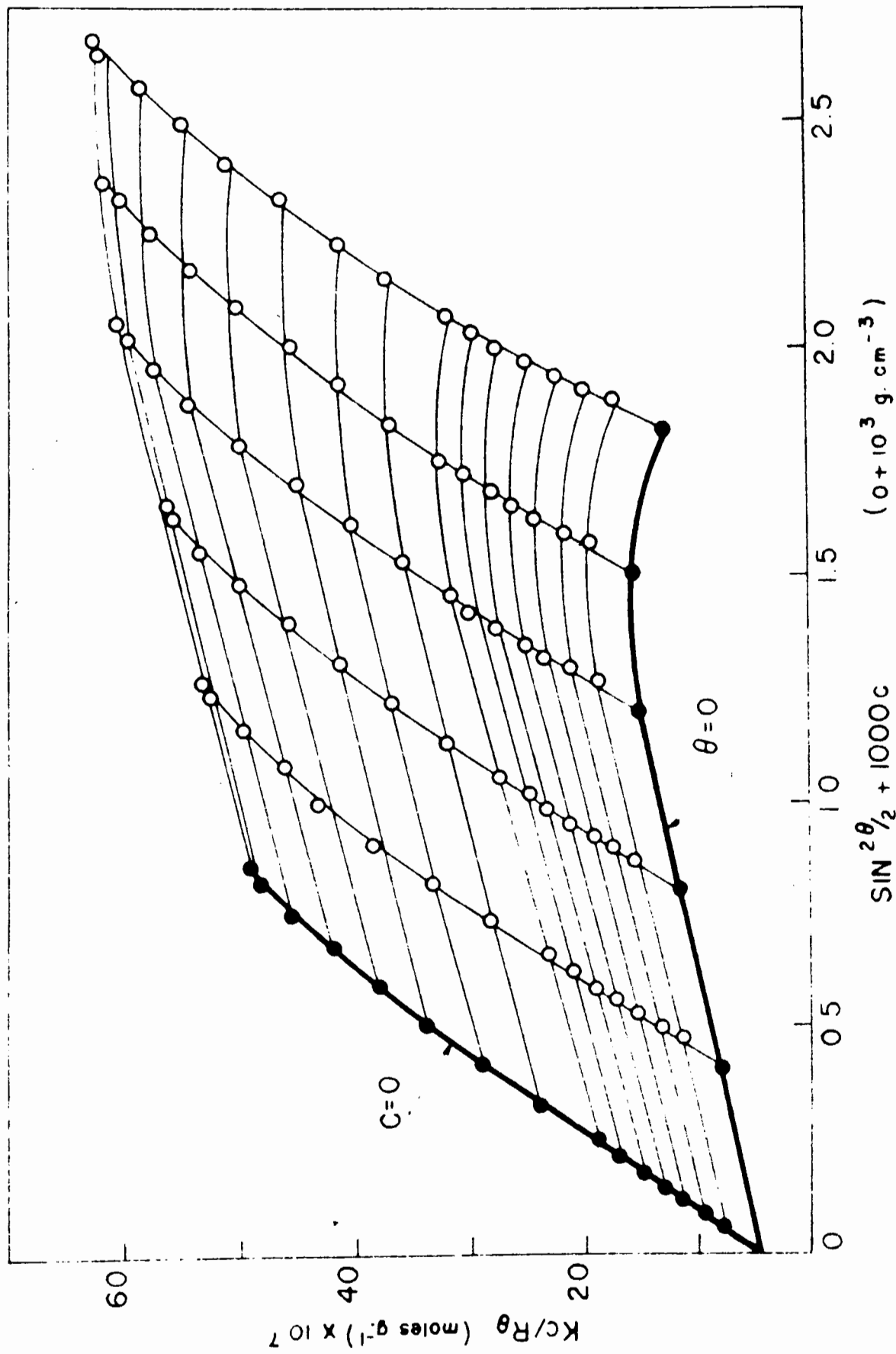
the curvature started $^{\#}$ depended on the molecular weight; c_c decreased approximately linearly with increasing molecular weight, as shown in Figs. 11 and 12 for acetone and ethyl acetate respectively. The curvature started at such low concentration in the case of the very high molecular weight fraction H-1 in acetone solution that extrapolation was impossible. The effect was also observed in solutions which were centrifuged for one hour or more instead of the usual 30 minutes. Thus the effect could not be caused by the presence of any debris-like material.

At about the same concentration at which the deviation from linearity of Zimm plots occurred, a curious optical phenomenon was noted. If the solution was centrifuged for 30 minutes at 55,000 g, placed in the light-scattering apparatus and the scattered beam observed in a mirror held at low angles, quite clear vertical striations, i.e. vertical bands of scattering substance could be seen. They were observed in nearly all samples provided that the concentration was sufficiently high.

$^{\#}$It would have been preferable to use the concentration at which $(Kc/R_\theta)_{\theta=0}$ attained a maximum value. It was not possible to obtain this point in all cases and, therefore, the critical concentration was taken to be the point at which a clear deviation from linearity was detected.

Fig. 11

Critical concentration vs. molecular
weight of the samples in acetone.
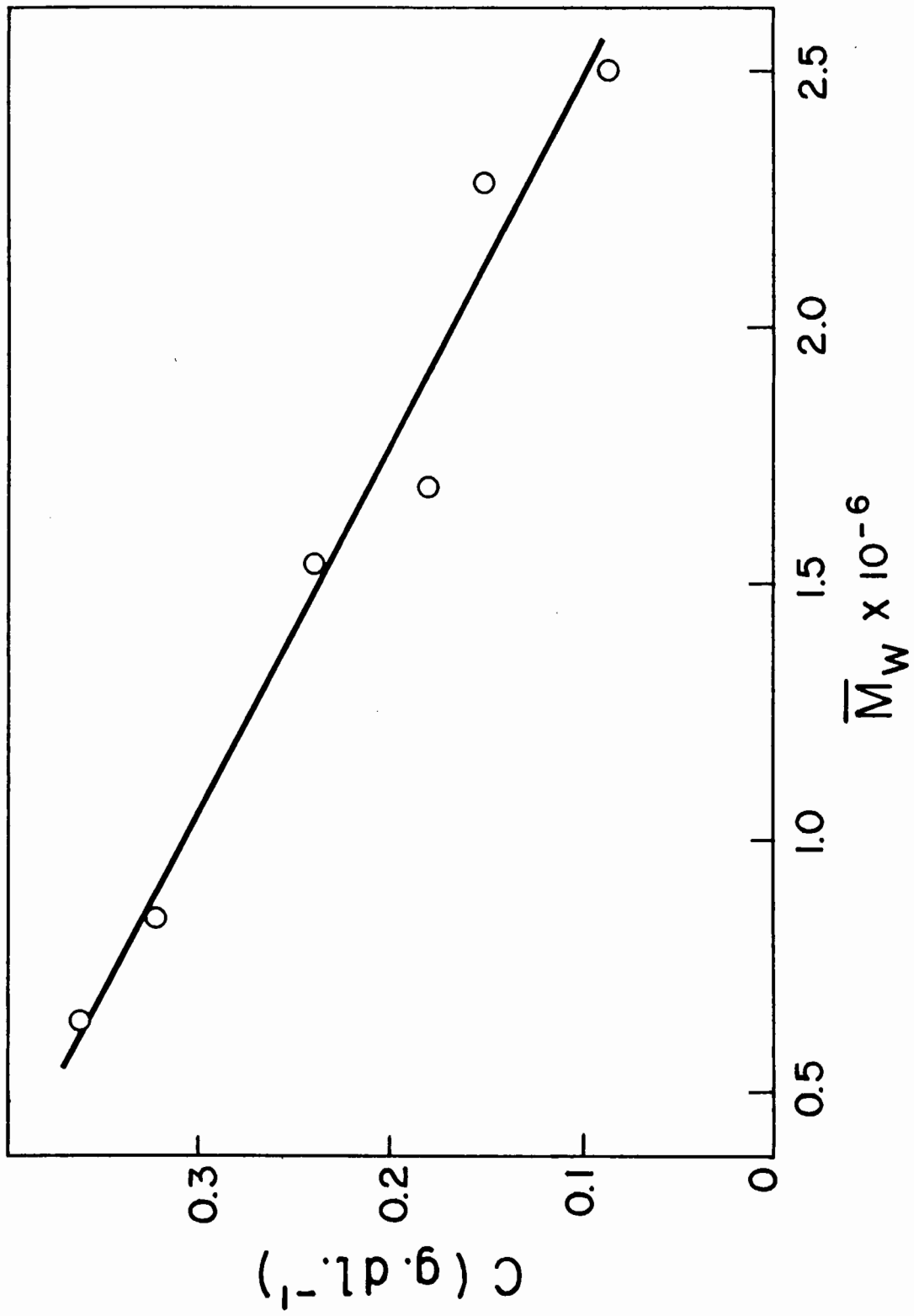
Fig. 12

Critical concentration vs. molecular
weight of the samples in ethyl acetate.
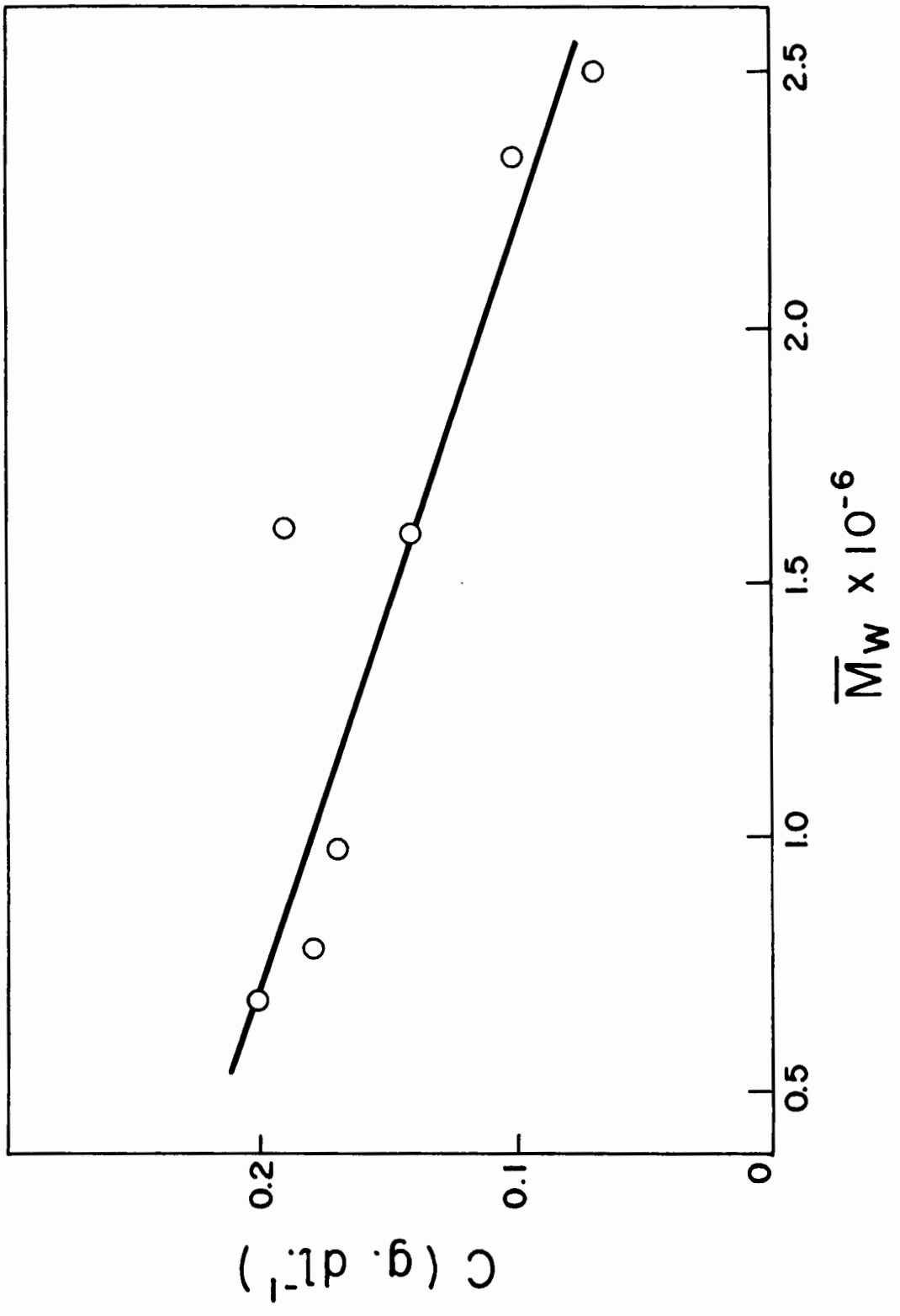
Striations occurred only on high speed centrifugation. No striation could be seen in a fresh, uncentrifuged solution. Thus the phenomenon was associated in some way with conditions produced by ultracentrifugation. If a centrifuged solution was allowed to stand, the striations gradually disappeared over a period of several hours, indicating that the process responsible for their production was reversible. In some solutions the discontinuities were not stationary but appeared to drift gradually.

The effect of striations on the scattering intensity was relatively small. A variation of intensity by about $\pm 5\%$ was found in successive measurements. No clear trend of increase or decrease in scattering intensity was noted on standing. Also, the polarization of the transmitted or scattered light was unaffected.

If the effect were due to the presence of gross aggregates, prolonged centrifugation should cause it to disappear. However, striations were observed in a sample centrifuged at 55,000 g for 5 hours. It was also possible that the discontinuities were caused by the mixing of a clear layer of solvent left by sedimentation at the top of the cell or at the conical walls. Experiments described in Appendix V proved that this was not the case.

A further possible cause could be an orientation of the molecules in the high fields used. If the CTN molecules possessed an intrinsic asymmetry in specific volume along the chain, it might orient on sedimentation and produce a micellar structure in which regions of varying refractive index would appear. Such orientation might be expected to produce an increase in the sedimentation constant with increase in the centrifugal field. No such increase was, in fact, detected. Sedimentation constants measured at 38,900 g and 259,000 g were equal within ±0.7%.

Experiments were carried out to test whether striations were associated with incipient gel-formation in the centrifuged solution. Small glass spheres were allowed to fall through the solution and attempts were made to detect irregularities in the sedimentation velocity of the spheres. Inadequate optics and the difficulty of eliminating thermal currents rendered the results inconclusive.

Greater details of these experiments are given in Appendix V and the possible causes of striations and the deviation from linearity of the Zimm plot are discussed further in a later section.

DISCUSSION

Variation of Radius of Gyration with Molecular Weight

The radius of gyration is a characteristic dimension
of the molecule in solution and, as expected, increased
with increasing molecular weight. (Tables V and VI). Also
for a given sample, $\sqrt{\overline{s^2}}$ was higher in ethyl acetate than
in acetone indicating greater extension in the former solvent.

In both solvents the relationship between $\overline{s^2_z}$ and
$\overline{M}_z$ was approximately linear as shown in Figs. 13 and 14. In
acetone the line passes through the origin and is expressed
by the equation

$$\overline{s^2_z} = 0.79 \text{ x } \overline{M}_z \qquad\qquad \ldots\ldots \text{ (6)}$$

For ethyl acetate the relationship is

$$\overline{s^2_z} = 1.33 \ \overline{M}_z - 3.55 \qquad\qquad \ldots\ldots \text{ (7)}$$

If the data for CTN in ethyl acetate obtained by Hunt et al.
(18) are included in Fig. 14, it is seen that below a mole-
cular weight of about 800,000 the graph curves towards the
origin. Similarly in Fig. 13 the data of Holtzer et al. (15)

Fig. 13

Z-average mean-square radius
of gyration vs. z-average mole-
cular weight of the CTN samples
in acetone.

        ○ - Present Work

        Χ - Holtzer et al. (15)

Fig. 14

Z-average mean-square radius of gyration vs. z-average molecular weight of the CTN samples in ethyl acetate.

○ - Present Work

χ - Hunt et al.(18)
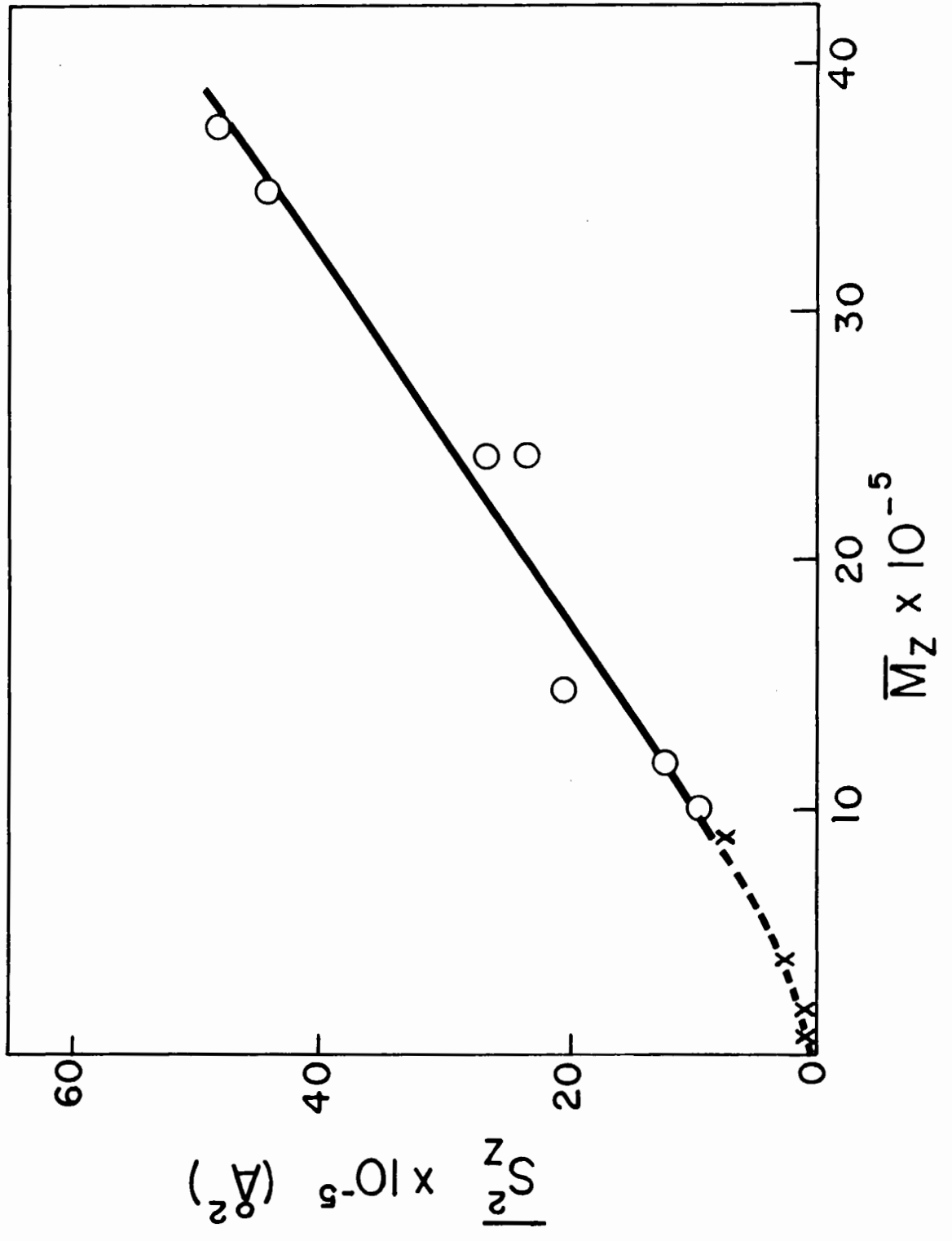
suggest a breakdown in the linearity at low molecular weight. Recently Notley and Debye (33) have noted a similar trend in the relationship between molecular dimensions and weights of polystyrene.

Configurational Change with Molecular Weight

The deviation from linearity in Figs. 13 and 14 could be expected if a transition to non-Gaussian behaviour occurred at low molecular weight. Such configurational changes have been treated theoretically by Benoit and Doty (4) in terms of a stiffness parameter, the persistence length, q. The persistence length was defined originally by Porod and Kratky (21, 38) as the mean value of the projection of an infinitely long chain along the direction of the first element in the chain. The expression deduced by Benoit and Doty is

$$\overline{s^2}_o = q^2 \left[\frac{x}{3} - 1 + \frac{2}{x} - 2(1-e^{-x})/x^2 \right] \quad \ldots \ldots (8)$$

where $\sqrt{\overline{s^2}_o}$ is the unperturbed radius of gyration (described later) and x is the number of units of length q in the fully extended molecule. The value of x is given by

$$x = \frac{r_{max}}{q} = \frac{D.P. \times \text{length of one monomer unit}}{q}$$

$$= \frac{\overline{M}}{M_o} \cdot \frac{\text{length of one monomer unit}}{q} \qquad \dots \dots (9)$$

r_{max} being the length of the fully extended chain. The length of one monomer unit was taken as 5.15 $\overset{o}{A}$.

For large x (i.e., large $\overline{M}$) Eqn. (8) reduces to

$$\frac{\overline{s_o^2}}{r_{max}} = \frac{q}{3} \qquad \dots \dots (10)$$

which is equivalent to constancy of $\overline{s_o^2}/\overline{M}$ for the Gaussian coil condition. For smaller x, the other terms significantly decrease the value of $\overline{s_o^2}/\overline{M}$ indicating an approach to the rod-like configuration.

After the manner of Hunt et al. (18), the experimentally determined values of $(\overline{s_o^2})_z/\overline{M}_z$ may be plotted against $\overline{M}_z$ and compared with the theoretical curve deduced from Eqn. (8). The unperturbed radius of gyration was obtained from the relationship

$$\sqrt{\overline{s_z^2}} = \propto \sqrt{(\overline{s_o^2})_z} \qquad \dots \dots (11)$$

where the expansion factor, α, was calculated from the second virial coefficient by the method of Orofino and Flory (35). As found by Hunt et al. for CTN in ethyl acetate, α was near to unity for all samples in both solvents (1.03 - 1.09) and showed a very slight increase with increasing molecular weight. The persistence length, q, required in Eqn. (8), was calculated by means of Eqn. (10), from $(\overline{s_0^2})_z$ and $\overline{M}_z$ for the two highest molecular weight samples. Averages of the values of q were 115 $\overset{o}{A}$ and 200 $\overset{o}{A}$ in acetone and ethyl acetate respectively. Hunt et al. (18) used a q value of 117 $\overset{o}{A}$ derived from the data on their three highest molecular weight samples.

In Figs 15 and 16, $(\overline{s_0^2})_z / \overline{M}_z$ is plotted against $\overline{M}_z$ for acetone and ethyl acetate respectively. Values of $(\overline{s_0^2})_z$ and $\overline{M}_z$ are given in Table VII. The data of Holtzer et al. (15) for CTN in acetone are included in Fig. 15 and the data of Hunt et al. (18) for CTN in ethyl acetate are included in Fig. 16.

As predicted by theory, the combined data in both cases show increase of $(\overline{s_0^2})_z / \overline{M}_z$ with $\overline{M}_z$. In the case of acetone, the results from the present investigation lie in the region of constant $(\overline{s_0^2})_z / \overline{M}_z$ while at lower molecular

Fig. 15

Dependence of $(\overline{s_o^2})_{z/\overline{M}_z}$ on $\overline{M}_z$ for
the CTN samples in acetone. The
solid curve is the theoretical one
based on Eqn. (8). The broken curve
is for a hypothetical helical configu-
ration of CTN in solution.

● — Present Work

○ — Holtzer et al. (15)
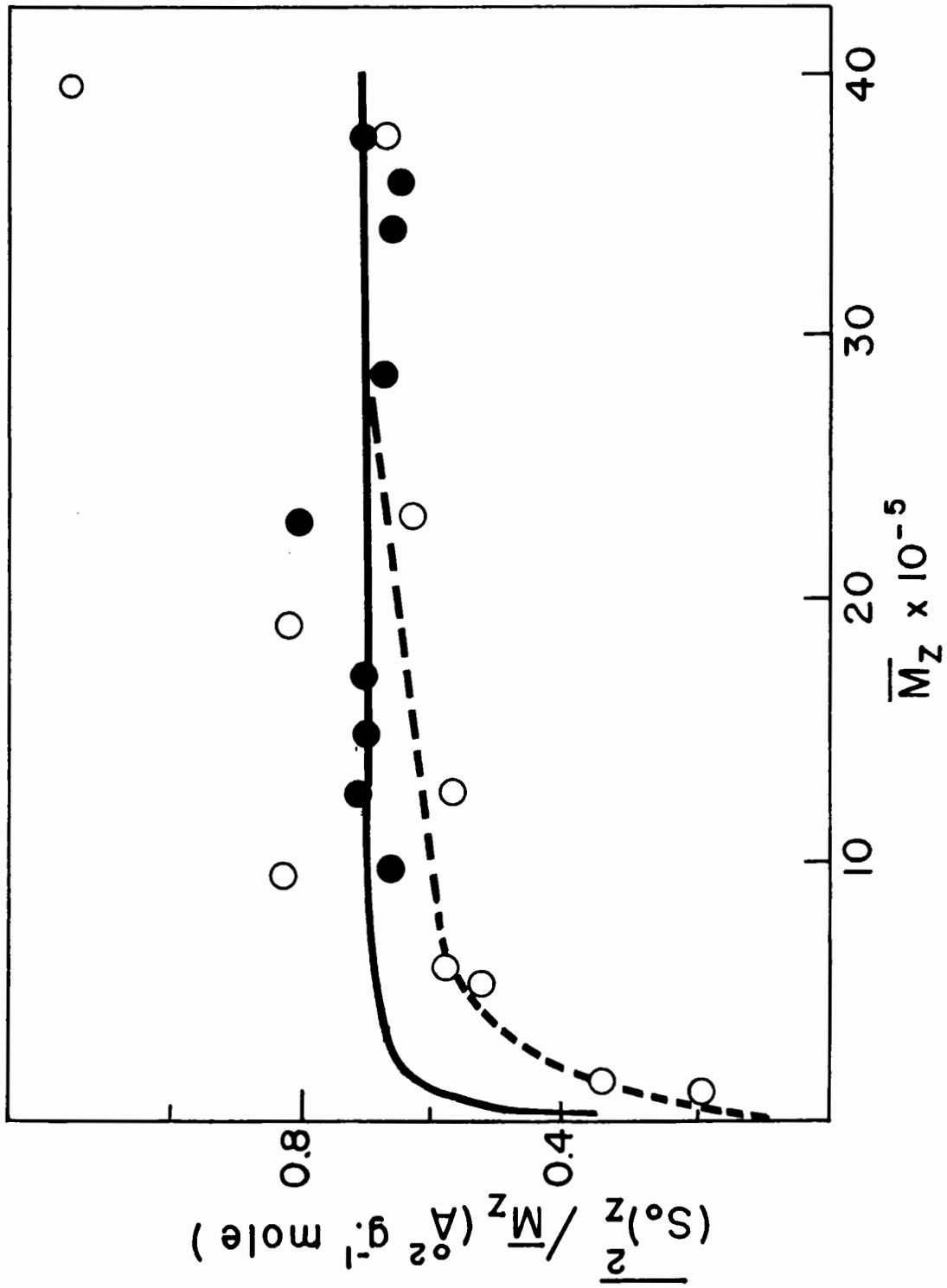
Fig. 16

Dependence of $(\overline{s_o^2})_{z}/\overline{M}_z$ on $\overline{M}_z$ for CTN
samples in ethyl acetate. The upper
solid curve is the theoretical one based
on Eqn. (8). The broken curve is for a
hypothetical helical configuration of
CTN in solution. The solid curve H is
the one proposed by Hunt et al. (18).

● - Present Work

○ - Hunt et al. (18)
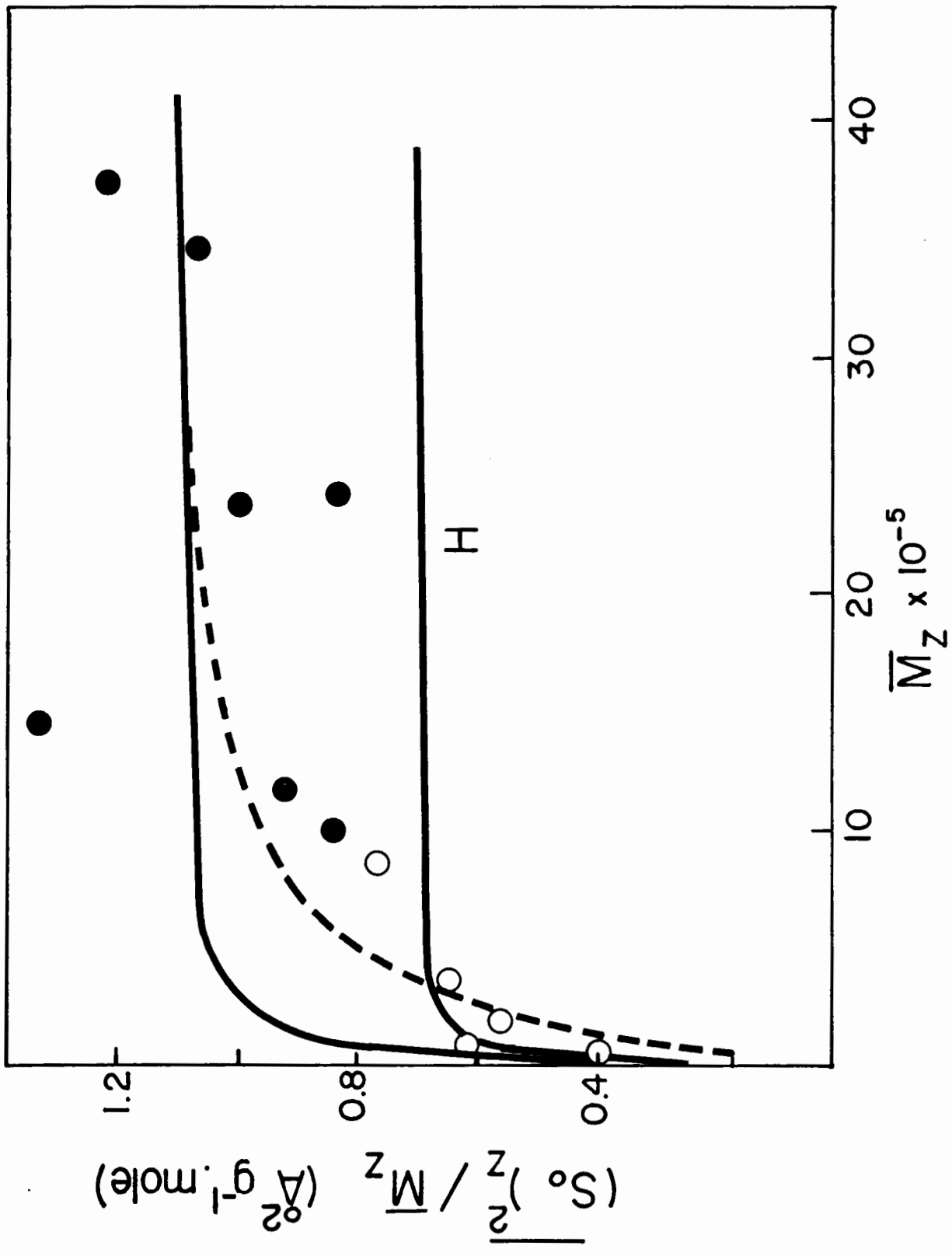
ERRATA

Page 47   Eqn.(6); read 0.80 for 0.79

Page 55   Table VII; column 2, row 6; read 2.54 for 2.86

TABLE VII

Molecular and Hydrodynamic Parameters

Sample	In Acetone			In Ethyl Acetate		
	$\bar{M}_z \times 10^{-6}$	$\overline{(s_o^2)}_z \times 10^{-6}$ $\overset{o}{A}{}^2$	$\Phi' \times 10^{-22}$	$\bar{M}_z \times 10^{-6}$	$\overline{(s_o^2)}_z \times 10^{-6}$ $\overset{o}{A}{}^2$	$\Phi' \times 10^{-22}$
T-8	0.98	0.66	2.34	1.01	0.85	2.95
T-6	1.26	0.80	2.90	1.17	1.08	2.83
M-3	1.49	1.04	3.05	1.47	1.98	1.96
P	1.71	1.21	2.97	-	-	-
M	2.30	1.85	2.21	2.42	2.01	3.52
M-2	2.86	1.93	2.62	2.39	2.47	2.86
M-1	3.42	2.27	3.91	3.48	4.07	2.64
H	3.57	2.32	4.32	-	-	-
H-2	3.75	2.63	4.11	3.75	4.59	3.28

weight the data of Holtzer et al. (15) show decrease in

$(\overline{s_0^2})_{z/\overline{M}_z}$. Their results indicated that at $\overline{M}_z$ values above
10^6 the molecule behaves like a Gaussian coil.
For ethyl acetate, except for one point, $(\overline{s_0^2})_{z/\overline{M}_z}$ increases
with $\overline{M}_z$ over the complete range of molecular weights.
This suggests that in the molecular weight range studied,
CTN does not attain the random coil configuration in ethyl
acetate. Curve H in Fig. 16 is the theoretical one given
by Hunt et al. which is based on a persistence length of
117 Å computed from the results for their three highest
molecular weight samples. The points from the present in-
vestigation are well above their theoretical line. This
discrepancy indicates that Hunt et al. (18) did not use a
high enough value of $\overline{M}_z$ in computing q. It must also be
noted that because of increasing trend of $(\overline{s_0^2})_{z/\overline{M}_z}$ with $\overline{M}_z$,
the value of q computed for samples M-1 and H-2 may
also be erroneously low.

The higher value of the persistence length in ethyl

acetate was unexpected since, to a first approximation, q

must depend only on orientation and steric factors in the

chain itself. It is possible, however, that the greater

solvation in ethyl acetate may cause an added inflexibility

due to more extensive packing of solvent molecules around the

polymer in the better solvent.

As shown in Figs. 15 and 16 the transition from rod-like to a coiled molecule appears too abrupt in the theoretical curves computed from Eqn. (8) when compared with the experimental data. It is interesting to note that a helical or spiral arrangement of the chain in solution would yield better agreement with experiment. For a large enough molecule, a flexible helix would assume a random coil configuration except that the extended length of the helix would be less than $r_{max.}$ by a factor depending on the pitch. If the length of the coiled helix is assumed to be 2/5 times the length of the fully extended molecule[#], the persistence length becomes $\frac{5}{2}$ q and the broken curves in Figs. 15 and 16 are obtained, which show better agreement with experimental points in the low and intermediate molecular weight region. This cannot be regarded as proof of a spiral configuration for CTN, although it is noteworthy that a helical arrangement has been proposed for the chemically similar polysaccharide, amylose (37, 39).

Variation of Intrinsic Viscosity with Molecular Weight

The intrinsic viscosity is a measure of the effective hydrodynamic volume of a solute and, as expected, $\left[\eta\right]_{500}$

[#]The arbitrary value, 2/5, was obtained by trial and error. The plot was sensitive to small changes in this factor.

TABLE VIII

Values of $\underline{a}$ and K

Investigator	Solvent	Range of M x 10^{-4}	Method	$G(sec.^{-1})$ for $[\eta]$	$\underline{a}$	K	Ref.
Holtzer et al.	Acetone	7.7-264	Light scattering	0	0.99	1.73×10^{-5}	15
#Holtzer et al.	"	64-264	"	0	0.91	5.37×10^{-5}	15
##Present	"	65-250	"	500	0.91	5.96×10^{-5}	
Newman et al.	Ethyl acetate	9.3-150	Ultra-centrifuge	500	0.99	4.82×10^{-5}	32
Hunt et al.	"	4.1-57.3	Light scattering	0	1.01	2.50×10^{-5}	18
Present	"	68-250	"	500	0.83	2.60×10^{-4}	
Present	"	68-250	"	0	0.86	1.66×10^{-4}	

a and K values derived from the six highest molecular weight sample.
The standard error in $\underline{a}$ was $0._{08}$ in all cases.

increased with $\overline{M}_W$. The values of the constants K and a in Eqn. (1) were obtained from plots of log $[\eta]_{500}$ vs. log $\overline{M}_W$ shown in Figs. 17 and 18 respectively for acetone and ethyl acetate solutions. The values are given in Table VIII along with the more recent values obtained by other workers. If $[\eta]_o$ at G=0 (obtained as described previously) is used a increases from 0.83 to 0.86 in ethyl acetate. Similar adjustment leaves a unchanged for acetone solutions since $[\eta]$ was found to be independent of G.

The intrinsic viscosity of CTN has been shown to vary considerably with small changes in the nitrogen content of the sample (25, 45). The intrinsic viscosity was corrected by the method of Lindsley and Frank (25) to a hypothetical value, $[\eta]^T$ corresponding to 14.14% nitrogen. The results are shown in Table IX. $[\eta]^T$ is considerably higher than the corresponding $[\eta]$ value given in Tables V and VI. Plots of log $[\eta]^T_{500}$ vs. log $\overline{M}_W$ yield a = 0.77 in ethyl acetate and a = 0.87 in acetone. With $[\eta]_o^T$ (i.e., $[\eta]^T$ at zero rate of shear) the value of a becomes 0.82 in ethyl acetate.

As mentioned in the Introduction, the value of a is influenced by two factors: (i) the configuration of the molecule and (ii) its permeability to solvent. Any increase in

Fig. 17

Log of intrinsic viscosity at a rate of shear of 500 sec.$^{-1}$ vs. log of molecular weight for the samples in acetone.
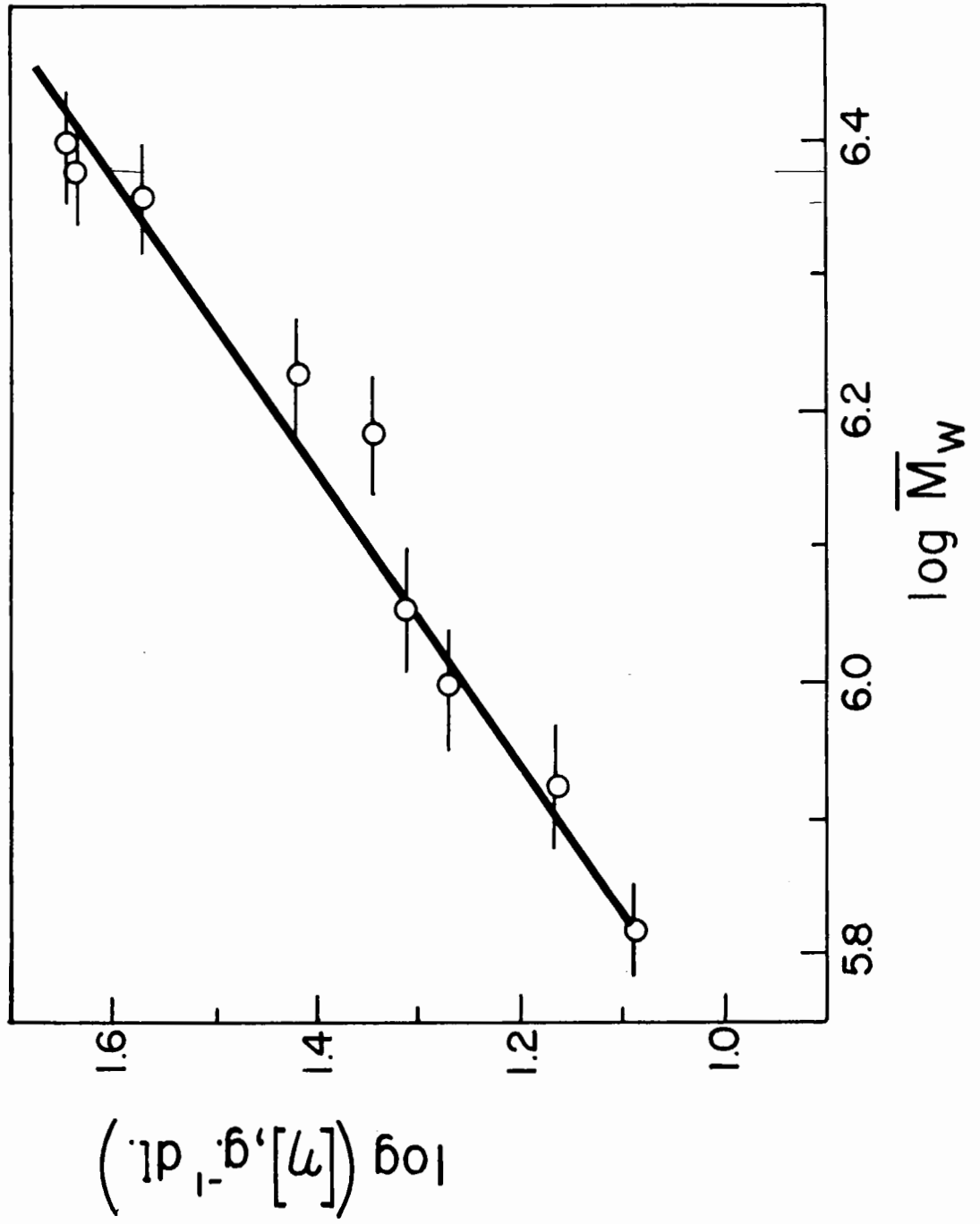
Fig. 18

Log of intrinsic viscosity of the samples
in ethyl acetate at a rate of shear of
500 sec.$^{-1}$ vs. molecular weight.
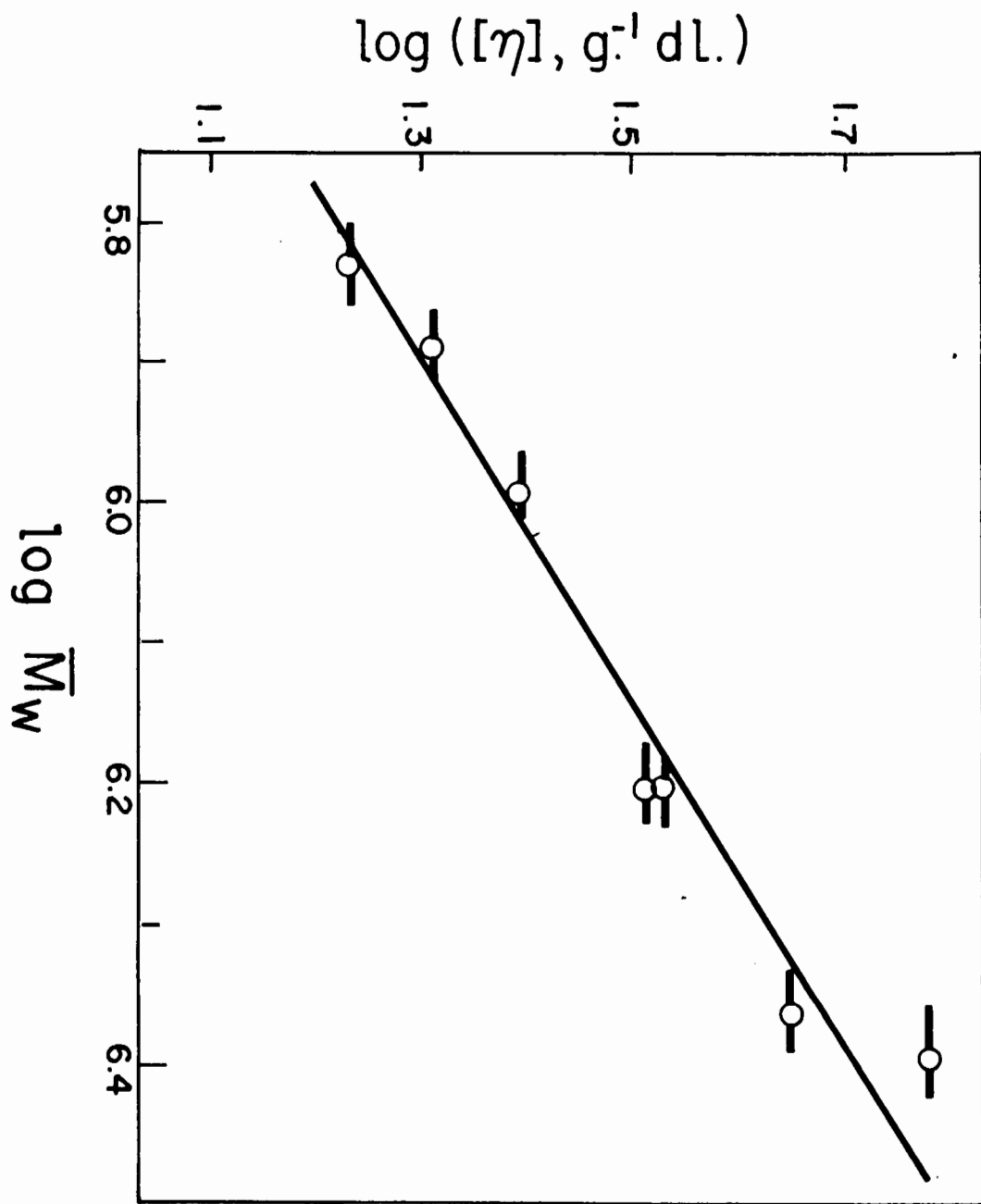
TABLE IX

Values of Intrinsic Viscosities after

Correction for Nitrogen Content

Sample	In Acetone $[\eta]_{500}^T$ dl.g.$^{-1}$	In Ethyl Acetate $[\eta]_{500}^T$ dl.g.$^{-1}$	$[\eta]_o^T$ dl.g.$^{-1}$	% Nitrogen
T-8	14.5	20.3	20.3	13.58
T-6	18.7	24.4	24.4	13.58
M-3	20.9	27.2	27.2	13.84
P	23.4	-	-	13.74
M	24.6	36.1	36.7	13.81
M-2	28.8	36.3	40.1	13.83
M-1	40.4	49.0	51.1	13.85
H	50.4	-	-	13.68
H-2	49.4	66.5	69.5	13.76

molecular extension would cause an increase in $\underline{a}$ whereas a change from the free-draining to the solvated (solvent immobilizing) state would cause $\underline{a}$ to decrease.

As shown in Table VIII, $\underline{a}$ was lower than unity in both solvents in contrast to the results of Holtzer $\underline{\text{et al.}}$ (15), Hunt $\underline{\text{et al.}}$ (16) and Newman $\underline{\text{et al.}}$ (32). The lower value of $\underline{a}$ in the high molecular weight range is in conformity with the expectation of Hunt $\underline{\text{et al.}}$ (18). Also, it is supported by the agreement between the present data and those for the six highest molecular weight samples of Holtzer $\underline{\text{et}}$ $\underline{\text{al.}}$ (15). Further, the low value of $\underline{a}$ is accentuated by the correction of the $\left[\eta\right]$ values for variation in nitrogen content. Thus the data supports in a general way the assumption of a more coiled configuration at high molecular weights as demonstrated by the light-scattering results.

Within experimental error $\underline{a}$ was equal in both acetone and ethyl acetate in the molecular weight range studied. This applies to the work of others (15, 18, 32) as well and is contrary to the behaviour of other polymers (e.g., polystyrene (3)) in good and bad solvents. This seeming anomaly may be due to the increased solvation in the good solvent which will decrease $\underline{a}$ by contributing to the solvent

immobilizing character and compensating for extension effects. The low a in ethyl acetate may also be related to the configurational behaviour discussed above. The data in Figs. 15 and 16 show that, while the configuration in acetone was constant in the present range, it changed continuously in ethyl acetate. For ethyl acetate, therefore, it is unlikely that the value of the exponent can be assigned with certainty to any model and a should remain an empirical quantity determined for various ranges of $\overline{M}$.

The Hydrodynamic Parameter Φ

It was of interest to compute the universal hydrodynamic parameter Φ introduced by Flory (47). Following the notations of Hunt et al. (18) the intrinsic viscosity may be related to the chain dimensions by the equation

$$\left[\eta \right] = \Phi' (\overline{s_0^2}/\overline{M})^{3/2} \overline{M}^{\frac{1}{2}} \propto^3 \qquad \dots\dots (12)$$

The prime is appended to Φ to indicate use of the radius of gyration instead of the end-to-end distance as customarily used (47). Values of Φ' for CTN in both solvents are given in Table VII. The detailed calculation of Φ' is described in Appendix VI.

As shown in Table VII, Φ' increases with molecular
weight in acetone. This is contrary to the conclusion of
Holtzer, Benoit and Doty (15) whose results suggested that
Φ' is constant. In ethyl acetate, on the other hand, Φ' is
seen to be virtually constant with a mean value of 2.86 (±0.33)
x 10^{22} which is close to the constant experimental value of
3.2 x 10^{22} obtained for the synthetic polymers.

The data can be further analyzed if Eqn. (12) is
written as

$$\Phi' = k \left[\eta\right] \overline{M}_{z} / (\overline{s_z^2})^{3/2} \qquad \ldots\ldots (13)$$

or

$$\Phi' = k. \frac{1}{\overline{s_z^2}/\overline{M}_z} . \left[\eta\right]/\sqrt{\overline{s_z^2}} \qquad \ldots\ldots (14)$$

where k is a constant for each solvent derived after the
manner of Hunt et al (18) and depends on the polydispersity
(See Appendix VI). For a random coil $\overline{s_z^2}/\overline{M}_z$ is constant
($\propto$ is taken as unity) according to Benoit and Doty (4) and
Hunt et al (18). Also, Kunst (48) has shown that $\left[\eta\right]$ is
directly proportional to $\sqrt{\overline{s_z^2}}$ for polyisobutylene in dif-
ferent solvents. Similar direct proportionality between
$\left[\eta\right]$ and $\sqrt{\overline{s_z^2}}$ can be derived from results on polystyrene
(49), polymethyl methacrylate (50) and polyvinyl acetate (51)

Fig. 19

Ratio of intrinsic viscosity to
root-mean-square z-average radius
of gyration vs. intrinsic viscosity
in acetone and ethyl acetate.

● - Ethyl Acetate

○ - Acetone

Figure with axes: horizontal axis labeled $[\eta]$ $(dl.g^{-1})$ with values 10, 20, 30, 40, 50, 60; vertical axis labeled $\dfrac{[\eta]}{\sqrt{\overline{S_Z^2}}}$ $(100\ cm^2\ g^{-1}) \times 10^{-6}$ with values 1.5, 2.0, 2.5.
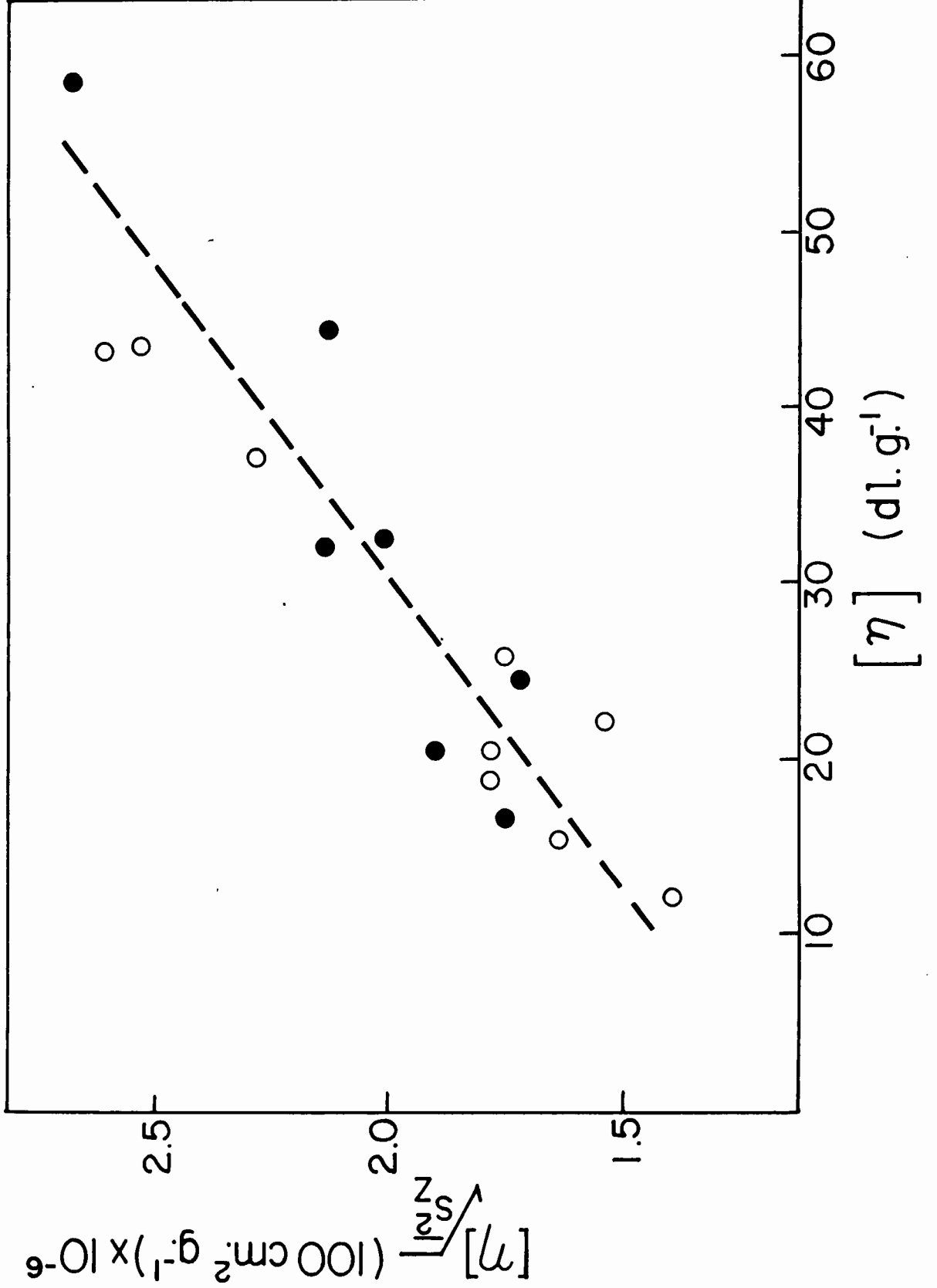
all of which have been shown to obey random flight statistics. Therefore, Φ' is constant for these polymers. In the case of CTN $[\eta]/\sqrt{\overline{s^2}_z}$ increases with intrinsic viscosity in ethyl acetate and acetone in the range investigated, as shown in Fig. 19. Since $\overline{s^2}_z/\overline{M}_z$ is constant in acetone Φ' will increase with increasing $\overline{M}$; whereas the increase of $\overline{s^2}_z/\overline{M}_z$ with $\overline{M}$ in ethyl acetate apparently just compensates the increase in $[\eta]/\sqrt{\overline{s^2}_z}$ leaving Φ' constant. The change of $[\eta]/\sqrt{\overline{s^2}_z}$ might be expected in ethyl acetate for which a configurational transition occurs throughout the range studied. In acetone, however, the light-scattering data suggest that a random coil configuration was attained. The increase of $[\eta]/\sqrt{\overline{s^2}_z}$ may, therefore be related to a decreasing degree of free-draining as the molecular weight increases.

Interaction Constants

The Huggins' interaction constant, k', is essentially an empirical quantity, but its value has been used as an indication of molecular branching (δ). It was, therefore, of interest to consider the variation of k' for change of solvent and shear rate. A typical set of results is shown in Table X. The value of k' is higher in the poor solvent, acetone, which is in agreement with the findings of Alfrey

TABLE X

Huggins' Interaction Constant, k', for Fraction H-2

in Two Solvents at Different Shear Rates

G (sec.$^{-1}$)	Acetone	Ethyl Acetate
300	0.514	0.366
400	0.450	0.310
500	0.407	0.274
600	0.364	0.232
700	0.330	0.206

et al. (1) for polymethyl methacrylate in different solvents. It may also be noted that k' decreases with increasing rate of shear, in agreement with the results of Masson and Goring (27) on carrageenin - a polygalactose sulphate - and Conrad et al.(6) on cellulose in cuprammonium and cupriethylenediamine. In consideration of the dependence of k' on such variables as solvent and rate of shear, one has to be cautious in using k' as a criterion for detecting branching, especially in the case of solutions showing non-Newtonian viscosity behaviour.

The variation of k'_{500} and A_2, the second virial coefficient in light scattering, with molecular weight is shown in Fig. 20 for both solvents. The graphs are irregular, but there is a significant decrease in k'_{500} with increase in $\overline{M}$ for both solvents. This is contrary to Huggins' (17) suggestion that it should be independent of molecular weight. Similar dependence of k'_{500} on molecular weight was found by Timell (43) for CTN in ethyl acetate and Alfrey et al. (1) for polymethylmethacrylate in different solvents.

The second virial coefficient, A_2, for a polymer-solvent system should decrease slowly with increasing molecular weight. For the same polymer the value of A_2 is

Fig. 20

The second virial coefficient, A_2, and
the Huggins' interaction constant, k',
vs. molecular weight of the samples in
acetone and ethyl acetate. Nitrogen
content of the samples have also been
included in the graph.

● – Ethyl Acetate

○ – Acetone

Χ – Nitrogen Content
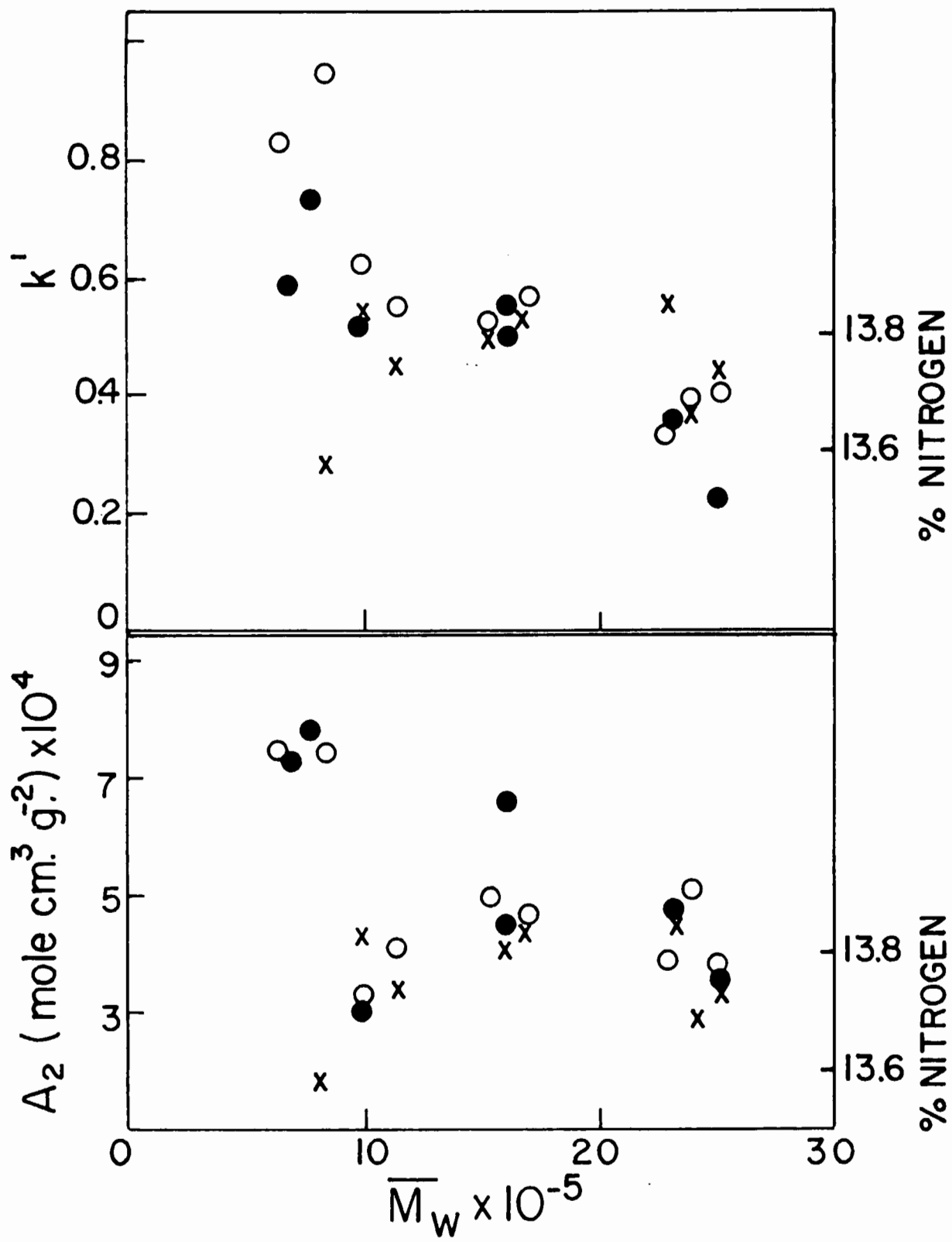
dependent on the nature of the solvent, being higher in a
good solvent. These two general characteristics of A_2 which
have been observed in the case of other polymers are not
found for CTN solutions. Holtzer et al. (15) found negligible
and irregular change of A_2 with molecular weight. In ethyl
acetate for low molecular weight fractions, Hunt et al. (18)
obtained values of A_2 which were practically the same as
found by Holtzer et al. except the lowest molecular weight
sample for which the value was slightly higher. In the pre-
sent investigation, values of A_2 were found to be the same,
within experimental error, in both solvents; a slight de-
crease in A_2 with increase of $\overline{M}_w$ can, however, be detected.

An obvious feature of Fig. 20 is the irregularity of
the data. Similar irregular results for the Huggins' constant
have been reported by other workers (1, 6, 43). Irregularities
in both k'_{500} and A_2 show the same trend in the two different
solvents, indicating that this behaviour is due to some in-
trinsic properties of the samples rather than to experimental
error. The nitrogen contents of the samples have been in-
cluded in Fig. 20. Except for two points, there is a rough
correlation between the nitrogen content and the eccentricities
in k'_{500} (19) and A_2. A more detailed study would be required
to elucidate more clearly the source of these irregularities.

DISCUSSION

Light-scattering Anomalies

As shown in the results, the light-scattering function, Kc/R_θ decreased with increase of c above a certain concentration which increased with decrease of molecular weight. Similar downward curvature of the $\theta = 0$ line of the Zimm plot was noted by Holtzer et al. (15) for their two highest molecular weight samples. The authors attributed this to possible experimental error. However, the consistency and regularity of the effect in the present study indicated that its cause is not trivial but is related to some fundamental property of the solution.

The phenomenon suggests the existence of a critical concentration above which the particle size increases. Such an increase could be due to an association-dissociation equilibrium, association being favoured by higher concentration.

It is possible that the critical concentration is related to the concentration at which the molecules form a close-packed array with molecular domains touching each other. Parent and Rinfret (36) suggested the existence of a critical concentration from discontinuities in heats of mixing measurements of polyvinyl acetate in methanol and s-tetrachloroethane.

Recently Cragg and Bigelow (7) came to similar conclusions from viscosity measurements of polymer-polymer-solvent systems.

Approximate calculations of the close-packing of molecular domains were computed from molecular dimensions derived in two ways:

a) The radius of an equivalent sphere was derived from the root-mean-square number average radius of gyration.

b) The radius of the equivalent Einstein sphere was calculated from the value of $[\eta]$.

The theoretical concentration of close-packing, c_a and c_b respectively from (a) and (b), are compared in Table XI with the experimentally determined critical concentration c_c. Evidently, in both solvents, c_c is considerably greater than c_a or c_b for the range of molecular weights studied. This suggests that considerable interpenetration of the chains must take place before the association reaction can occur to any extent. Such interpenetration might be quite possible in the case of cellulose nitrate because of the pronounced extension of the chain.

The phenomenon of striations seemed to be related to the downward curvature of the Zimm plot because it occurred in approximately the same region of concentration. A somewhat

TABLE XI

Calculated and Measured Critical Concentrations

Number-average molecular weight	Acetone			Ethyl Acetate		
	Calculated		Measured	Calculated		Measured
	c_a	c_b	c_c	c_a	c_b	c_c
0.33×10^6	0.035	0.155	0.36	0.026	0.111	0.20
1.25×10^6	0.017	0.043	0.08_5	0.008	0.032	0.07

Concentration in g./100 cc.

74

analogous observation was described as a "stippled" appearance in the light-scattering beam by Holtzer et al. who found the effect to disappear on prolonged centrifugation. These authors attributed this to the presence of aggregation.

In the present investigation, this phenomenon was observed in all samples. The experiments described earlier showed that its cause was probably not trivial, i.e., it was not caused by convection currents set up due to concentration or temperature gradients. The constancy of sedimentation constant over a wide range of centrifugal field suggested that molecular orientation did not occur. This was also supported by the absence of perceptible depolarization in the transmitted beam in the presence of striations.

Another possible cause was incipient gelation caused by the high compression experienced by the solution during ultracentrifugation. This might produce macroscopic regions of slightly different refractive index which could give the observed effect. However, no indication could be found in the literature supporting the occurrence of gelation with pressure. The sedimentation experiments with falling beads were designed to test this idea; for reasons given in an earlier section, preliminary results of these experiments were inconclusive.

An elucidation of the anomalous light-scattering
might also be reached by an analogy with the macroscopic
behaviour of cellulose fibre in suspension. When fibres
in suspension are allowed to sediment, flocculation takes
place due to mechanical entanglement induced by differential
sedimentation (12). The degree of flocculation depends,
among other factors, on the axis ratio and the concentration
of the fibres. A fully extended CTN molecule has a much
greater axis ratio than a cellulose fibre and would, there-
fore, be susceptible to molecular entanglements during sedi-
mentation in a high centrifugal field. Such flocculation,
if extensive, might produce the visible inhomogeneities
and the increase in scattered intensity observed at higher
concentrations.

APPENDICES

APPENDIX I

HISTORICAL REVIEW

HISTORICAL REVIEW

Cellulose nitrate is probably the most important of all cellulose derivatives. Its application in such diverse fields as explosives, lacquers and plastics necessitated solution of many problems, out of which has grown an extensive technical literature on the subject. The elucidation of the structure of cellulose, its recognition as a high-polymeric substance and the development of a method of nitration of cellulose without degradation (8) have aroused renewed interest in the study of cellulose nitrate. The fact that it is easily made in the laboratory and is soluble in many organic solvents facilitates its use in studying the molecular properties of the parent substance cellulose which is either insoluble or unstable in solution in certain special reagents.

Cellulose is known to consist of long chains of β-glucopyranose units joined to each other through 1-4 positions (9). The length of one β-glucopyranose unit in the molecule is 5.15 $\overset{o}{\text{A}}$. In the cellulose molecule there are, for each unit, two secondary and one primary hydroxyl groups. The polymer is, therefore, a polyhydric alcohol and undergoes many typical alcohol reactions such as esterification,

etherification.

Cellulose nitrate has essentially the same skeletal structure as cellulose. It is obtained by nitration of cellulose with various nitrating mixtures. Cellulose can be nitrated to various degrees of substitution. The degree of substitution is defined as the average number of nitrate groups per anhydro-glucose unit.

Nitration of cellulose for technical purposes is carried out mostly with nitric acid-sulphuric acid mixtures. This method of nitration involves degradation of the cellulose and complete nitration cannot be achieved (10). Staudinger and Mohr (10) developed a method of nitration which leads to complete nitration without appreciable degradation. The process, in which nitric acid-phosphoric acid mixture is used for nitration, was later improved by Alexander and Mitchell (8). The solubility and viscosity of cellulose nitrate solution are dependent to a large extent on the degree of nitration (10). In view of this fact, it is necessary to use samples with as high a nitrogen content as possible.

In a sample of cellulose all molecules are not of the same length, i.e., a certain degree of polydispersity

exists (11). Also celluloses obtained from different sources

do not have the same average molecular weight (11). If a

cellulose trinitrate is prepared by a suitably mild nitra-

tion, its molecular properties, deduced by well-known physico-

chemical methods, can be related back to the properties of

the original sample of cellulose. Extensive investigation

of this type has been made by Timell (12, 13) and Conrad

and co-workers (14). However, it is important that funda-

mental properties such as molecular weight or configuration

can be related correctly to observed phenomena such as vis-

cosity or light-scattering. As discussed elsewhere, there

is considerable uncertainty in this respect for high mole-

cular weight cellulose trinitrate.

Several physico-chemical methods are available for

determination of the molecular weight, molecular size and

shape of polymers in solution. These are based on measure-

ments of osmotic pressure, sedimentation and diffusion,

viscosity, streaming double refraction and light-scattering.

Theoretical and practical aspects of these methods are

adequately described in text-books (6, 15, 16). All of

these methods have been employed to gain an insight into

the size and configuration of cellulose nitrate in solution.

Gralen (11) considered cellulose nitrate and cellulose as unsolvated oblong ellipsoids. From sedimentation and diffusion measurements the author calculated the major and minor axes for a number of unfractionated samples. For cellulose nitrates the minor axes for the samples were constant and lower than that for the corresponding celluloses. The author suggested that when the nitrate groups are attached to the cellulose molecule it would be elongated by stretching. This was attributed to the marked dipole character and large volume of the nitrate group which reduced bending between the glucose units.

Earlier, Mosimann (17) compared the axis ratios calculated from sedimentation and diffusion and from streaming double refraction with those obtained by using Burgers' (18) viscosity equation for ellipsoidal particles with axis ratios much greater than unity and showing strong Brownian motion. The values from streaming double refraction were about 25% lower than those from sedimentation measurements. Axis ratios using Burgers' equation were higher than those from the other two methods. Jullander (19) corroborated the latter observation of Mosimann.

Viscosity equations developed by Kuhn (20), Huggins (21, 22), Burgers (18) and Simha (23) for asymmetric

particles showing strong Brownian motion were used by Campbell and Johnson (24) to calculate the axis ratios of cellulose nitrate fractions (12.2% N) of low molecular weight from viscosity measurements. Kuhn and Huggins based their theoretical treatments on rigid, rod-like molecules and rigid, randomly kinked molecules respectively. Burgers and Simha took as their model elongated ellipsoids with axis ratios much greater than unity. Huggins also considered the viscosity of solutions of flexible chains. Campbell and Johnson found good agreement between axis ratios calculated from the equations of Kuhn and Simha but these values differed widely from those calculated from the other equations.

These early investigations were based on models which cannot be expected to correspond to the actual molecules in solution. Besides, the influence of such factors as rate of shear (14) and the nitrogen content (25) on the viscosity was not fully appreciated until recently. The introduction of light-scattering by Debye (26) and its further improvement by Zimm (27) and others (15) for measuring directly the molecular dimensions of long chain polymers, combined with the theoretical developments (28,

29, 30, 31) in understanding the hydrodynamic properties of polymers in solution advanced the study of cellulose trinitrate.

The light-scattering experiments of Badger and Blaker (32) were limited to very low molecular weight samples. The authors, however, showed that cellulose nitrate is relatively stiff compared to the vinyl polymers. Their inferences were, in general, corroborated by the later work of Holtzer et al. (33). Working with fractionated and unfractionated samples of highly nitrated cellulose in acetone solution in a wide range of molecular weight, Holtzer et al. came to the conclusion that the existing hydrodynamic theories were inadequate to explain some of their observations. These authors used a few samples of very high molecular weight (up to 2.64×10^6) but the results for these were treated with considerable reservations because of some anomalous observations during light-scattering measurements. The expected change in the viscosity-molecular weight relationship at high molecular weight (discussed in the Introduction) was not observed by these authors. This is in contrast to the observations of Münster (35) and Badger and Blaker (32).

With a view to exploring the limitations of the existing hydrodynamic theories, Hunt et al.(34) carried out an investigation on the configuration and frictional properties of low molecular weight fractions of cellulose nitrate in ethyl acetate. Their conclusions were similar to those of Holtzer et al. (33). The authors suggested that the disagreement with the theories for their samples arose primarily from severe deviations from random flight statistics at such low molecular weight, and predicted that at high molecular weight better agreement with the theories would be achieved.

In view of this prediction and the conflicting data in the published literature, an investigation of the configurational behaviour of high molecular weight cellulose nitrate was undertaken, the results of which are reported in the present work.

APPENDIX II

THE MULTI-SHEAR VISCOMETER

THE MULTI-SHEAR VISCOMETER

The viscometer is shown in Fig. 1-A. It was of the suspended-level type with a large bulb which permitted dilution in situ. For clarity the horizontal scale of the diagram has been increased. The dimensions of its different parts were so chosen as to allow interpolation of viscosity values to a shear rate of 500 sec.$^{-1}$.

The radius of the capillary was 0.02254 cm. A curved tube, 3 mm. internal diameter, joined the capillary to the bulbs. By this arrangement a hydrostatic head small enough to produce the necessary low rates of shear was obtained. The capillary length was 12 cm. and the volume of the mixing bulb was about 100 cm.^{3}. The volume of the bulbs, the mean hydrostatic head, h_m, for each bulb and efflux times of acetone are given in Table I-A.

The mean head, h_m, was calculated from the relationship

$$h_m = \frac{h_1 - h_2}{\ln h_1/h_2} \qquad \dots \text{(1-A)}$$

where h_1 and h_2 are the distances between the upper and lower marks on each bulb respectively and the lower end of the capillary.

<u>Fig. 1-A</u>

The multi-shear viscometer

CAPILLARY
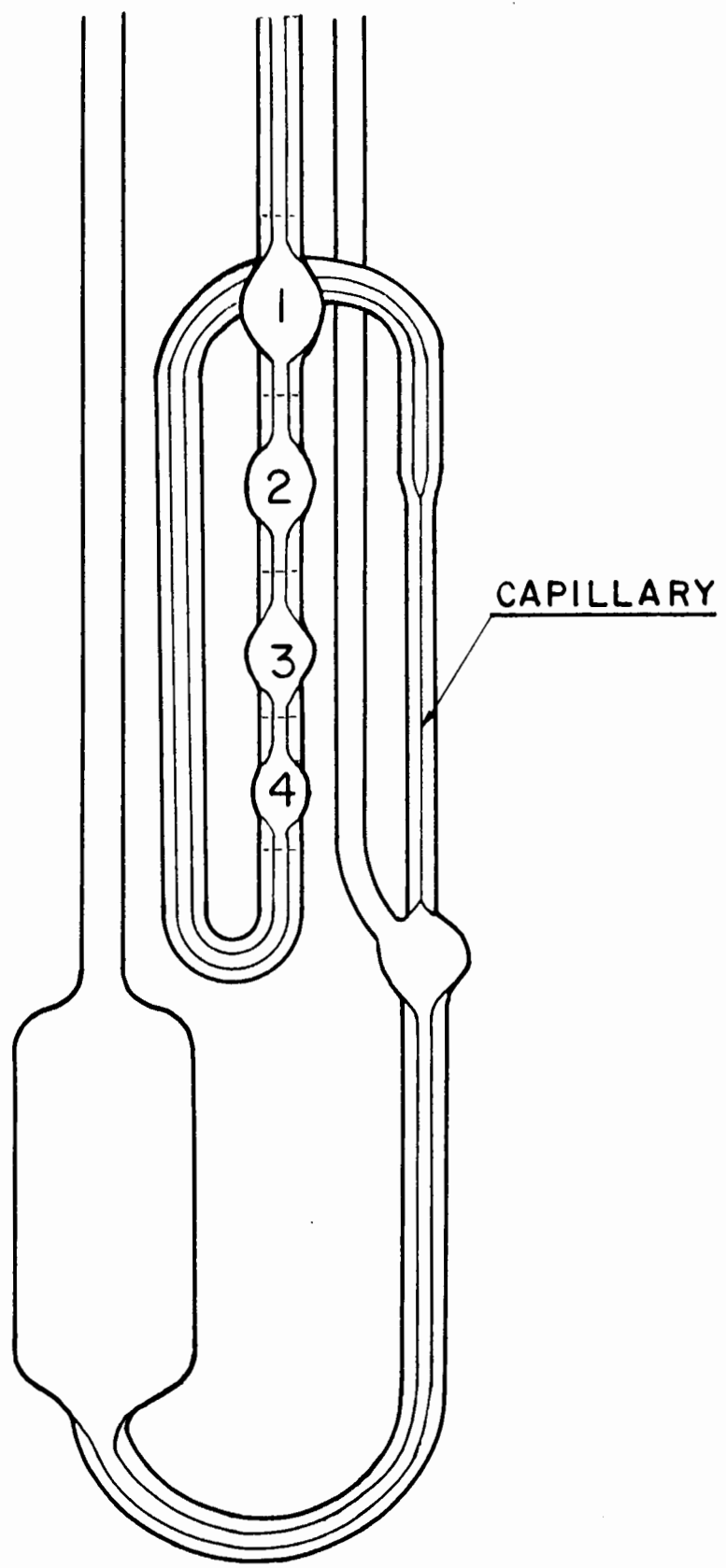
TABLE I-A

Data for Multi-shear Viscometer

Bulb No.	Volume cm.^{3}	h_m cm.	Efflux time of acetone sec.
1	2.74	17.0	78.4
2	1.98	12.0	80.0
3	1.75	7.1	119.4
4	0.83	3.1	130.8

APPENDIX III

ANOMALOUS VISCOSITY BEHAVIOUR

AT LOW CONCENTRATIONS

ANOMALOUS VISCOSITY BEHAVIOUR AT LOW CONCENTRATION

It was observed that the solvent efflux times with a freshly cleaned viscometer capillary differed significantly from that measured directly after an experiment in a solvent-rinsed viscometer. Table II-A gives the efflux times of distilled ethyl acetate before and after viscosity measurements.

The difference in efflux times, although only 0.6 sec., is considerably greater than the experimental error of ± 0.1 sec. The efflux time did not change on repeated washing with solvent but was reduced to its original value by routine cleaning with chromic acid.

Since all conditions were identical in both cases the increase in the efflux time after viscosity measurements indicated a decrease in the effective capillary radius, probably due to some sort of film adhering to the capillary wall. The presence of such adsorbed layer has been proposed by Ohrn (4), to explain the upward curvature of $\frac{\eta_{sp}}{c}$ vs. c line at low concentration. He found a dependence of the thickness of the layer on concentration.

Takeda and Eno (5) have calculated the thickness of the adsorbed layer from a solution of polyvinyl chloride in

TABLE II-A

Efflux Times of Ethyl Acetate before

and after Viscosity Measurements

Clean capillary	. After viscosity measurement and washing of capillary and bulb three times with solvent.
Sec.	Sec.
83.9	84.5
84.0	84.5
83.9	84.5

cyclohexanone and found values of 1500 to 3,300 $\overset{\text{o}}{\text{A}}$.

The effective capillary radius was calculated from the two efflux times and the known capillary radius. The difference, 3,200 $\overset{\text{o}}{\text{A}}$, may be taken as the effective thickness of the adsorbed layer. The value falls in the range of values calculated by Takeda and Eno (5).

This, however, is not conclusive evidence of the adsorption layer being the cause of the upward curvature in the plot of $\dfrac{\eta_{sp}}{c}$ vs. c. Further experimental work is required.

APPENDIX IV

DEVELOPMENT OF LIGHT-SCATTERING

TECHNIQUES

DEVELOPMENT OF LIGHT-SCATTERING TECHNIQUES

Experiments which led to the adoption of Dandliker and Kraut's method of ultraclarification of solutions and the consequent modification of the Brice-Phoenix light-scattering photometer are described in this appendix.

Preliminary Measurements

Measurements prior to modification were made in the original Brice-Phoenix apparatus with cylindrical cells. The wave length of light used was $4358 \, \mathring{A}$.

The symmetry of the cells and the apparatus for θ from $30°$ to $135°$ was tested with an aqueous solution of fluorescein. The graph of I_θ (scattered intensity corrected for volume change by the factor $\sin \theta$) vs. θ is shown in Fig. 2-A. The envelope is symmetrical and constant to $\pm 1\%$.

The results of similar experiments with distilled and filtered toluene and acetone are shown in Fig. 3-A. The absence of marked irregularities in the graphs indicated low intensity of secondary reflections.

The calibration of the instrument was checked with Cornell standard polystyrene in toluene and the turbidity was found to be in fair agreement with the published values.

91

Fig. 2-A

Scattered intensity (corrected for volume
change) at different angles vs. angle, θ ,
for an aqueous alkaline solution of fluores-
cein in the light-scattering apparatus before
and after modification.
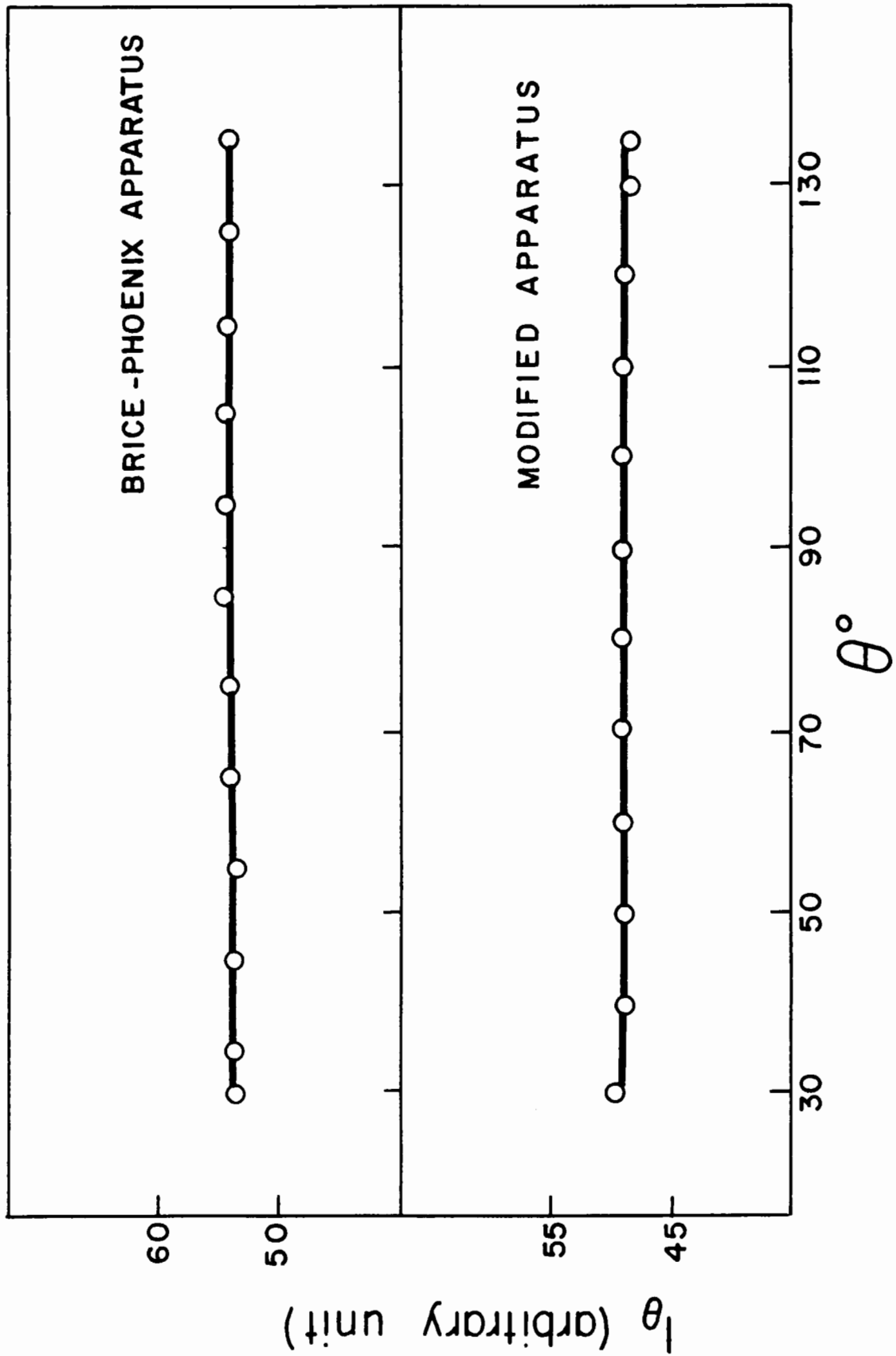
Fig. 3-A

Scattered intensity (corrected for volume
change) at different angles vs. angle, θ ,
for distilled and filtered toluene and acetone
in the Brice-Phoenix apparatus with cylindrical
cells.
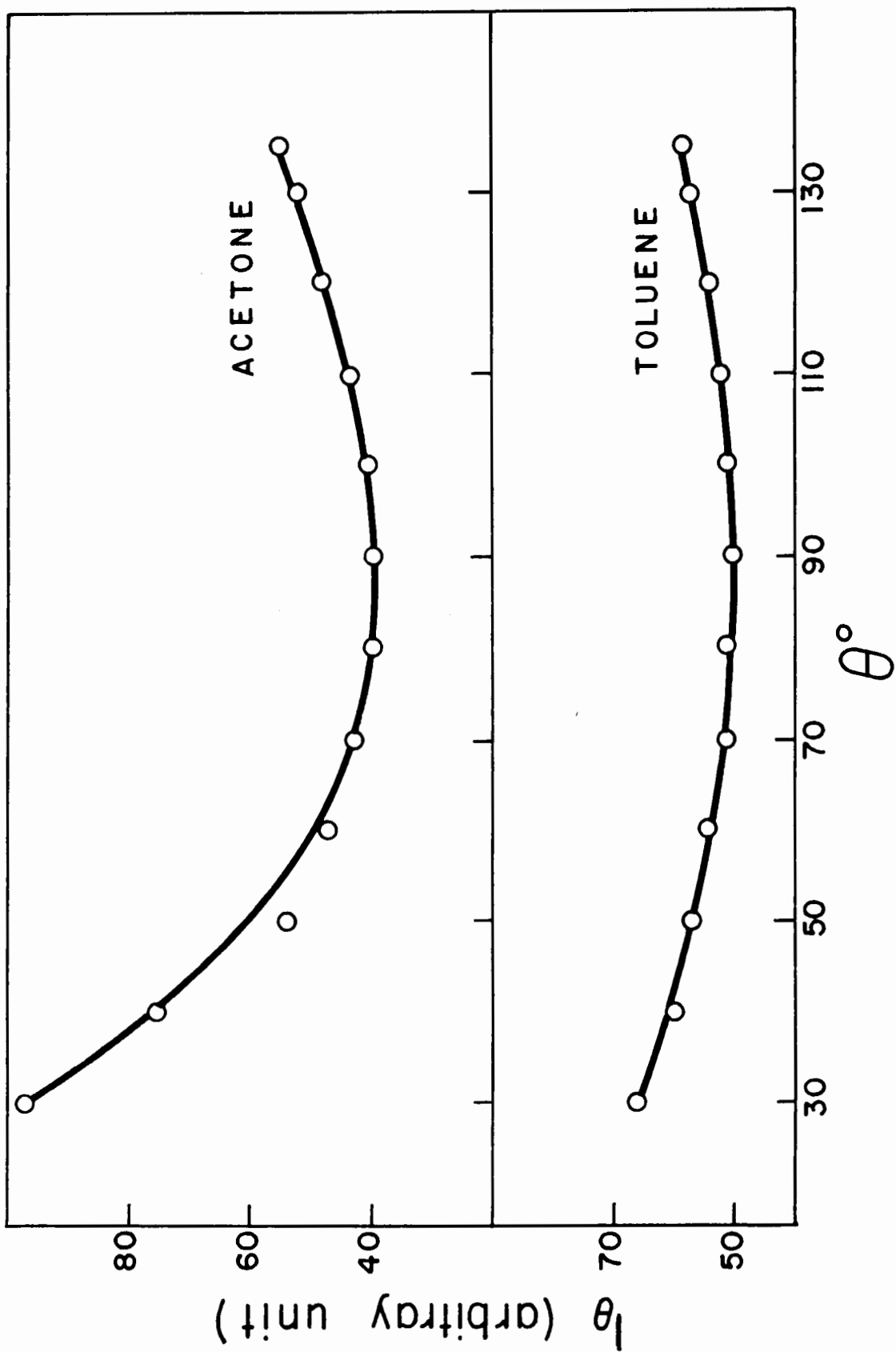
Clarification of Solvents and Solutions

Filtered reagent grade acetone was first used as solvent. Early in the work it was found that one batch gave very high scattering value. This was traced to a fluorescent impurity. Hence reagent grade solvents were used only after redistillation and filtration through ultrafine sintered glass filter.

Both filtration and centrifugation were tried for the clarification of the solutions. In an attempted filtration through an ultrafine sintered glass filter it was found that the filtrate contained only 3% of the solute. The rest of the solute remained adsorbed on the filter.

Centrifugation at 24,000 g in an International centrifuge with high speed attachment was tried. The time of centrifugation was limited by the rise of temperature of the rotor. When the rotor was pre-cooled to $4^{o}C$, the temperature of the rotor increased to about $50^{o}C$ on centrifugation for 45 minutes. This rise in temperature was undesirable because of the possibility of degradation of CTN. However, concentration measurements before and after centrifuging showed that there was no marked sedimentation of CTN in the high field used.

Centrifugation at 45,000 g for one hour in a Spinco model L ultracentrifuge using stainless steel tubes with polyethylene gaskets was found to give satisfactory clarification. However, in spite of elaborate precautions to eliminate extraneous dust particles during transfer to light-scattering cells and subsequent dilution reproducible results could not be obtained. For example, duplicate measurements on a sample having intrinsic viscosity 36.8 g.$^{-1}$ dl. in acetone gave molecular weights differing by 19 percent. Moreover, two samples whose intrinsic viscosities differ by 10 units gave the same molecular weight.

The basic weakness in the above mentioned methods of clarification lies in the fact that the solution must be transferred from the container where it is cleaned to the cell in which measurements are made. The best arrangement would be a light-scattering cell which could be centrifuged. Such a cell has recently been described by Dandliker and Kraut (1). Certain other advantages of this type of cell are:(a) the volume required is small, (b) they are relatively easy to make and (c) the part of the cell where the incident light beam enters is conical in shape, thus reflecting the stray light out of the plane of the incident and scattered beams. In consideration of these advantages and more efficient clarification of the solution, it was

decided to use this method of ultraclarification. This necessitated changes in the cell table and in the optical system of the Brice-Phoenix apparatus.

Modification of the Apparatus

(a) The Scattering Cell

Fig. 4-A shows a cell with dimensions. Cells were made from selected glass tubing. The drawn-out tip at the bottom of the cell should be gradually tapering as shown. If the bottom was flat or thin the cells tended to crack during centrifugation.

Before use in light-scattering measurements, the cells were tested by spinning them at 55,000 g. A 75% solution of glycerol in water was used as a floating medium in the centrifuge cups. A frequent cause of breakage was traced to improper vacuum seal of the centrifuge cups. The seal was improved by a thin film of vacuum grease applied on the rubber gaskets in the cups. After centrifugation, the cells were carefully washed with detergent and water to remove any grease that might adhere to the cell, rinsed with clean acetone, wiped with lens paper and then placed in the cell assembly for taking measurements.

Fig. 4-A

The light-scattering cell used in the present work. The dimensions of the cell are to scale.
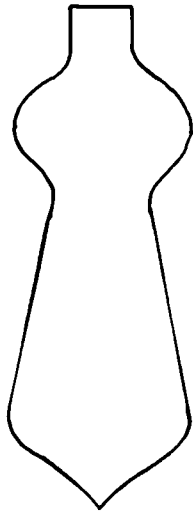
cm.

(b)   The Cell Assembly

The cell assembly (Fig. 4) consisted of a cylindrical vessel, B, and a device for holding the cell upright in the vessel; B was made from a carefully selected beaker of outside diameter 55 mm. A brass ring 2 mm. thick held the vessel in position; but it could be taken out for periodic cleaning. The scattering cell SC was held in position by means of a sturdy, bent metal strip which was permanently fixed to the ring. At the end of the strip there was a V-slot and spring clip to hold the cell vertically at the centre of the vessel B. A circular blackened teflon sheet with a conical hole at the centre sat at the bottom of B. This conical hole served to centre the bottom of the cell.

A new table was made from a block of an aluminium alloy to replace the Brice-Phoenix table. The table top was flat with a rim 3 mm. wide and 6 mm. deep. Three small bolts, 120° apart, through the rim permitted centering of the cell assembly. These bolts were securely positioned by means of three Allen screws on top of the rim of the table. After optical alignment two of the bolts were tightened permanently. The other was slackened whenever the cell assembly was removed. By means of suitable marks the table, the cell assembly and each cell were always located in the same respective position. All metal parts were

painted dull black except for the marks which were dots of white paint.

(c) Changes in the Optical System

The purpose of modifying the optical system was to decrease the size of the incident beam and the scattering volume. This was achieved by means of suitable slits and lenses in the incident and scattered beams.

The main lens of the Brice-Phoenix system was replaced by the lens L_1, having a diameter of 29 mm. and focal length of 76 mm. (Fig. 3). The lens was fitted in a metal ring and was secured in the collimating tube by means of an Allen screw. The diaphragms S_1 (8 mm. x 4 mm.) on the lamp housing and S_2 (20 mm. x 8 mm.) on the metal ring holding the lens L_1 limited the primary beam.

Cylindrical lenses were placed in the incident and scattered beams to compensate for the aberrations produced by the curvature of the vessel B. The cylindrical lens CL_1 was glued to a brass plate with a circular hole of 13 mm. diameter. The plate replaced the cell table diaphragm of the original apparatus. The receiving system consisted of an achromatic objective L_2 of diameter 11 mm. and focal length 18 mm. and the cylindrical lens CL_2. CL_1 and CL_2 were spectacle lenses cut to diameters of 18 mm. and

13 mm. respectively. The lenses L_2 and CL_2 were fixed in a newly-built nose-piece. The lens L_2 was painted dull black except for an opening (4 mm. x 2.5 mm.) to admit the scattered beam. The nose-piece was removable and was locked to the photomultiplier housing by means of a screw.

(d) Optical Alignment

The position of the lens L_1 was fixed by focussing an image of the diaphragm S_1 at the centre of the solvent-filled vessel. The lens was then secured to the collimating tube by means of the Allen screw. The position of the lens L_2 was determined in the following way. A lamp was placed in the photomultiplier housing and an image of the diaphragm S_4 focussed at the centre of the table by changing the position of the lens. The lens was then glued to the nose-piece. The nose-piece was designed to leave a small gap between the lenses L_2 and CL_2. After alignment the distances of lenses L_1 and L_2 from the centre of the table were 110 mm. and 28 mm. respectively.

Tests of the Modified Apparatus

The graph of I_θ vs. θ in Fig. 2-A for a solution of fluorescein shows that the scattering is symmetrical around 90°. Fig. 5-A shows the envelopes of toluene and

<u>Fig. 5-A</u>

Scattered intensity (corrected for folume
change) at different angles vs. angle, θ ,
for distilled and filtered toluene and
acetone in the modified apparatus.
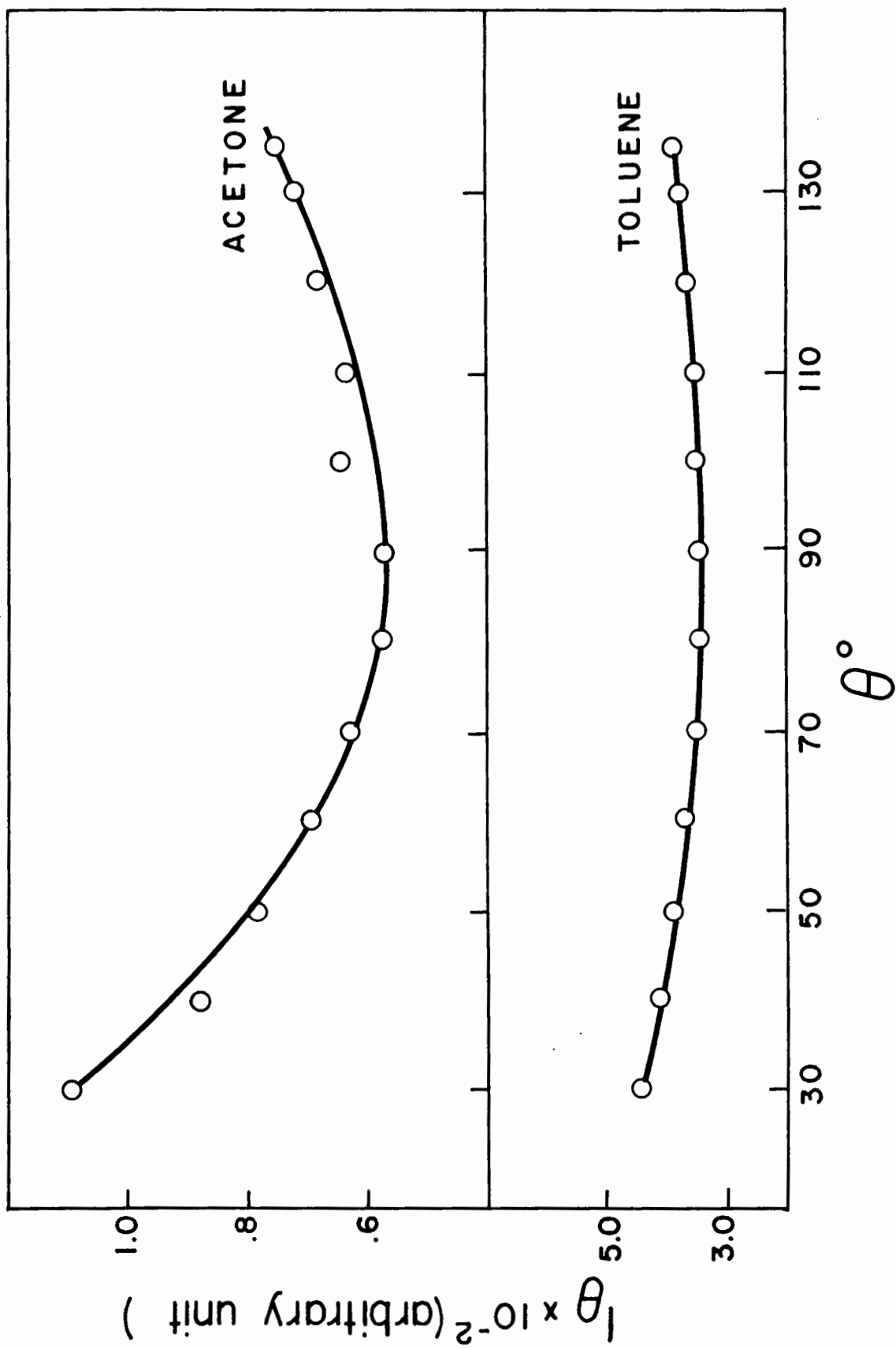
acetone. The envelope for toluene was regular but slight irregularity was observed in the case of low angle scattering of acetone. This caused no error because the solvent scattering was always subtracted from the scattering by the solution.

Fig. 6-A is a graph of galvanometer deflections near $\theta = 0°$. It can be seen that the maximum intensity was at $+ 0.5°$ when the working standard was in position. Without the working standard the maximum intensity coincided with the zero of the scale. Thus the diffusing plate in the working standard deflected the incident beam slightly. Since all intensities at $\theta = 0°$ were measured with the working standard in position, readings for transmitted intensities were taken with the scale placed at $+ 0.5°$.

Calibration

The apparatus was calibrated with Ludox suspensions made from a 30% stock suspension. Suspensions of 3%, 2%, 1%, 0.5%, and 0.25% nominal concentrations were made by diluting the stock with 0.05 M aqueous NaCl (2). The solvent and the stock suspension were filtered through ultrafine and coarse sintered glass filters, respectively, before dilution. Turbidities of these suspensions were measured in a Beckman

Fig. 6-A

Galvanometer deflection vs. angle, θ, near $\theta = 0^{o}$.
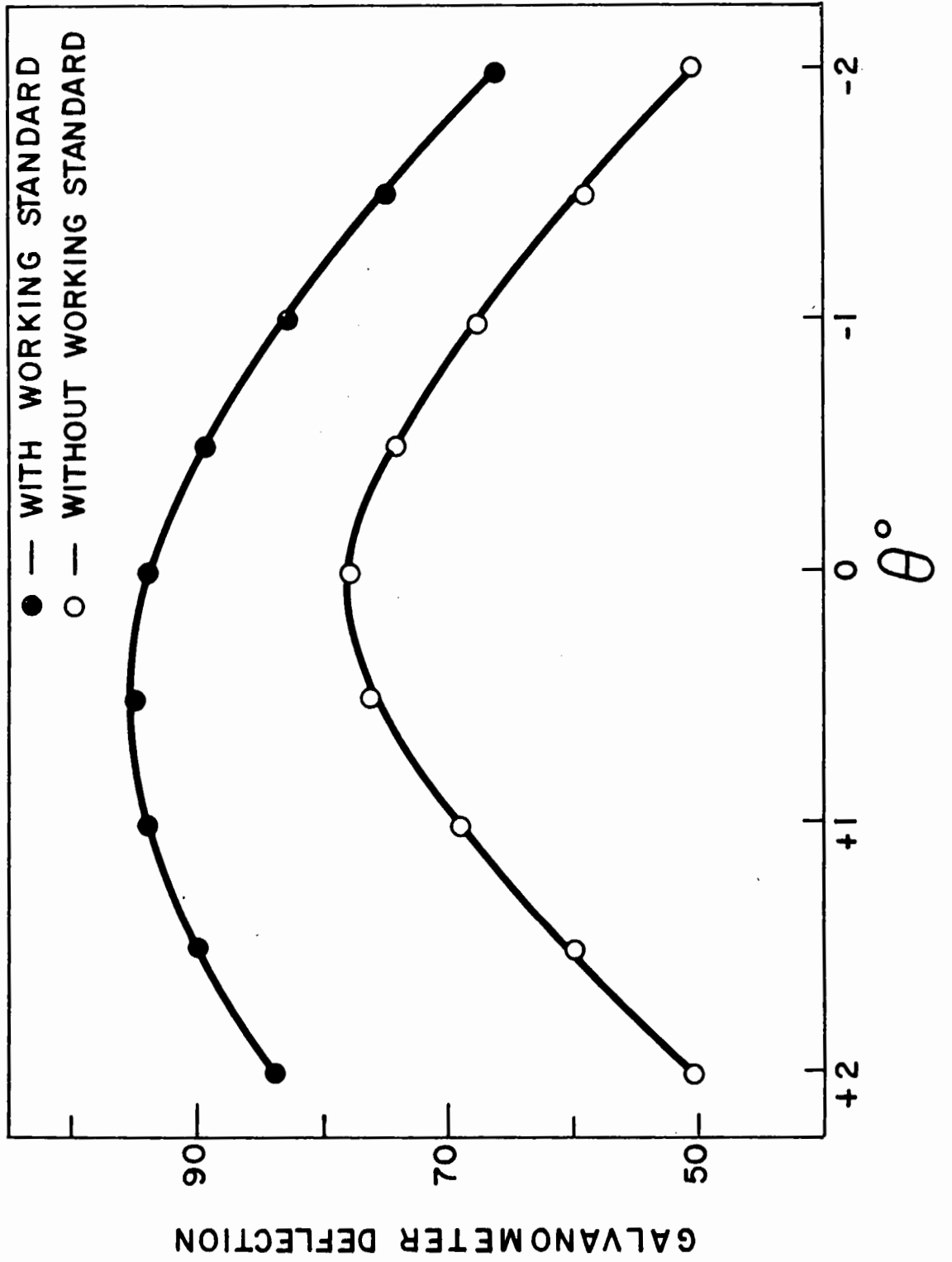
DU spectrophotometer with 10 cm. matched cells at $\lambda = 4358 \overset{o}{A}$. From galvanometer readings at 90° and 0°, i_{90} was computed for each of the cells at all concentrations in the light-scattering apparatus. The working standard was in place during measurement of intensity at $\theta = 0^o$.

From the spectrophotometric data c/τ (c is concentration in g./cm.^{3} and τ is turbidity in cm.$^{-1}$) was plotted against c and extrapolated to $c = 0$ (Fig. 7-A). The c/i_{90} values from light-scattering measurements were plotted against concentration and a linear extrapolation to $c = 0$ gave $(c/i_{90})_{c=0}$. Fig. 8-A shows such plots for two cells.

The calibration factor, C, was calculated from

$$(c/i_{90})_{c=0} = C(c/\tau)_{c=0} \qquad \ldots\ldots \text{(2-A)}$$

The mean value of $(c/i_{90})_{c=0}$ for all the cells used was $(2.61 \pm 0.01) \times 10^{-3}$. The value of $(c/\tau)_{c=0}$ from spectrophotometric measurements was 0.0525. Thus $C = 4.99 \times 10^{-2}$ and τ is given by

$$\tau = 4.99 \times 10^{-2}.i_{90} \qquad \ldots\ldots \text{(3-A)}$$

For measurements in non-aqueous systems a refraction correction must be applied (3) to give

Fig. 7-A

$c/_{\tau}$ vs. c for Ludox suspensions
at different concentrations from
measurements in a Beckman DU
spectrophotometer.

$C/\tau \ (g.cm.^{-2})$

$C \ (g.cm.^{-3})$

0.03   0.02   0.01   0

0.09   0.07   0.05
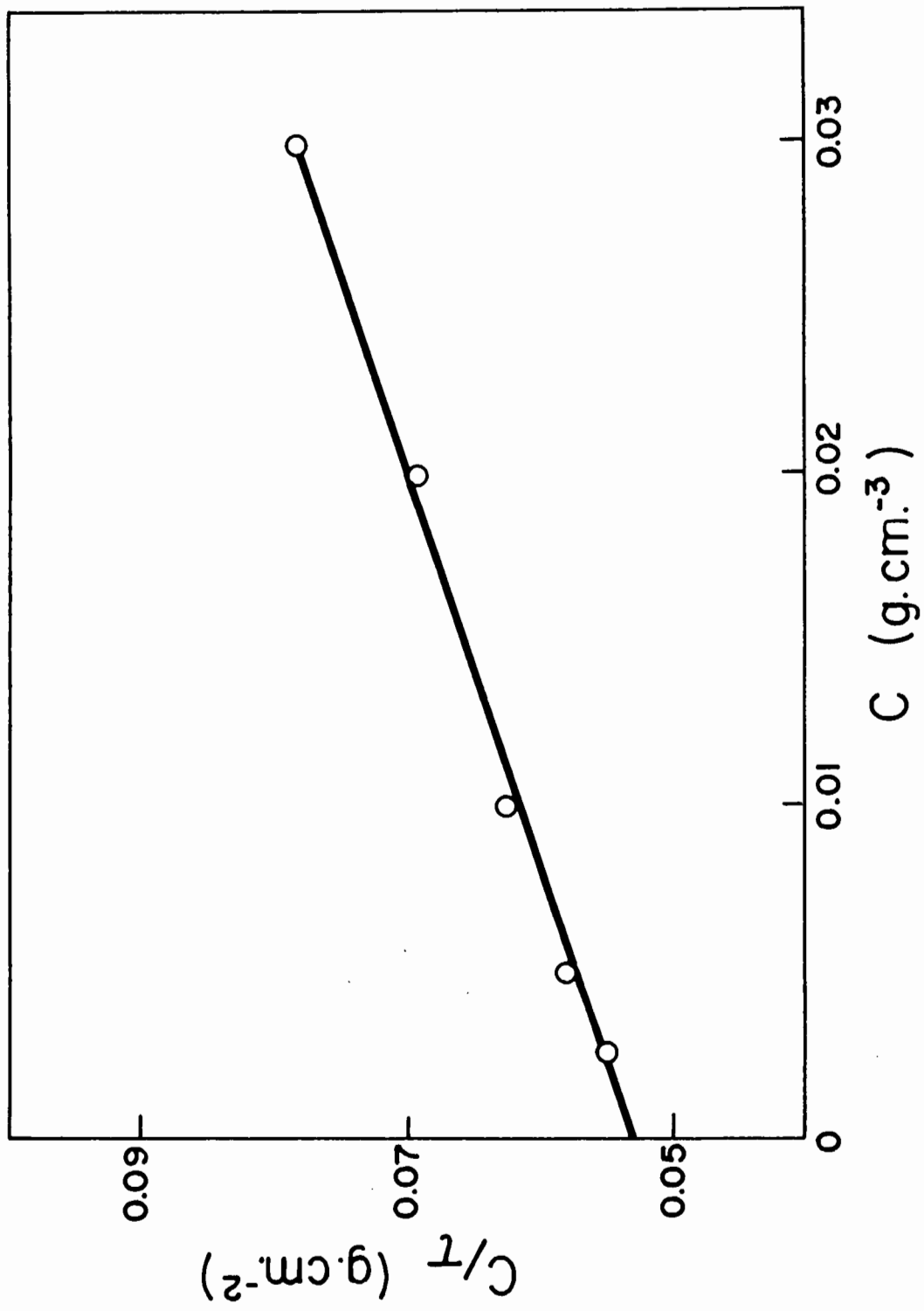
Fig. 8-A

c/i_{90} vs. c for Ludox suspensions
of different concentrations in two
light-scattering cells (Fig. 4-A)
from measurements in the modified
light-scattering apparatus.

C (g.cm.⁻³)

$C/I_{90} \times 10^3$ (g.cm.⁻³)
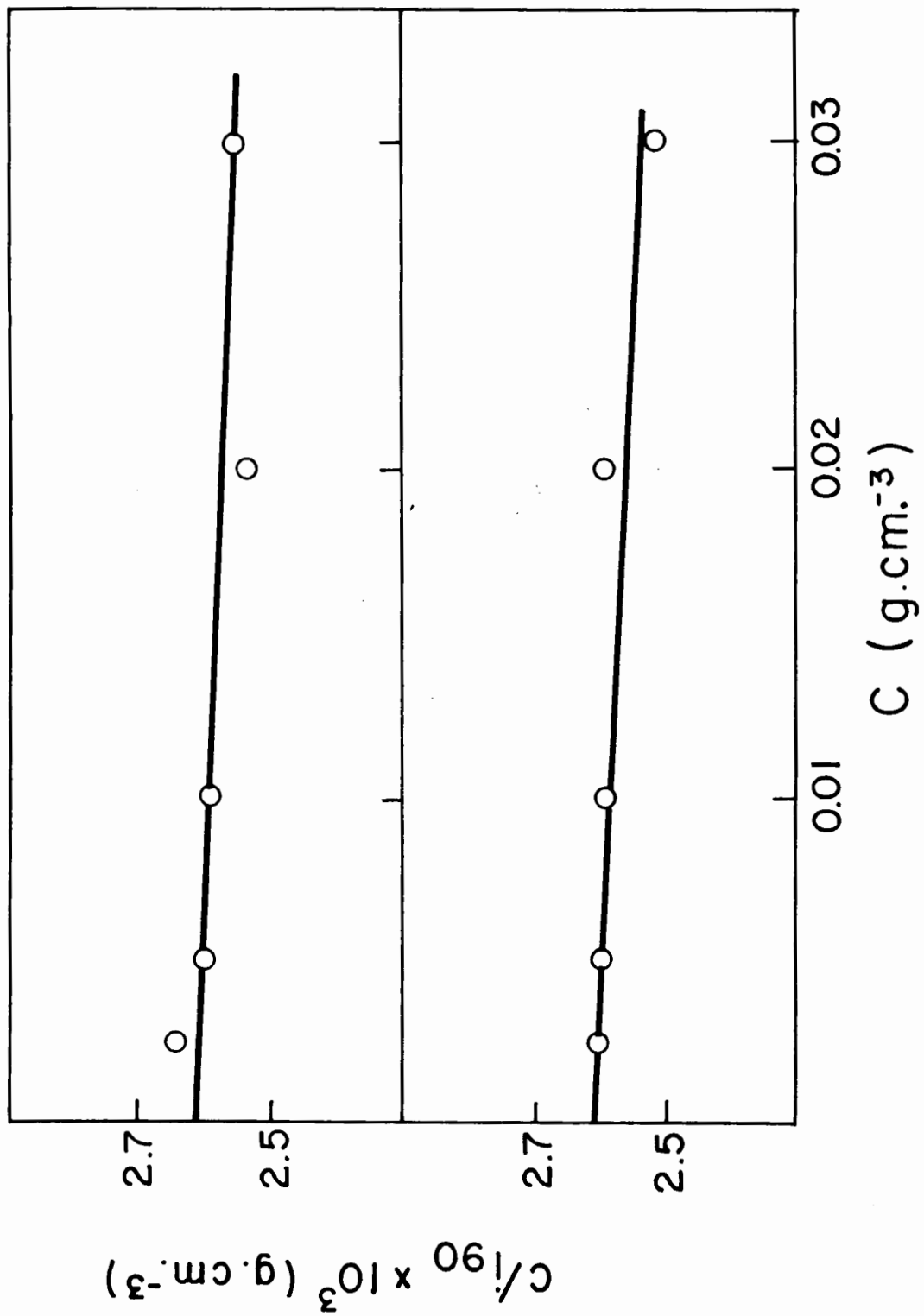
$$\tau = 4.99 \times 10^{-2} \cdot i_{90} \cdot \left(\frac{n_s}{n_w}\right)^2 \qquad \ldots\ldots \text{(4-A)}$$

The relationship between the turbidity and the Rayleigh ratio at $90°$, R_{90}, is

$$\tau = \frac{16\,\pi}{3}\ R_{90} \qquad \ldots\ldots \text{(5-A)}$$

from which

$$R_{90} = \frac{3}{16\,\pi} \cdot C \cdot i_{90} \cdot \left(\frac{n_s}{n_w}\right)^2 \qquad \ldots\ldots \text{(6-A)}$$

and

$$R_\theta = \frac{3}{16\,\pi} \cdot C \cdot i_\theta \cdot \left(\frac{n_s}{n_w}\right)^2 \cdot \frac{\sin\theta}{1 + \cos^2\theta}$$

$$= 2.98 \times 10^{-3} \cdot i_\theta \cdot \left(\frac{n_s}{n_w}\right)^2 \cdot \frac{\sin\theta}{1 + \cos^2\theta} \quad \ldots \text{(7-A)}$$

which is equation (4) of the main text.

As mentioned previously in the main text, the calibration was confirmed by measurement of the scattering of a liquid of known τ. Results in good agreement with published values were obtained.

APPENDIX V

FORMATION OF STRIATIONS

THE FORMATION OF STRIATIONS

Experiments which showed some of the characteristics of the phenomenon of striations are described in this Appendix.

Effect of Striation on Scattered Intensity

An example of the order of variation of scattered intensity observed in solutions showing striation is given in Table III-A. The solution was centrifuged at about 55,000 g for 30 minutes. Values of i_θ obtained at different times after putting the cleaned cell in the apparatus and at different angles, θ, are shown in this Table.

A solution showing striation was centrifuged for 5 hours at about 55,000 g. Striations were again observed although the intensity of the scattered light was diminished. The variation of scattered intensity with time in this solution is shown in Table IV-A.

Effect of Mixing Added Solvent

That the striations were not caused by mixing a clear layer of solvent left by sedimentation either at the top of the cell or at the conical walls was shown by the

TABLE III-A

i_θ at Different Times and Angles for a Solution
Showing Striations

(Time of centrifugation – 30 minutes)

Angle	Immediately after centrifuging	After 10 minutes	After 15 minutes
30°	0.1695	0.1627	0.1820
35°	0.1302	0.1204	0.1359
40°	0.1013	0.0934	0.1045
50°	0.0690	0.0636	0.0721
60°	0.0476	0.0443	0.0502

TABLE IV-A

i_θ at Different Times and Angles for a Striated Solution

(Time of centrifugation $\doteq$ 5 hours)

Angle	Immediately after centrifuging	After 10 minutes	After 15 minutes
$30°$	0.0990	0.1119	0.1071
$35°$	0.0731	0.0839	0.0827
$40°$	0.0595	0.0664	0.0657
$50°$	0.0389	0.0437	0.0431
$60°$	0.0305	0.0300	0.0292

experiments described below. Solutions which were known
to show striations were used for these experiments.

A layer of solvent was introduced on top of the
solution in a light-scattering cell. No striation was
observed for 4 hours when the experiment was stopped.

A centrifuged solution was left overnight when the
striations disappeared. A layer of solvent was then put
on the top. Again there was no discontinuity in the scat-
tered beam even after 3 hours standing.

A cell containing a fresh solution was cooled in
a refrigerator to about $5^{\circ}C$ and then a solvent layer intro-
duced on top of it. No striation was observed.

After each of the above experiments, pure solvent
was injected into the solution by means of a syringe. A
momentary discontinuity was observed which disappeared soon
after the injection was stopped.

A special cell was made in order to test whether the
striations were caused by a separation of a layer of solvent,
left under the sloping walls of the cell, on centrifugation.
In the new cell (Fig. 9-A) the upper bulb was eliminated.
The conical walls were radial to the centre of the rotor,
so that no solvent layer could accumulate under the conical

Fig. 9-A

A conical light-scattering cell for
investigation of striations.
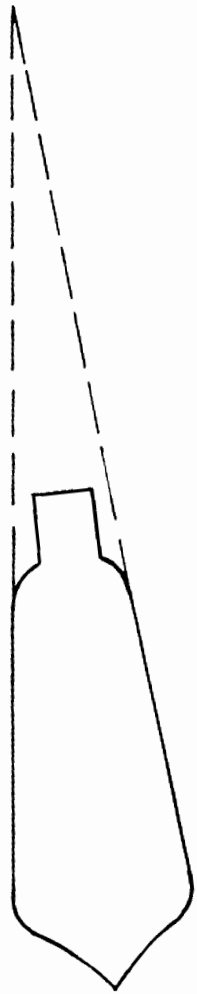
Fig. 10-A (a)

Ultracentrifuge diagrams for fraction
P in acetone at a field of 259,700 g.
at different time intervals.
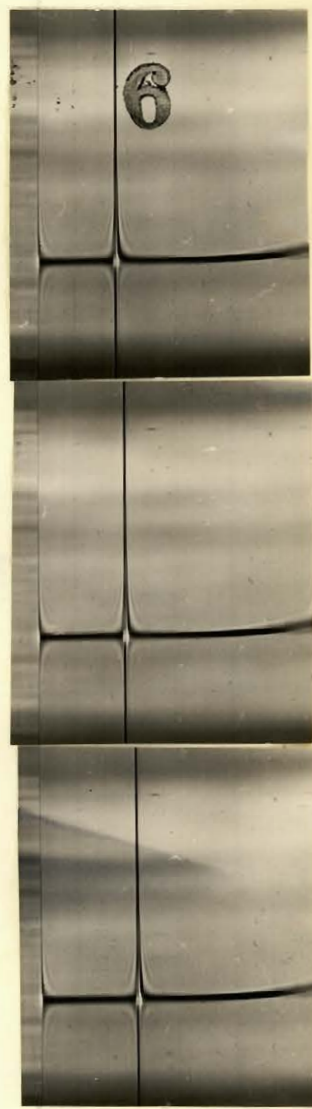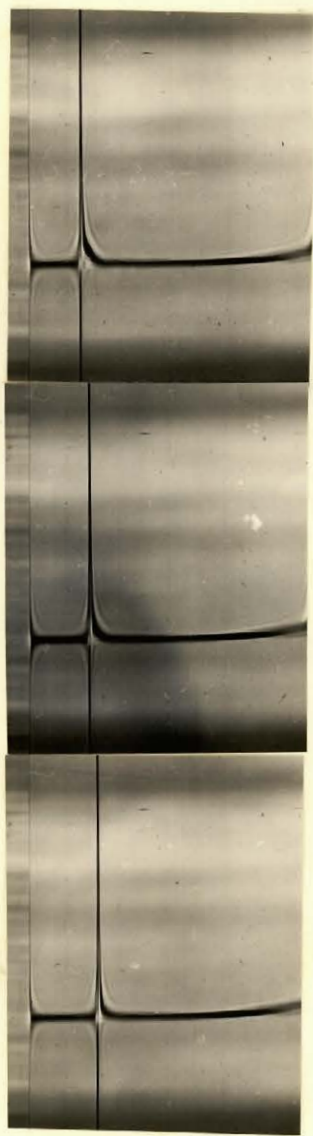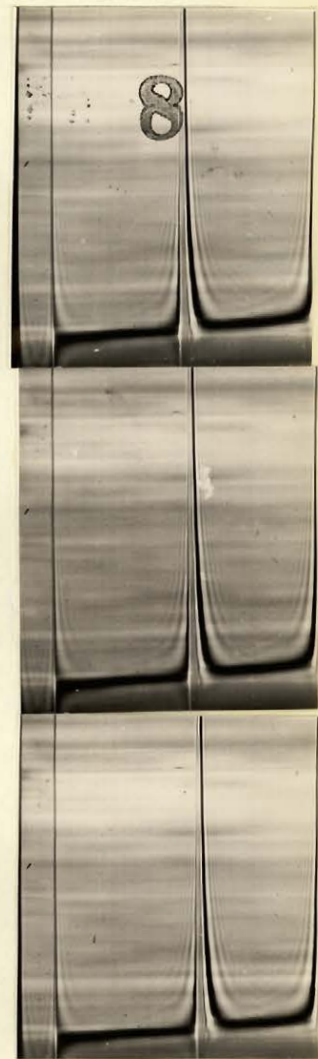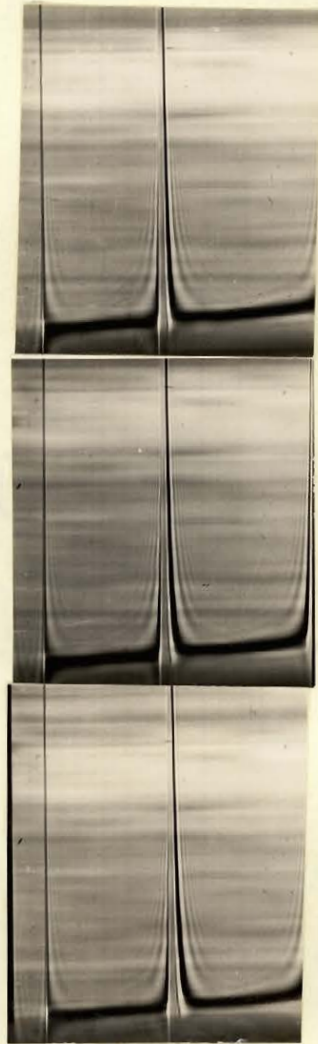
Fig. 11-A

Log of the distance, x_2, of the
boundary from the centre of the rotor
vs. time. Centrifugal field $=$ 38,900 g.
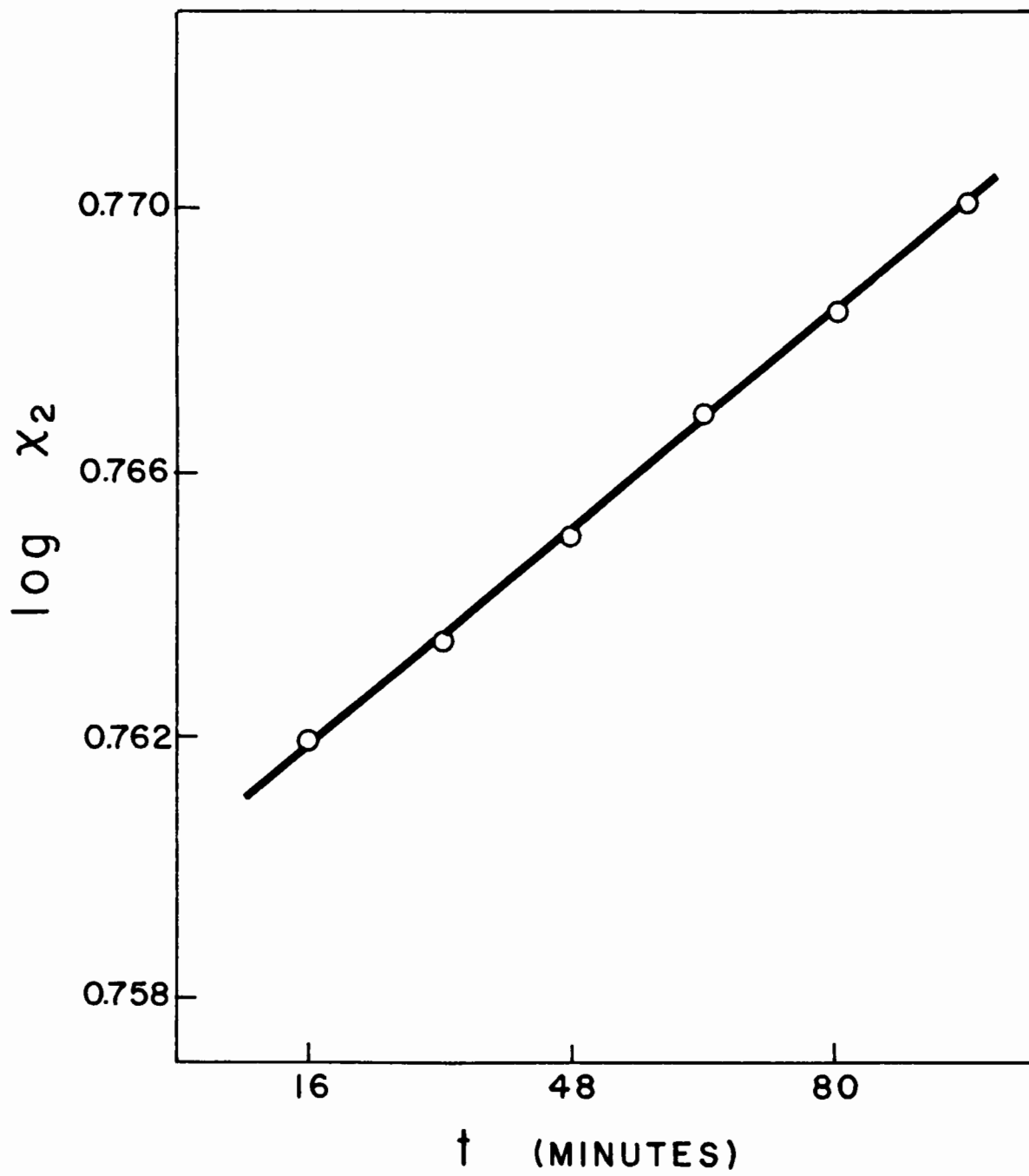
Fig. 12-A

Log of the distance, x_2, of the
boundary from the centre òf the
rotor vs. time. Centrifugal field
$= 259,700$ g.
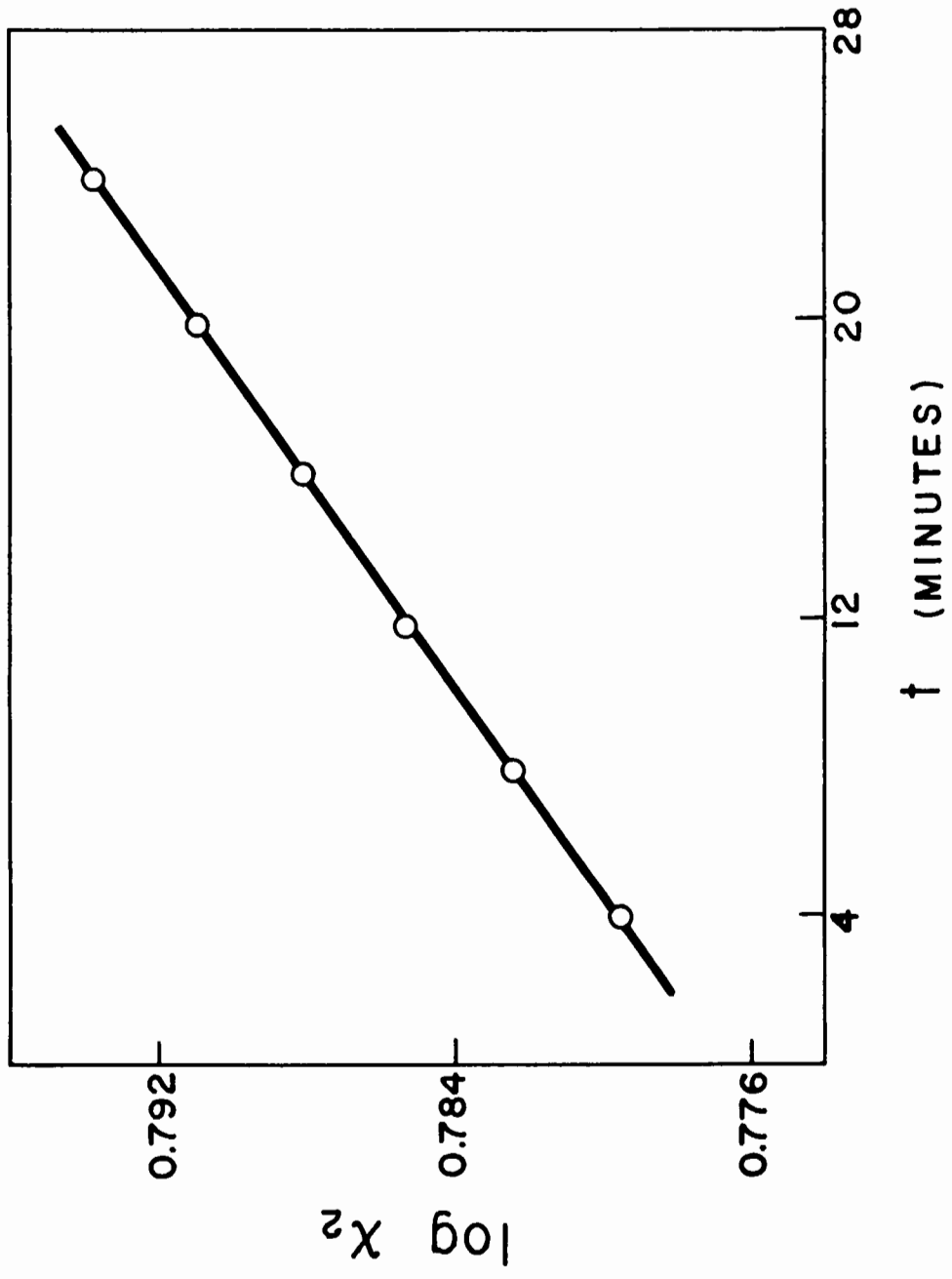
Fig. 13-A

Log of the distance, x_2, of the boun-
dary from the centre of the rotor vs.
time after reducing the field to 38,900 g.

lines. The values of the constants were corrected for
viscosity (temperature dependent) and density (temperature
and field dependent) in the usual way (6). The values,
referred to 20°C, were 6.76 S, 6.70 S and 6.73 S respec-
tively in the three stages of the experiment.

Sedimentation of Glass Spheres

Experiments to test whether striations were caused
by incipient gel formation were attempted. The experiments
consisted in observing the rate of fall of tiny glass spheres,
about 10 or 100 μ diam., through a striated solution of CTN
in a cell designed and made for the purpose. The cell was
similar in dimension to the conical light-scattering cell
(Fig. 9-A) except that it was cylindrical in shape, the
vertical portion having an outside diameter of 24 mm. The
cell could be centrifuged. The falling spheres were ob-
served with a differential sedimentation apparatus similar
to one described by Anderson (7).

The presence of gel-like aggregates would cause
gross discontinuities in the rate of sedimentation of the
particles. No conclusion, however, could be drawn from
these experiments because of optical limitations of the
instrument and the mechanical difficulty of eliminating
thermal currents produced in the solution by the light

source used for illuminating the particle. Given enough time, the difficulties could be surmounted; the results are expected to give valuable information about the cause of striations.

APPENDIX VI

CALCULATION OF Φ'

CALCULATION OF Φ'

After the manner of Hunt et al. (34) the exponent
a in the empirical intrinsic viscosity-molecular weight
relation (Eqn. 1) can be expressed as

$$a = 0.5 + 3a_1 + 1.5a_2 + a_3 \qquad \ldots\ldots \text{(8-A)}$$

where a_1, a_2 and a_3 are defined by

$$
\left.
\begin{aligned}
a_1 &= d \ln \alpha / d \ln \bar{M} \\
a_2 &= d \ln \overline{s_o^2} / \bar{M} / d \ln \bar{M} \\
a_3 &= d \ln \Phi' / d \ln \bar{M}
\end{aligned}
\right\} \qquad \ldots\ldots \text{(9-A)}
$$

and

Equations (8-A) and (9-A) result from differentiation of
the equation obtained by combining the logarithms of Eqns.
(1) and (12).

According to Hunt et al. (34) Eqn. (12) can be
written as

$$\Phi' = q_\Phi \left[\eta\right] \bar{M}_w / (\overline{s_z^2})^{3/2} \qquad \ldots\ldots \text{(10-A)}$$

where q_Φ is a polydispersity correction factor given by

$$q_{\Phi} = \left[\Gamma(y + 3 + 2a_1 + a_2)\right]^{3/2}(y+1)^{-2}$$

$$\left[\Gamma(y + 2)\right]^{-\frac{1}{2}} \left[\Gamma(y + 3/_2 + 3a_1 + 3a_{2/_2})\right]^{-1}$$

$$\ldots\ldots (11\text{-}A)$$

where y is a parameter which characterizes the polydispersity by $\overline{M}_z : \overline{M}_w : \overline{M}_n = (y+2):(y+1):y$.

In the present work y has been taken as 1. In acetone $\propto$ was found to be practically constant, then a_1 can be taken as zero. Similarly a_2 was also zero in acetone. Substituting in Eqn. (11-A), q_{Φ} comes out to be 1.95. By substitution of this value for q_{Φ} in Eqn. (10-A) the values of $\bigoplus$' as given in Table VII were computed for CTN in acetone.

In ethyl acetate $\overline{s_z^2}/M_z$ was found to increase slowly with $\overline{M}_z$ over the range studied; thus a_2 could not be assumed to be zero. The value of a_2 obtained from a plot of $\ln(\overline{s_o^2})_{z/\overline{M}_z}$ vs. $\ln \overline{M}_z$ was 0.26. As in acetone a_1 was zero. The value of q_{Φ}, calculated from Eqn. (11-A), was then 2.36 from which $\bigoplus$' values were calculated by substitution in Eqn. (10-A).

Equation (10-A) may be written as

$$\Phi' = k \ [\eta] \ \overline{M}_z/(\overline{s_z^2})^{3/2} \qquad\qquad \ldots\ldots (12\text{-A})$$

where k is a constant different for each solvent and equal to $q_\Phi / 1.5$.

APPENDIX VII

DETAILED DATA FROM VISCOSITY MEASUREMENTS

DETAILED DATA FROM VISCOSITY MEASUREMENTS

The viscosity data from which the results described in the main text were derived are given in this Appendix. The specific viscosities of the samples in acetone at different concentrations and rates of shear obtained from measurements in the four bulbs of the viscometer described in Appendix II are given in Table V-A. The same quantities for solutions in ethyl acetate are given in Table VI-A. The specific viscosities were corrected for kinetic energy. Concentrations are expressed in grams per 100 cc.

TABLE V-A

Specific Viscosities in Acetone of the Samples of Different Concentrations and Rates of Shear

Sample	Bulb No.	$c_1=11.01 \times 10^{-2}$		$c_2=8.32 \times 10^{-2}$		$c_3=6.66 \times 10^{-2}$		$c_4=4.76 \times 10^{-2}$		$c_5=3.33 \times 10^{-2}$	
		$\eta_{sp.}$	G sec.$^{-1}$	$\eta_{sp.}$	G sec.$^{-1}$	$\eta_{sp.}$	G sec.$^{-1}$	$\eta_{sp.}$	G sec.$^{-1}$	$\eta_{sp.}$	G sec.$^{-1}$
T-8	1	2.736	744	1.750	1008	1.265	1221	0.803	1531	0.513	1815
	2	2.811	519	1.798	706	1.301	857	0.821	1080	0.525	1286
	3	2.879	303	1.848	413	1.334	503	0.845	636	0.543	759
	4	2.925	133	1.877	181	1.359	220	0.864	279	0.552	334

Sample	Bulb No.	$c_1=9.19 \times 10^{-2}$		$c_2=5.52 \times 10^{-2}$		$c_3=3.94 \times 10^{-2}$		$c_4=2.76 \times 10^{-2}$		$c_5=2.12 \times 10^{-2}$	
T-6	1	3.276	647	1.463	1119	0.898	1448	0.569	1745	0.414	1930
	2	3.414	448	1.522	782	0.936	1016	0.591	1233	0.437	1362
	3	3.533	259	1.571	456	0.968	595	0.611	725	0.446	806
	4	3.611	112	1.604	199	0.989	260	0.626	318	0.462	354

Sample	Bulb No.	$c_1=6.56 \times 10^{-2}$		$c_2=4.92 \times 10^{-2}$		$c_3=3.93 \times 10^{-2}$		$c_4=2.46 \times 10^{-2}$		$c_5=1.64 \times 10^{-2}$	
M-3	1	2.056	934	1.350	1210	0.992	1424	0.555	1813	0.349	2079
	2	2.111	647	1.381	843	1.014	995	0.567	1273	0.358	1464
	3	2.168	372	1.417	487	1.043	576	0.582	742	0.465	858
	4	2.211	157	1.442	207	1.056	245	0.592	317	0.369	368

TABLE V-A Contd.

Sample	Bulb No.	$c_1=5.50 \times 10^{-2}$ $\eta_{sp.}$	G sec.$^{-1}$	$c_2=4.13 \times 10^{-2}$ $\eta_{sp.}$	G sec.$^{-1}$	$c_3=2.75 \times 10^{-2}$ $\eta_{sp.}$	G sec.$^{-1}$	$c_4=1.83 \times 10^{-2}$ $\eta_{sp.}$	G sec.$^{-1}$	$c_5=1.18 \times 10^{-2}$ $\eta_{sp.}$	G sec.$^{-1}$
P	1	1.741	1042	1.159	1321	0.689	1682	0.423	1983	0.260	2230
	2	1.794	721	1.195	916	0.705	1174	0.433	1393	0.265	1570
	3	1.853	414	1.228	530	0.728	682	0.446	813	0.273	921
	4	1.899	175	1.260	224	0.739	291	0.454	348	0.276	396

Sample	Bulb No.	$c_1=5.17 \times 10^{-2}$ $\eta_{sp.}$	G sec.$^{-1}$	$c_2=3.86 \times 10^{-2}$ $\eta_{sp.}$	G sec.$^{-1}$	$c_3=2.57 \times 10^{-2}$ $\eta_{sp.}$	G sec.$^{-1}$	$c_4=1.93 \times 10^{-2}$ $\eta_{sp.}$	G sec.$^{-1}$	$c_5=1.29 \times 10^{-2}$ $\eta_{sp.}$	G sec.$^{-1}$
M	1	1.700	986	1.146	1237	0.680	1572	0.482	1777	0.309	2005
	2	1.766	976	1.183	854	0.700	1094	0.498	1239	0.313	1408
	3	1.854	384	1.239	489	0.728	633	0.514	720	0.322	824
	4	1.929	161	1.286	206	0.749	269	0.527	308	0.329	354

Sample	Bulb No.	$c_1=4.18 \times 10^{-2}$ $\eta_{sp.}$	G sec.$^{-1}$	$c_2=3.14 \times 10^{-2}$ $\eta_{sp.}$	G sec.$^{-1}$	$c_3=2.51 \times 10^{-2}$ $\eta_{sp.}$	G sec.$^{-1}$	$c_4=1.79 \times 10^{-2}$ $\eta_{sp.}$	G sec.$^{-1}$	$c_5=1.14 \times 10^{-2}$ $\eta_{sp.}$	G sec.$^{-1}$
M-2	1	1.633	1011	1.092	1268	0.818	1456	0.537	1715	0.318	1991
	2	1.705	693	1.137	875	0.841	1014	0.553	1199	0.327	1397
	3	1.798	394	1.192	502	0.879	586	0.579	696	0.343	816
	4	1.882	165	1.241	212	0.908	249	0.594	298	0.349	352

TABLE V-A Contd.

M-1

Sample	Bulb No.	$\eta_{sp.}$ ($c_1=1.42\times10^{-2}$)	G sec.$^{-1}$	$\eta_{sp.}$ ($c_2=1.14\times10^{-2}$)	G sec.$^{-1}$	$\eta_{sp.}$ ($c_3=0.81\times10^{-2}$)	G sec.$^{-1}$	$\eta_{sp.}$ ($c_4=0.52\times10^{-2}$)	G sec.$^{-1}$
M-1	1	0.546	1709	0.424	1849	0.293	2031	0.178	2220
	2	0.566	1188	0.440	1289	0.303	1421	0.183	1561
	3	0.598	686	0.466	747	0.318	829	0.193	915
	4	0.635	290	0.490	318	0.336	355	0.205	393

H

Sample	Bulb No.	$\eta_{sp.}$ ($c_1=3.91\times10^{-2}$)	G sec.$^{-1}$	$\eta_{sp.}$ ($c_2=2.93\times10^{-2}$)	G sec.$^{-1}$	$\eta_{sp.}$ ($c_3=1.95\times10^{-2}$)	G sec.$^{-1}$	$\eta_{sp.}$ ($c_4=1.47\times10^{-2}$)	G sec.$^{-1}$	$\eta_{sp.}$ ($c_5=0.98\times10^{-2}$)	G sec.$^{-1}$
H	1	2.405	839	1.620	1088	0.856	1451	0.672	1691	0.914	1983
	2	2.681	548	1.771	727	1.026	991	0.718	1165	0.442	1384
	3	3.089	289	1.979	396	1.115	557	0.771	664	0.472	797
	4	3.675	109	2.273	155	1.233	227	0.833	276	0.508	336

H-2

Sample	Bulb No.	$\eta_{sp.}$ ($c_1=4.46\times10^{-2}$)	G sec.$^{-1}$	$\eta_{sp.}$ ($c_2=3.34\times10^{-2}$)	G sec.$^{-1}$	$\eta_{sp.}$ ($c_3=2.67\times10^{-2}$)	G sec.$^{-1}$	$\eta_{sp.}$ ($c_4=1.67\times10^{-2}$)	G sec.$^{-1}$	$\eta_{sp.}$ ($c_5=1.03\times10^{-2}$)	G sec.$^{-1}$
H-2	1	3.257	672	2.062	932	1.485	1146	0.797	1576	0.450	1941
	2	3.612	436	2.251	619	1.600	772	0.847	1083	0.473	1352
	3	4.180	228	2.526	334	1.769	425	0.916	613	0.507	772
	4	4.944	85	2.895	130	1.992	169	1.006	252	0.549	325

TABLE VI-A

Specific Viscosities in Ethyl Acetate of the Samples at Different Concentrations and Rates of Shear

Sample	Bulb No.	$c_1=7.19\times10^{-2}$		$c_2=5.39\times10^{-2}$		$c_3=4.31\times10^{-2}$		$c_4=3.08\times10^{-2}$		$c_5=2.16\times10^{-2}$	
		$\eta_{sp.}$	G sec.$^{-1}$	$\eta_{sp.}$	G sec.$^{-1}$	$\eta_{sp.}$	G sec.$^{-1}$	$\eta_{sp.}$	G sec.$^{-1}$	$\eta_{sp.}$	G sec.$^{-1}$
T-8	1	2.013	751	1.324	972	0.977	1141	0.638	1373	0.422	1578
	2	2.077	522	1.373	676	1.012	797	0.660	964	0.437	1111
	3	2.137	304	1.412	395	1.047	465	0.679	566	0.447	656
	4	2.179	132	1.433	173	1.064	203	0.689	248	0.453	289

Sample	Bulb No.	$c_1=6.42\times10^{-2}$		$c_2=4.81\times10^{-2}$		$c_3=3.85\times10^{-2}$		$c_4=2.75\times10^{-2}$		$c_5=1.93\times10^{-2}$	
T-6	1	2.521	649	1.614	873	1.173	1048	0.755	1295	0.494	1517
	2	2.621	447	1.669	606	1.213	730	0.781	906	0.506	1068
	3	2.730	257	1.731	350	1.257	424	0.806	529	0.523	627
	4	2.802	111	1.772	152	1.275	184	0.825	230	0.532	274

Sample	Bulb No.	$c_1=5.11\times10^{-2}$		$c_2=3.83\times10^{-2}$		$c_3=2.55\times10^{-2}$		$c_4=1.70\times10^{-2}$		$c_5=1.09\times10^{-2}$	
M-3	1	2.018	765	1.318	994	0.772	1296	0.473	1554	0.288	1772
	2	2.099	525	1.367	687	0.799	901	0.487	1087	0.296	1245
	3	2.191	298	1.420	393	0.826	521	0.503	632	0.303	727
	4	2.284	125	1.470	166	0.851	221	0.519	269	0.312	311

TABLE VI-A Contd.

Sample	Bulb No.	$c_1=3.63\times10^{-2}$ $\eta_{sp.}$	G sec.$^{-1}$	$c_2=2.59\times10^{-2}$ $\eta_{sp.}$	G sec.$^{-1}$	$c_3=1.81\times10^{-2}$ $\eta_{sp.}$	G sec.$^{-1}$	$c_4=1.40\times10^{-2}$ $\eta_{sp.}$	G sec.$^{-1}$	$c_5=1.01\times10^{-2}$ $\eta_{sp.}$	G sec.$^{-1}$
M	1	1.713	849	1.068	1112	0.677	1367	0.495	1531	0.338	1705
	2	1.823	574	1.123	762	0.705	946	0.515	1063	0.349	1192
	3	1.966	321	1.201	431	0.750	542	0.546	613	0.373	690
	4	2.125	131	1.283	179	0.795	228	0.574	259	0.391	294

Sample	Bulb No.	$c_1=4.33\times10^{-2}$ $\eta_{sp.}$	G sec.$^{-1}$	$c_2=3.25\times10^{-2}$ $\eta_{sp.}$	G sec.$^{-1}$	$c_3=2.16\times10^{-2}$ $\eta_{sp.}$	G sec.$^{-1}$	$c_4=1.44\times10^{-2}$ $\eta_{sp.}$	G sec.$^{-1}$	$c_5=0.93\times10^{-2}$ $\eta_{sp.}$	G sec.$^{-1}$
M-2	1	2.388	692	1.535	910	0.874	1228	0.524	1503	0.315	1736
	2	2.560	458	1.628	619	0.920	846	0.553	1043	0.331	1213
	3	2.755	253	1.744	347	0.976	482	0.582	601	0.348	704
	4	3.000	103	1.881	143	1.047	201	0.619	254	0.373	300

Sample	Bulb No.	$c_1=3.21\times10^{-2}$ $\eta_{sp.}$	G sec.$^{-1}$	$c_2=2.41\times10^{-2}$ $\eta_{sp.}$	G sec.$^{-1}$	$c_3=1.60\times10^{-2}$ $\eta_{sp.}$	G sec.$^{-1}$	$c_4=1.07\times10^{-2}$ $\eta_{sp.}$	G sec.$^{-1}$	$c_5=0.69\times10^{-2}$ $\eta_{sp.}$	G sec.$^{-1}$
M-1	1	2.003	769	1.311	998	0.764	1303	0.469	1558	0.287	1773
	2	2.195	509	1.416	673	0.815	893	0.500	1079	0.305	1237
	3	2.456	276	1.557	372	0.887	504	0.537	618	0.326	715
	4	2.773	109	1.730	150	0.969	208	0.582	259	0.352	302

TABLE VI-A Contd.

Sample	Bulb No.	$c_1=3.35 \times 10^{-2}$		$c_2=2.51 \times 10^{-2}$		$c_3=1.67 \times 10^{-2}$		$c_4=1.26 \times 10^{-2}$		$c_5=0.91 \times 10^{-2}$	
		$\eta_{sp.}$	G sec.$^{-1}$	$\eta_{sp.}$	G sec.$^{-1}$	$\eta_{sp.}$	G sec.$^{-1}$	$\eta_{sp.}$	G sec.$^{-1}$	$\eta_{sp.}$	G sec.$^{-1}$
H-2	1	2.821	605	1.808	823	1.032	1133	0.725	1332	0.506	1522
	2	3.251	384	2.032	537	1.137	761	0.792	906	0.546	1048
	3	3.938	193	2.370	283	1.280	418	0.878	507	0.600	594
	4	5.009	68	2.857	106	1.474	166	0.993	205	0.666	246

APPENDIX VIII

DETAILED DATA OF LIGHT-SCATTERING

MEASUREMENTS

TABLE VII-A

$R_\theta \times 10^5$ for the CTN Samples in Acetone for Different Concentrations and Different Angles.

	T-8						T-6					
Angle θ \ $c \times 10^{-3}$	3.75	2.48	1.99	1.52	1.00	0.51	3.43	2.46	1.97	1.52	1.02	0.51
30°	11.72	8.71	7.79	6.83	5.48	3.61	10.88	8.79	8.06	7.15	6.18	4.45
35	11.39	8.49	7.48	6.55	5.32	3.42	10.65	8.70	7.84	6.98	5.90	4.18
40	11.05	8.26	7.46	6.38	5.12	3.29	10.47	8.47	7.69	6.77	5.74	3.93
45	10.71	8.12	7.22	6.18	4.95	3.13	10.22	8.28	7.38	6.56	5.50	3.68
50	10.45	7.98	7.02	5.96	4.90	3.03	9.95	8.04	7.22	6.26	5.18	3.45
60	9.75	7.46	6.90	5.59	4.33	2.60	9.42	7.63	6.84	5.83	4.80	3.07
70	9.22	7.11	6.24	5.25	3.98	2.30	8.84	7.25	6.45	5.45	4.30	2.66
80	8.89	6.72	5.86	4.89	3.66	2.11	8.45	6.84	6.06	5.02	3.88	2.36
90	8.45	6.42	5.48	4.57	3.40	1.91	7.93	6.41	5.67	4.61	3.43	2.10
100	8.04	6.03	5.18	4.25	3.17	1.76	7.51	6.06	5.28	4.31	3.24	1.89
110	7.69	5.73	4.90	4.08	2.96	1.63	7.22	5.76	5.01	4.13	3.08	1.77
120	7.45	5.54	4.74	3.89	2.81	1.52	6.83	5.54	4.77	3.97	2.92	1.66
130	7.05	5.36	4.54	3.74	2.74	1.55	6.58	5.22	4.52	3.74	2.81	1.61
135°	6.88	5.17	4.44	3.68	2.64	1.49	6.43	5.11	4.41	3.61	2.74	1.56

TABLE VII-A, continued

	M-3					P				
Angle θ / $\delta \times 10^{-3}$	2.50	1.98	1.50	1.00	0.50	2.35	1.76	1.16	0.79	0.40
30°	15.46	13.76	10.29	8.79	5.74	13.08	11.30	9.26	7.36	4.56
35	14.62	12.40	9.52	8.01	5.25	12.08	10.37	8.37	6.72	4.24
40	13.46	11.34	8.98	7.33	4.73	11.26	9.66	7.72	6.26	3.84
45	12.34	10.56	8.24	6.83	4.24	10.58	9.18	7.23	5.75	3.52
50	11.22	9.60	7.74	6.34	3.94	10.02	8.64	6.71	5.31	3.22
55	10.83	9.37	7.42	6.00	3.75	9.30	8.07	6.19	5.11	2.89
60	10.33	8.84	7.00	5.63	3.37	9.00	7.74	5.99	4.65	2.67
70	9.19	8.00	6.46	4.99	2.91	8.32	7.05	5.34	4.05	2.28
80	8.46	7.18	5.69	4.40	2.50	7.63	6.41	4.78	3.54	1.96
90	7.73	6.55	5.20	3.95	2.23	7.03	5.91	4.32	3.17	1.74
100	7.12	6.02	4.77	3.61	1.98	6.53	5.41	3.91	2.87	1.53
110	6.66	5.62	4.48	3.33	1.81	6.10	5.05	3.64	2.61	1.41
120	6.30	5.37	4.29	3.20	1.72	5.83	4.84	3.47	2.47	1.31
130	6.05	5.10	4.02	3.05	1.64	5.54	4.63	3.34	2.40	1.27
135°	5.98	5.08	3.95	2.98	1.61	5.38	4.47	3.29	2.39	1.24

TABLE VII-A, continued

Angle θ / $c \times 10^{-3}$	M					M-2				
	2.80	1.91	1.63	0.94	0.48	1.74	1.39	1.04	0.70	0.35
30°	17.08	12.21	11.13	8.52	6.10	12.69	10.94	9.67	7.84	4.93
35	14.84	11.05	10.01	7.71	5.28	11.36	10.03	8.67	6.96	4.32
40	13.68	10.19	9.14	7.06	4.67	10.49	9.31	7.91	6.22	3.81
45	12.70	9.60	8.74	6.51	4.22	9.82	8.61	7.20	5.67	3.40
50	11.82	9.06	8.34	6.01	3.86	9.18	8.09	6.76	5.22	3.09
55	11.20	8.57	7.76	5.68	3.50	8.63	7.90	6.35	4.80	2.70
60	10.60	8.10	7.27	5.24	3.14	8.44	7.33	5.91	4.43	2.45
70	9.71	7.37	6.58	4.56	2.66	7.57	6.47	5.24	3.73	2.01
80	8.89	6.71	6.01	3.98	2.28	6.80	5.80	4.60	3.27	1.73
90	8.19	6.11	5.48	3.59	2.02	6.24	5.23	4.13	2.89	1.55
100	7.68	5.69	5.07	3.27	1.80	5.72	4.69	3.73	2.60	1.38
110	7.21	5.36	4.73	3.03	1.67	5.26	4.48	3.45	2.39	1.25
120	6.70	5.00	4.40	2.78	1.51	5.07	4.25	3.32	2.29	1.19
130	6.36	4.76	4.18	2.69	1.48	4.85	4.09	3.15	2.21	1.15
135°	6.16	4.68	4.16	2.69	1.50	4.72	4.07	3.13	2.18	1.13

TABLE VII-A, continued

Angle θ / $c \times 10^{-3}$	M-1					H				
	1.82	1.51	1.20	0.81	0.41	0.98	0.66	0.50	0.33	0.24
30°	19.65	14.34	11.85	9.69	6.52	10.36	8.17	6.74	5.33	4.41
35	16.98	12.83	10.61	8.54	5.72	9.46	7.37	6.15	4.72	3.82
40	15.17	11.53	9.61	7.77	4.97	8.74	6.78	5.52	4.15	3.38
45	13.57	10.60	8.83	7.04	4.39	8.27	6.23	4.98	3.66	2.98
50	12.25	9.92	8.08	6.41	3.94	7.67	5.70	4.62	3.31	2.67
55	11.36	9.10	7.38	6.03	3.60	6.98	5.19	4.01	3.14	2.50
60	10.56	8.54	7.05	5.43	3.24	6.62	4.96	3.84	2.77	2.19
70	9.10	7.55	6.21	4.69	2.68	5.90	4.33	3,32	2.36	1.84
80	8.12	6.75	5.52	4.05	2.27	5.30	3.88	2.93	2.04	1.59
90	7.28	6.06	4.94	3.60	1.97	4.83	3.49	2.63	1.81	1.42
100	6.59	5.53	4.44	3.27	1.75	4.41	3.22	2.37	1.63	1.28
110	6.10	5.10	4.07	2.97	1.63	4.09	2.94	2.21	1.53	1.21
120	5.71	4.82	3.86	2.79	1.52	3.95	2.80	2.11	1.44	1.14
130	5.39	4.61	3.72	2.66	1.44	3.81	2.68	1.99	1.40	1.10
135°	5.37	4.50	3.66	2.65	1.42	3.70	2.65	1.97	1.36	1.09

TABLE VII-A, continued

H-2

Angle θ / $c \times 10^{-3}$	0.83	0.62	0.43	0.21
30°	10.76	8.67	6.65	4.05
35	9.44	7.55	5.75	3.51
40	8.33	6.70	5.06	3.02
45	7.52	6.01	4.47	2.67
50	6.86	5.47	4.06	2.31
55	6.23	4.85	3.60	2.08
60	5.80	4.54	3.27	1.85
70	4.94	3.84	2.73	1.53
80	4.36	3.36	2.36	1.30
90	3.82	2.96	2.08	1.12
100	3.45	2.68	1.86	1.00
110	3.13	2.41	1.69	0.90
120	2.99	2.28	1.61	0.85
130	2.88	2.22	1.57	0.84
135°	2.84	2.16	1.54	0.82

TABLE VIII-A

$R_\theta \times 10^5$ for the CTN Samples in Ethyl Acetate at Different Concentrations and Different Angles.

Angle θ / $c \times 10^{-3}$	T-8						T-6			
	2.34	1.96	1.50	1.00	0.54		1.87	1.39	0.67	0.34
30°	9.60	7.63	6.59	5.39	3.68		9.12	6.56	4.45	2.62
35	9.10	7.34	6.53	5.16	3.50		8.56	6.33	4.20	2.45
40	8.67	7.20	6.23	4.89	3.37		8.14	6.06	3.95	2.28
45	8.35	6.86	5.91	4.63	3.10		7.78	5.78	3.74	2.13
50	7.85	6.53	5.62	4.44	2.92		7.44	5.53	3.50	2.01
60	7.27	6.07	5.23	3.95	2.51		6.75	5.09	3.06	1.69
70	6.75	5.66	4.77	3.56	2.24		6.16	4.65	2.66	1.45
80	6.28	5.21	4.37	3.20	2.00		5.69	4.24	2.36	1.29
90	5.76	4.83	4.04	2.93	1.80		5.24	3.89	2.14	1.14
100	5.39	4.48	3.76	2.71	1.62		4.85	3.58	1.94	1.04
110	5.05	4.25	3.56	2.56	1.54		4.55	3.33	1.81	0.93
120	4.85	4.06	3.39	2.43	1.46		4.47	3.19	1.70	0.89
130	4.59	3.82	3.15	2.26	1.38		4.21	3.00	1.63	0.87
135°	4.54	3.81	3.13	2.26	1.35		4.12	2.93	1.58	0.84

TABLE VIII-A, continued

Angle θ / $c \times 10^{-3}$	M-3				M			
	1.97	1.50	1.01	0.52	1.91	1.52	1.12	0.76
30°	13.75	10.39	7.65	4.48	10.39	8.83	7.73	6.53
35	11.85	8.97	6.59	3.90	9.38	8.08	7.03	5.93
40	10.53	8.09	5.93	3.40	8.51	7.43	6.55	5.39
45	9.52	7.35	5.42	3.20	7.85	6.95	6.05	4.89
50	8.64	6.79	4.94	2.90	7.26	6.45	5.56	4.49
55	7.90	6.25	4.53	2.55	6.71	5.97	5.08	4.23
60	7.63	5.90	4.30	2.42	6.45	5.77	4.94	3.89
70	6.74	5.22	3.75	2.05	5.90	5.09	4.31	3.34
80	5.97	4.69	3.29	1.79	5.32	4.59	3.86	2.92
90	5.41	4.20	2.98	1.58	4.86	4.14	3.47	2.61
100	4.92	3.83	2.68	1.42	4.47	3.80	3.17	2.34
110	4.55	3.55	2.47	1.30	4.16	3.51	2.93	2.18
120	4.36	3.44	2.34	1.28	3.96	3.36	2.77	2.07
130	4.12	3.25	2.26	1.19	3.77	3.15	2.63	1.96
135°	4.08	3.16	2.19	1.16	3.70	3.11	2.60	1.89

TABLE VIII-A, continued

Angle θ / $c \times 10^{-3}$	M-2					M-1				H-2			
	1.52	1.26	0.79	0.60	0.41	1.01	0.83	0.61	0.40	0.70	0.59	0.47	0.24
30°	12.39	9.87	7.48	6.30	4.87	10.00	8.26	6.70	4.98	8.58	7.31	6.19	3.52
35	10.95	8.57	6.42	5.43	4.17	8.72	7.26	5.85	4.30	7.37	6.16	5.25	2.99
40	9.66	7.71	5.71	4.76	3.66	7.62	6.47	5.14	3.70	6.40	5.40	4.50	2.54
45	8.75	7.06	5.13	4.27	3.25	6.85	5.78	4.57	3.26	5.63	4.75	3.91	2.19
50	8.15	6.47	4.74	3.92	2.91	6.14	5.27	4.20	2.93	4.99	4.15	3.46	1.85
55	7.51	5.97	4.30	3.52	2.60	5.78	4.95	3.95	2.79	4.60	3.84	3.17	1.68
60	6.93	5.67	3.98	3.20	2.37	5.24	4.44	3.43	2.38	4.17	3.46	2.87	1.49
70	6.13	4.91	3.40	2.73	1.96	4.44	3.75	2.89	1.86	3.48	2.89	2.36	1.20
80	5.44	4.36	2.99	2.36	1.68	3.80	3.27	2.46	1.63	2.96	2.43	2.01	1.00
90	4.89	3.91	2.65	2.06	1.48	3.39	2.86	2.15	1.44	2.61	2.16	1.75	0.89
100	4.47	3.54	2.41	1.85	1.32	3.06	2.54	1.94	1.31	2.32	1.92	1.56	0.79
110	4.17	3.27	2.21	1.72	1.23	2.81	2.37	1.80	1.20	2.15	1.77	1.42	0.72
120	3.91	3.05	2.06	1.61	1.15	2.64	2.23	1.67	1.11	2.02	1.67	1.34	0.66
130	3.75	2.95	2.00	1.56	1.12	2.52	2.10	1.61	1.04	1.95	1.59	1.31	0.65
135°	3.67	2.91	1.96	1.53	1.09	2.50	2.09	1.58	1.06	1.95	1.58	1.30	0.64

139

CLAIMS TO ORIGINAL RESEARCH

1. The Brice-Phoenix Light-scattering Photometer was modified
   to accommodate small cells in which solutions could be
   clarified for light-scattering measurements by ultracen-
   trifugation.

2. Light-scattering measurements on high molecular weight
   cellulose trinitrate in two solvents – acetone and ethyl
   acetate – have been carried out.

3. It has been shown that in acetone, cellulose trinitrate
   assumes a random coil configuration above a molecular
   weight of 600,000 but in ethyl acetate such configuration
   is not achieved even at the highest molecular weight
   studied (2.5×10^6).

4. The intrinsic viscosity in acetone has been shown to be
   independent of shear rate in the range of shear rate from
   700 to 300 sec.$^{-1}$ even for the highest molecular weight
   fraction investigated. In ethyl acetate the intrinsic
   viscosity was independent of shear rate for values less
   than 30 dl. g.$^{-1}$. For $[\eta] > 30$ dl. g.$^{-1}$ a linear rela-
   tionship with the rate of shear could be extrapolated
   to obtain the value of zero shear rate.

5. The exponent <u>a</u> in the intrinsic viscosity-molecular weight
relationship for high molecular weight cellulose trinitrate
was found to be approximately equal but less than unity
in both solvents.

6. Certain anomalous observations in light-scattering have
been shown to be genuine effects. Tentative suggestions
have been made to explain these phenomena.

SUGGESTIONS FOR FURTHER WORK

1. A study of cellulose trinitrate solutions at very low
    rates of shear in a Couette type of viscometer.

2. A more detailed investigation of the anomalous increase
    of $\frac{\eta_{sp}}{c}$ at very low concentrations, e.g., dependence
    on capillary size, rate of shear and molecular weight.

3. Further investigation of the anomalies found in light-
    scattering. For example, parallel light-scattering
    and viscosity measurements may reveal a viscometric
    analogy to the deviation from linearity of $(Kc/R_\theta)_{\theta=0}$
    vs. c line at relatively high concentration.

4. A more careful study of the sedimentation of glass
    beads might indicate the origin of striations in cen-
    trifuged solution.

5. Study of the influence of nitrogen content on molecular
    dimensions and interaction constants.

6. Light-scattering and viscosity study of cellulose tri-
    nitrate in a poor solvent at the Θ temperature.

BIBLIOGRAPHY

BIBLIOGRAPHY

Main Text

1. Alfrey, T., Goldberg, A. I. and Price, J. A.,
        J. Colloid Sci., 5, 251 (1950).

2. Badger, R. M. and Blaker, R. H.,
        J. Phys. & Colloid Chem., 53, 1056 (1949).

3. Bawn, C. E. H., Freeman, R. E. J. and Kamaliddin, A. R.,
        Trans. Faraday Soc., 46, 1107 (1950).

4. Benoit, H. and Doty, P.,
        J. Phys. Chem., 57, 958 (1953).

5. Brinkman, H. C.,
        Proc. Amsterdam Acad., 50, No. 6 (1947).

6. Conrad, C. M., Tripp, V. W. and Mares, T.,
        J. Phys. & Colloid Chem., 55, 1474 (1951).

7. Cragg, L. H. and Bigelow, C. C.,
        J. Polymer Sci., 24, 429 (1957).

8. Cragg, L. H. and Bigelow, C. C.,
        J. Polymer Sci., 14, 177 (1955).

9. Dandliker, W. B. and Kraut, J.,
        J. Am. Chem. Soc., 78, 2380 (1956).

10. Daniels, F., Mathews, J. H. and Williams, J. W.,
        Experimental Physical Chemistry. 4th Ed.
        McGraw-Hill Book Company, Inc., New York.
        1949. P. 434.

11. Debye, P. and Bueche, A. M.,
        J. Chem. Phys., 16, 573 (1948).

12. Favis, D. V., Robertson, A. A. and Mason, S. G.,
        Can. J. Tech., 30, 294 (1952).

13. Goring, D. A. I., Senez, M., Melanson, B. and Huque, M. M.,
         J. Colloid Sci., (in press).

14. Hermans, J. J. and Levinson, S.,
         J. Opt. Soc. Am., 41, 460 (1951).

15. Holtzer, A. M., Benoit, H. and Doty, P.,
         J. Phys. Chem., 58, 624 (1954).

16. Houwink, R.,
         J. prakt. Chem., 157, 15 (1940).

17. Huggins, M. L.,
         J. Am. Chem. Soc., 64, 2716 (1942).

18. Hunt, M. L., Newman, S., Scheraga, H. A. and Flory, P. J.,
         J. Phys. Chem., 60, 1278 (1956).

19. Immergut, E. H., Rånby, B. G. and Mark, H. F.,
         Ind. Eng. Chem., 45, 2483 (1953).

20. Kirkwood, J. G. and Riseman, J.,
         J. Chem. Phys., 16, 565 (1948).

21. Kratky, O. and Porod, G.,
         Rec. trav. chim., 68, 1106 (1949).

22. Kroeplin, H.,
         Kolloid Z., 47, 294 (1929).

23. Kuhn, W.,
         Kolloid Z., 87, 3 (1939).

24. Kushner, L. M.,
         J. Opt. Soc. Am., 44, 155 (1954).

25. Lindsley, C. H. and Frank, M. B.,
         Ind. Eng. Chem., 45, 2491 (1953).

26. Maron, S. H. and Lou, R. H.,
         J. Polymer Sci., 14, 273 (1954).

27. Masson, C. R. and Goring, D. A. I.,
         Can. J. Chem., 33, 895 (1955)

28. Mitchell, R. L.,
                  Ind. Eng. Chem., 45, 2526 (1953).

29. Münster, A.,
                  J. Polymer Sci., 8, 633 (1952).

30. Nawab, M. A.,
                  Ph. D. Thesis. McGill University. 1957.

31. Newman, S. and Flory, P. J.,
                  J. Polymer Sci., 10, 121 (1953).

32. Newman, S., Loeb, L. and Conrad, C. M.,
                  J. Polymer Sci., 10, 463 (1953).

33. Notley, N. T. and Debye, P.,
                  J. Polymer Sci., 24, 275 (1957).

34. Öhrn, O. E.,
                  J. Polymer Sci., 17, 137 (1955).

35. Orofino, T. A. and Flory, P. J.,
                  J. Chem. Phys., 26, 1067 (1957).

36. Parent, M. and Rinfret, M.,
                  Can. J. Chem., 33, 971 (1955).

37. Paschall, E. F. and Foster, J. F.,
                  J. Polymer Sci., 9, 73, 85 (1952).

38. Porod, G.,
                  Monatsh., 80, 251 (1949).

39. Rundle, R. H. and French, D.,
                  J. Am. Chem. Soc., 65, 1707 (1943).

40. Schurz, J. and Immergut, E. H.,
                  J. Polymer Sci., 9, 281 (1952).

41. Takeda, M. and Eno, R.,
                  J. Phys. Chem., 60, 1202 (1956).

42. Timell, T. E.,
                  Svensk Papperstidning, 57, 777 (1954).

43. Timell, T. E.,
                  Svensk Papperstidning, 57, 913 (1954).

44. Timell, T. E.,
      Ind. Eng. Chem., 47, 2166 (1955).

45. Wannow, H. A.,
      Kolloid Z., 102, 29 (1943).

46. Zimm, B. H.,
      J. Chem. Phys., 16, 1093, 1099 (1948).

47. Flory, P. J.,
      Principles of Polymer Chemistry. Cornell
      University Press, Ithaca, New York. 1953.

48. Kunst, E. D.,
      Rec. trav. chim., 69, 125 (1950).

49. Outer, P., Carr, C. I. and Zimm, B. H.,
            J. Chem. Phys., 18, 830 (1950).

50. Bischoff, J. and Desreux, V.,
            Bull. soc. chim. Belg., 61, 10 (1952).

51. Shultz, A. R.,
      J. Am. Chem. Soc., 76, 3422 (1954).

Appendices

1. Dandliker, W. B. and Kraut, J.,
    J. Am. Chem. Soc., 78, 2380 (1956).

2. Goring, D. A. I., Senez, M., Melanson, B. and Huque, M. M.,
    J. Colloid Sci., (in press).

3. Hermans, J. J. and Levinson, S.,
    J. Opt. Soc. Am., 41, 460 (1951).

4. Öhrn, O. E.,
    J. Polymer Sci., 17, 137 (1955).

5. Takeda, M. and Eno, R.,
    J. Phys. Chem., 60, 1202 (1956).

6. Alexander, A. E. and Johnson, P.,
    Colloid Science. Oxford. At the Clarendon
    Press, London. 1949.

7. Anderson, O.,
    Svensk Papperstidning, 59, 540 (1956).

8. Alexander, W. J. and Mitchell, R. L.,
    Anal. Chem., 21, 1497 (1949).

9. Cellulose and Cellulose Derivatives, edited by E. Ott
    and H. M. Spurlin. Interscience Publishers,
    Inc., New York. 1954.

10. Staudinger, H. and Mohr, R.,
    Ber., 70, 2296 (1937).

11. Gralen, N.,
    Dissertation. University of Uppsala. 1944.

12. Timell, T. E.,
    Ind. Eng. Chem., 47, 2166 (1955).

13. Timell, T. E.,
    Svensk Papperstidning, 58, 1 (1955).

14. Newman, S., Loeb, L. and Conrad, C. M.,
    J. Polymer Sci., 10, 463 (1953).

15. Stacey, K. A.,
    Light-scattering in Physical Chemistry.
    Butterworths Scientific Publications,
    London. 1956.

16. Flory, P. J.,
    Principles of Polymer Chemistry, Cornell
    University Press, Ithaca, New York. 1953.

17. Mosimann, H.,
    Helv. Chim. Acta., $\underline{26}$, 61, 369 (1943).

18. Burgers, J. M.,
    Second Report on Viscosity and Plasticity,
    Amsterdam. 1938. P. 134.

19. Jullander, I.,
    Arkiv. Kemi Mineral. Geol., $\underline{A21}$, No. 8
    (1945).

20. Kuhn, W.,
    Kolloid Z. $\underline{68}$, 2 (1934).

21. Huggins, M. L.,
    J. Phys. Chem., $\underline{42}$, 911 (1938).

22. Huggins, M. L.,
    J. Phys. Chem., $\underline{43}$, 439 (1939).

23. Simha, R.,
    J. Phys. Chem. $\underline{44}$, 25 (1940).

24. Campbell, H. and Johnson, P.,
    Trans. Faraday Soc., $\underline{40}$, 221 (1944).

25. Lindsley, C. H. and Frank, M. B.,
    Ind. Eng. Chem., $\underline{45}$, 2491 (1953).

26. Debye, P.,
    J. Appl. Phys., $\underline{15}$, 338 (1944).

27. Zimm, B. H.,
    J. Chem. Phys., $\underline{16}$, 1093, 1099 (1948).

28. Debye, P. and Bueche, A. M.,
    J. Chem. Phys., $\underline{16}$, 573 (1948).

29. Kirkwood, J. G. and Riseman, J.,
    J. Chem. Phys., $\underline{16}$, 565 (1948).

30. Brinkman, H. C.,
        Proc. Amsterdam Acad., 50, No. 6 (1947).

31. Fox, T. G. and Flory, P. J.,
        J. Am. Chem. Soc., 73, 1904, 1909, 1915
        (1951).

32. Badger, R. M. and Blaker, R. H.,
        J. Phys. & Colloid Chem., 53, 1056 (1949).

33. Holtzer, A. M., Benoit, H. and Doty, P.,
        J. Phys. Chem., 58, 624 (1954).

34. Hunt, M. L., Newman, S., Scheraga, H. A. and Flory, P. J.,
        J. Phys. Chem., 60, 1278 (1956).

35. Münster, A.,
        Z. physik. Chem., 197, 17 (1951).